Compounds Derived from Birch Trees that Inhibit HIV-1 Replication

A DISSERTATION
SUBMITTED TO THE FACULTY OF THE GRADUATE SCHOOL
OF THE UNIVERSITY OF MINNESOTA
BY

Casey R. Dorr

IN PARTIAL FULFILLMENT OF THE REQUIREMENTS
FOR THE DEGREE OF
DOCTOR OF PHILOSOPHY

Adviser: Louis Mansky

February 2011

Acknowledgements

There numerous people that I need to thank. First, I want to thank my Mom and Dad for always supporting me. Without their support I would not have made it through 26 years of education. Also, my brother Nate has been my closest friend through my whole life and I am grateful for his support. I thank Emily Mara for the support over the past years and spending her day off helping me edit the thesis. I want to thank my grandparents Cliff and Mabel Bahr and Wesley and Betty Dorr for always believing in me. Thanks also to my extended family on both sides for being a great family.

Thank you labmates for helping me troubleshoot experiments and prepare for presentations. Thank you to Dr. Louis Mansky for mentoring, lab space, educational opportunities and for teaching me retrovirology. Also, miigwech to the American Indian Community; especially Rick Smith and Dr. Ben Clarke at University of Minnesota Duluth. Without Rick and Ben's motivational support and help finding financial assistance, I likely would not have got through undergraduate college. They have also assisted me through the graduate education. Miigwech to the Mille Lacs Band of Ojibwe and the Mille Lacs Band of Ojibwe Scholarship Program for many years of encouragement and support. Thank you to Drs. Pavel Krasutsky, Igor Kolomitsyn, Oksana Kolomitsyna, and Sergiy Yemets for an excellent chemistry and biology collaboration. Thank you to Dr. Eric Freed for reagents and research advice. Thank you to Dr. Jocelyn Shaw for academic advising in my first few years of graduate school. Thank you to Dr. Nik Somia and Dr. Reuben Harris for critical advisement and scientific discussions during the final year of my education. Also thank you to committee members Dr. Ronald Phillips and Dr. David Largaespada for helping direct me through my education. I thank anyone in advance who takes the time to read this thesis.

This research was funded by the Continuing Umbrella of Research Experiences Supplement to the Cancer Biology Training Grant: T32CA009138, Research Supplements to Promote Diversity in Health-Related Research to NIH grant GM56615 and the University of Minnesota's Diversity of Views and Experiences Fellowship. The research in the prologue was funded by a NIH Minority Access to Research Careers Training Program, the U of MN Undergraduate Research Opportunities Program, and the NIH Minority International Research Training Program.

Dedication

This dissertation is dedicated to my mother Darlene Rae (Bahr) Dorr and my father Ronald Wesley Dorr.

Abstract

Human Immunodeficiency Virus type-1 (HIV-1) replication is introduced in **Chapter 1** with an emphasis on the late phase of viral replication. Literature about the production of infectious HIV-1 is reviewed in **Chapter 1** while focusing on targets for suppressive HIV-1 therapy. **Chapter 2** describes the discovery of triterpene compounds derived from birch trees that inhibit HIV-1 replication reformatted from *Bioorganic and Medicinal Chemistry Letters*. **Chapter 3** investigates the anti-HIV-1 mechanisms of the triterpenes described in **Chapter 2**. Virus release assays conclude that the triterpene compounds target and prevents cleavage of the HIV-1 Gag product CA-SP1. Virus release assays and transmission electron microscopy indicate that the triterpene compounds SY33 and Bevirimat have a secondary mechanism of action by causing 55 kDa Gag to accumulate in cells. The Gag accumulation in cells was observed in both wild-type HIV-1 and the mutant SP1-A1V. The SP1-A1V mutant causes a decrease in susceptibility, by viral replication and CA-SP1 processing, to SY33 and Bevirimat. An **Epilogue** describes recommended future experiments. **Appendix A** describes genotypic results of an experiment to select for HIV-1 resistant to SY33 and Bevirimat using wild type and SP1-A1V as the founder viruses. The data in **Appendix A** suggest SP1-A1V causes reduced susceptibility to SY33 and Bevirimat. **Appendix B** describes the initial discovery of fatty acid derivatives with anti-HIV-1 activity.

Table of Contents

List of Tables

List of Figures

Prologue

Since attending Bemidji High School (Minnesota) in the mid-1990's, I thought that plants could answer many world problems such as hunger and disease. In 1998, while hiking through a Belizean rainforest, a Mayan medicine man taught me about the many plants near his village of Blue Creek, Belize. The plants have been used for centuries to cure diseases and malcontent. This trip to Belize, and a return in 1999, spurred my interest in biology and specifically the use of plants for therapeutic purposes.

After high school, I began college at University of Minnesota-Duluth (UMD) in fall 1999. In summer 2001, I joined Professor Ronald Phillips's lab at University of Minnesota in Saint Paul and learned essential molecular genetics techniques. In Professor Phillips's Lab, my enthusiasm for plant biology was sparked, as I studied the molecular genetics of wild rice (*Zizania palustris L.*). My experiences in Dr. Phillips' lab, led to a one year project working with Professor Arun Goyal, as an undergraduate student at UMD. In Professor Goyal's lab, I studied the ethics of wild rice research and plant biotechnology. I used *Agrobacterium* gene transfer [1] to engineer Poplar trees to express the jellyfish, *Aquorea victoria*, derived Green Fluorescent Protein (GFP). To do this, I co-cultured Poplar tissue (leaf, stem, or root) with *Agrobacterium tumefaciens*. I engineered the *Agrobacterium* to deliver the GFP gene into the plant tissue. Following co-culture, the plants were regenerated, resulting in Poplar trees that glowed green under UV light (See **Figure 1**). Since GFP expression is only in exterior of leaves, the plants are likely chimeric GFP and wild type. The GFP expression in Poplar could be used as a transgenic reporter system. Alternatively, fluorescent plants could be sold commercially.

Figure 1: Green Fluorescent Protein Expression in *Populus* Plant
GFP expression is evident under long-wave UV light (right picture). The picture to the left is both GFP expressing and wild-type (WT) *Populus* strain NM6 under normal light. GFP expression is only in the exterior regions of the leaf, which indicates a possible chimeric *Populus* plant. The six-week-old *Populus* plants were regenerated from root tissue that was engineered by *Agrobacterium* mediated gene transfer.

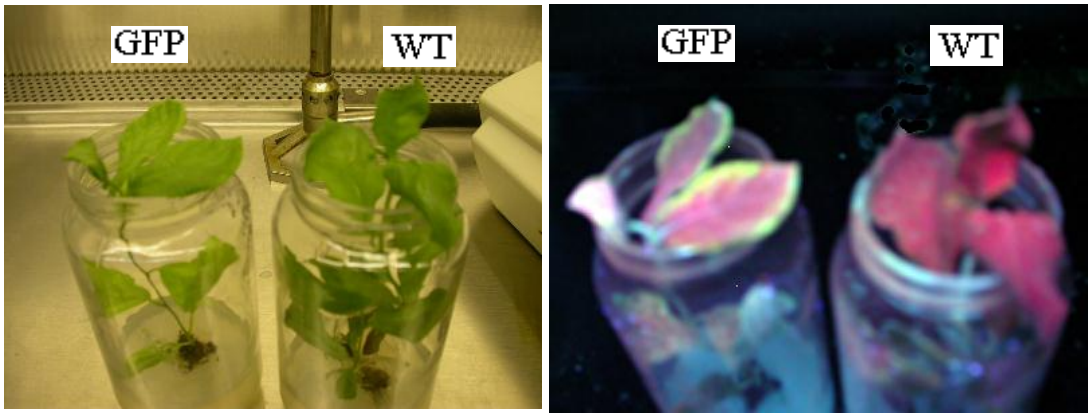

My desire to use plant biology techniques in human health continued in Rome, Italy. In 2003, I pursued a research project in Professor Eugenio Benvenuto and Selene Baschieri's lab at the Italian National Agency for New Technologies, Energy and Environment (ENEA-Casaccia). In Rome, I engineered Potato Virus X (PVX) to express an epitope from the HIV-1 envelope protein on PVX's surface. The chimeric PVX/HIV-1 was later published by Benvenuto's lab named pPVX*Sma*-P18DD [2]. The recombinant pPVX*Sma*-P18DD virus was able to systemically infect the tobacco plant *Nicotiana benthamiana* [2]. The goal of this project was to produce an HIV-1 vaccine, by expressing HIV-1 antigens in plants. The potential vaccine could then be harvested, and used to elicit anti-HIV-1 immune responses in humans. Due to time constraints, I did not test the immunogenicity of pPVX-*Sma*P18DD. However, Dr. Benvenuto's Lab was able to elicit human and murine HIV-1 specific antibodies, in a murine model, using recombinant-PVX as an HIV-1 immunogen [3].

Figure 2: Recombinant HIV-1/Potato Virus X Systemically Infects Tobacco
Five week-old *Nicotiana benthamiana* plants were infected with PVX*Sma* or PVX*Sma*-P18DD. Lesions and signs of onset chlorosis became detectable five days after infection with PVX-Sma and PVX-P18DD. This photo shows that the HIV-1 envelope epitope expressing PVX*Sma*-P18DD systemically infects tobacco plants with a similar phenotype as the wild-type PVX*Sma* virus. RT-PCR analysis verified expression of the HIV-1 epitope in the tobacco plant.

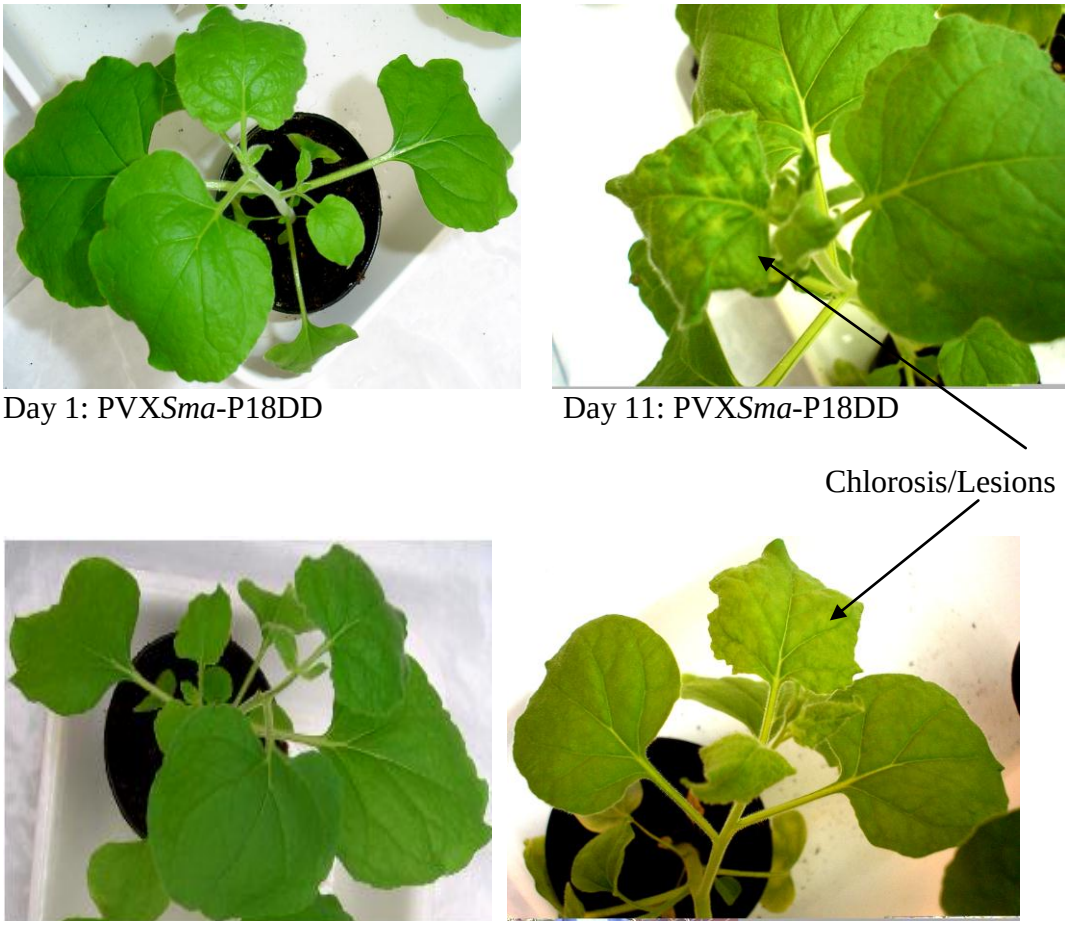

In 2005 I joined graduate school at the University of Minnesota-Twin Cities and refocused my strategy of using plants to address human problems. During graduate school, I turned my attention to the biological problem instead of the plant as the therapeutic. I studied retrovirology in Professor Louis Mansky's lab focusing on the biology of HIV-1. When I joined Professor Mansky's Lab, we formed a collaboration

with Professor Pavel Krasustky's Lab at UMD's Natural Resource Research Institute (NRRI). Dr. Krasutsky's research group specializes in extracting compounds from natural sources (like plants), purifying the compounds, than chemically modifying the compounds with organic chemistry. Professor Krasutsky has numerous patents filed describing the synthesis of novel compounds with therapeutic use and potential. Using the tools of retrovirology in the Mansky Lab and organic chemistry in the Krasutsky Lab, we set out to find novel anti-viral strategies against HIV-1. To begin the project, I developed a single-round HIV-1 replication assay to screen a large library of compounds derived from the Birch tree *Betula Paprifrya* [4].

On July 31, 2006, I was working at the FACScan flow cytometer, collecting data when I got my first "hit". I observed that sample OK256 (compound **19**, **Chapter 2**) was potent at inhibiting HIV-1 replication. We recently published the anti-HIV-1 activity of OK256 2,2-Dimethyl-4-[(28-oxolup-20-en-3β-yl)oxy]-4-oxobutanoic acid [4]. After discovery of OK256, I worked with Drs. Pavel Krasutsky, Oksana Kolomitsyna, Sergiy Yemets, and Igor Kolomistyn to design thousands of novel compound structures that might be active at inhibiting HIV-1 replication. The compounds can be derived from triterpene (**Chapters 2** and **3**) or fatty acid (**Chapter 4**) fractions of Birch bark extract. I spent much of my thesis research screening these novel compounds for anti-HIV-1 activity. While screening compounds, I also did numerous experiments investigating the mechanism of anti-HIV-1 activity.

Figure 3: Birch Trees near Bemidji, Minnesota, United States of America
The white bark of these birch trees, *Betula papyrifera*, is the starting material for the compounds described in this thesis. The compounds described in **Chapter 2** and **3** were derived from triterpene fractions of Birch bark extracts. The compounds in **Appendix B** can be derived from suberin fractions of the Birch bark extracts.

This thesis begins with a background of HIV-1 replication, while focusing on potential therapeutic targets in the late phase of HIV-1 replication. **Chapter 2**, is a reformatted manuscript that was published in *Bioorganic and Medicinal Chemistry Letters* describing the discovery of anti-HIV-1 triterpenes. **Chapter 3** investigates the molecular target of the newly discovered anti-HIV-1 compounds. The research in **Chapters 2** and **3** was presented at the Retroviruses conference in Cold Spring Harbor, New York in May of 2009 [5] and at the Centennial Retrovirus Meeting in Prague, Czech Republic in April and May of 2010 [6]. **Appendix A** shows the genotypic results from passaging HIV-1 in human T-cells in high concentrations of SY33. **Appendix B** is a short data set describing initial findings on a new class of fatty acid derivatives with anti-HIV-1 activity. Finally, there is an epilogue describing future directions for this research.

Chapter 1

Drug Targets during the Production of HIV-1

With great honor, this dissertation is being written during the 100 year anniversary of the beginning of retrovirology when Peyton Rous discovered a filterable agent that caused sarcoma in chickens [7, 8]. The filterable agent was later named Rous Sarcoma Virus (RSV). Rous's discovery of the retrovirus RSV is generally noted as the start of the scientific study of retrovirology [9]. Since early in the discovery of retroviruses, it was noted that this family of enveloped viruses could have serious health implications to the infected hosts [7, 8]. This remains true as the retrovirus, Human Immunodeficiency Virus type-1 (HIV-1) has quickly become a worldwide health problem infecting over 33 million people [10].

HIV-1 and the related virus HIV-2 are the etiological agents that cause Acquired Immunodeficiency Syndrome (AIDS) [11-15]. AIDS is defined by the Center for Disease Control to include all HIV infected persons with 200 $CD4^+$ T-lymphocytes/µL, or a CD4+ T-lymphocyte percentage of total lymphocytes of less than 14 [16]. If HIV-1 is left untreated, nearly all HIV-1 infected individuals will succumb to the fatal AIDS. To date, the biggest advancement in AIDS research is the development of highly active antiretroviral therapy (HAART). HAART is a suppressive viral therapy that slows, and possibly prevents, the progression of HIV infection to AIDS. A significant problem with HAART is the continual development of drug resistant virus [17]. Thus, it is important to develop antiretroviral compounds that inhibit drug resistant HIV.

The two primary types of HIV are type 1 (HIV-1) and type 2 (HIV-2) [18]. HIV-1 is more pathogenic than HIV-2 and leads to higher incidences of AIDS progression [10]. HIV-1 and HIV-2 are from the retrovirus genus lentiviridae (*lenti-*, latin for "slow"). Lentiviruses are slow viruses [19] that incubate in the host for a prolonged period prior to onset of disease. There are a number of retroviruses in the lentiviridae genus including: Bovine Immunodeficiency Virus (BIV), Visna/Maedi Virus, Feline Immunodeficiency Virus (FIV), and Simian Immunodeficiency Virus (SIV). It is generally accepted that HIV-1 evolved from SIV and crossed host species from non-human primates to humans [20]. Each lentivirus particle has 2 copies of a single-stranded viral RNA (vRNA) genome. The RNA genome is reverse transcribed by the viral Reverse Transcriptase (RT) into viral DNA (vDNA) [21], and then integrated into a host cell's genome by the viral Integrase (IN). Lentiviruses can infect [22, 23] and integrate the viral genome into non-dividing cells.

This thesis will concentrate on the production of infectious HIV-1 from virus producing cells. Furthermore, this chapter will introduce HIV-1 replication while paying close attention to the late phase of HIV-1 replication. Specifically, **Chapter 1** is a review of literature describing scientific findings related to expression of the HIV-1 *GagPol* gene, assembly and budding of *GagPol* gene products Gag and GagProPol, Lastly, this chapter will explore anti-viral strategies that target the late phase of HIV-1 replication.

Figure 1: HIV-1 Replication Cycle
HIV-1 replication can be divided into the early and late phases of replication. The early phase of replication consists of viral entry, reverse transcription, nuclear import of the viral DNA and integration of the viral DNA into the host cell's genome. The late phase consists of viral transcription, translation of viral proteins, trafficking and assembly of the viral proteins at the plasma membrane, budding and release of the viral particle from the cell, and viral maturation.

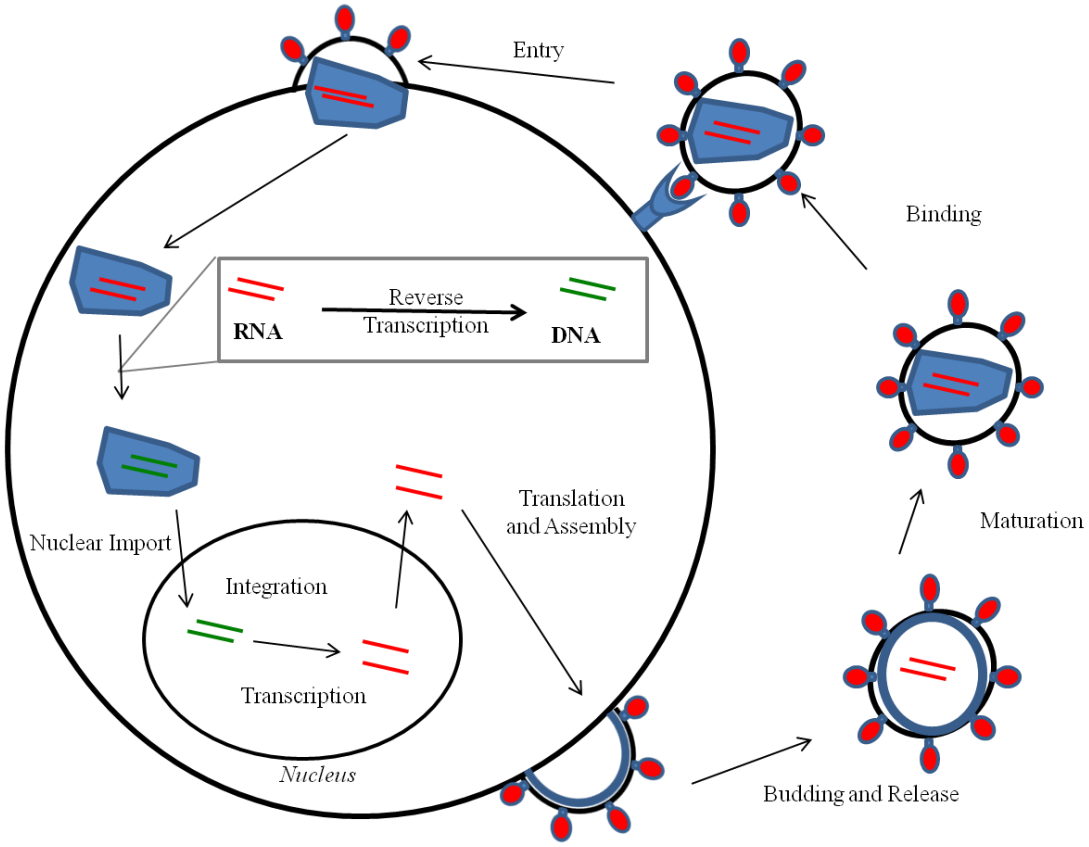

HIV-1 Replication Cycle

The HIV-1 replication cycle can be divided into the early and late phases of viral replication. The early phase of viral replication is from the time HIV-1 binds and enters the permissive target cell through integration. The late phase of viral replication is when the viral genes are expressed through maturation of the virus (**Figure 1**).

The early phase of replication begins with the virus envelope protein attaching to the CD4 receptor [24, 25], and recognition of one the co-receptors CXCR4 [26] or CCR5 [27, 28]. CCR5 is a co-factor for macrophage-tropic HIV-1[29], while CXCR4 is a co-factor for T-cell-tropic HIV-1 [26]. Subsequently, the viral membrane fuses with the cell membrane and the viral core enters the cytoplasm [30]. During viral entry, reverse transcription of the genomic RNA (gRNA) begins by the viral RT enzyme. As the viral core enters the cell, HIV-1's RT synthesizes vDNA while the core degrades during viral uncoating. The vDNA is imported into the host cell nucleus. Once in the nucleus, the vDNA integrates into the host cell genome catalyzed by the viral enzyme IN [31]. The process of viral entry to integration is the early phase of HIV-1 replication.

Reverse transcription was discovered by David Baltimore [32], Satoshi Mizutami, and Howard Temin [21] in 1970 when they observed that retroviral gRNA was reverse transcribed into viral DNA (vDNA) by an RNA dependent DNA polymerase. The enzyme was later named Reverse Transcriptase (RT). RT is a heterodimer and has an RNAseH domain that degrades RNA [33-36]. HIV-1's RT has a 1:1 ratio of p66 and p51 subunits [37]. The discovery of RT revolutionized the fields of molecular biology and virology. Prior to the discovery of RT, the central dogma of molecular biology was that genetic information is stored in DNA [38, 39] and was expressed in a stringent pathway. The dogma stated that DNA is transcribed into RNA and the RNA is translated into protein [40, 41]. The discovery of RT redefined the central dogma of molecular biology by proving that genetic information can be stored in RNA and reverse transcribed into DNA.

The late phase of the HIV-1 replication cycle consists of viral gene expression, Gag trafficking, viral components assembling at the viral membrane, budding of the virus from the membrane, and release of the particle into the extracellular milieu [42]. The late phase of HIV-1 replication continues after the virus is released from the cell and the virus matures into an infectious virus [43]. The viral Protease (PR) is active as a homodimer [44] and catalyzes reactions that cleave the Gag structural protein into the components Matrix (MA), Capsid (CA), Spacer Peptide 1 (SP1), Nucleocapsid (NC), Spacer Peptide 2 (SP2), and p6 [45]. HIV-1's PR is an aspartic acid protease [46]. During maturation, RT, the NC coated gRNA, and other viral components are encapsidated by the CA protein forming the viral core. Once the virus matures, the virus life cycle is complete rendering an infectious nascent HIV-1 particle.

Figure 1 shows the HIV-1 replication cycle. Virtually any step in HIV-1 replication can be targeted for suppressive therapy. Current HIV-1 drugs inhibit viral replication by interfering with reverse transcription, integration, viral fusion, viral entry, and protease activity. This chapter will review literature about the late phase of replication and then investigate current progress targeting the late phase of HIV-1 replication for antiretroviral drug development.

GagPol: The Quintessential Retroviral Gene

Retroviruses have two essential genes, *GagPol* and *Env*. However, the envelope (expressed from the *Env* gene) from other viruses can be supplied *in trans* and the virus can still replicate. For example, the vesicular stomatitis virus glycoprotein (VSV-G) can

be expressed *in trans* to "pseudotype" the envelope defective HIV-1 so the virus can infect a permissive cell [47] (see **Chapter 2, Figure 1**) . Since, envelope can be supplied *in trans*, *GagPol* is thus the quintessential gene that maintains retroviral integrity.

HIV-1 encodes multiple RNAs transcribed by the host DNA dependent RNA polymerase Pol II. Many of the HIV-1 RNAs are poly-cistronic (encode more than one protein product per RNA). For instance, the *Env* mRNA is translated to a 1:1 ratio of Envelope (Env) and Vpu proteins. The *GagPol* gene encodes two major proteins GagProPol and Gag (**Figure 2**).

Figure 2: Maps of *GagPol* Gene Products Gag and GagProPol
The *GagPol* gene expresses both the 55 kDa protein Gag and 160 kDa protein GagProPol. Gag and GagProPol expression is regulated by ribosomal frameshifting during translation. The lines between each protein domain indicate PR cleavage sites. Prior to cleavage, The **M** region functions in membrane binding, **I** in Gag and GagProPol self-association, and **L** functions in viral budding.

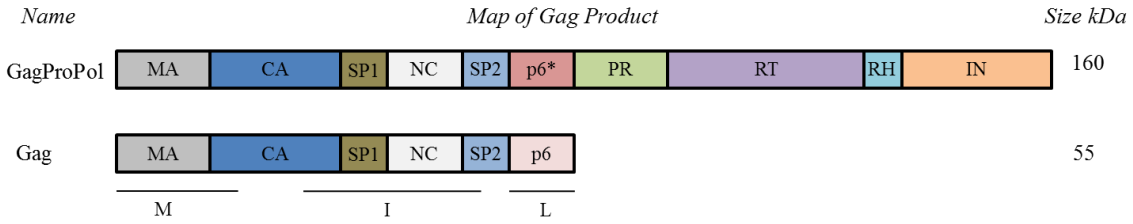

Gag and GagProPol regions play important roles in HIV-1 assembly, release, and maturation. During assembly of viral particles, the membrane binding (**M**) region [18] is composed of the MA protein and N-terminus of CA. The **M** region of the Gag or GagProPol protein is essential for targeting the proteins toward the plasma membrane (PM). The intermediate (**I**) region [18], is composed of the C-terminus of CA, SP1, and NC. **I** functions in Gag, GagProPol, and RNA multimerizations. The late (**L**) region [18] is primarily the p6 protein and SP2 region. The p6 protein interacts with ESCRT proteins and functions in the budding process of virus production and cytokinesis of the virus from the cell.

During maturation, GagProPol is processed into nine proteins after the viral protease (PR) cleaves itself out of the GagProPol precursor. The nine proteins are MA, CA, SP1, NC, SP2, p6*/TFP, PR, RT, IN. PR then cleaves Gag into the five proteins MA, CA, SP1, NC, SP2, and p6. The maps of Gag and GagProPol in **Figure 2** indicate the the protein products after Gag and GagProPol cleavages.

GagPol Gene Expression

GagPol is an essential retroviral gene that is expressed via a highly regulated process. Following *GagPol* transcription, by the host cell's RNA polymerase, the *GagPol* mRNA transcript is trafficked out of the nucleus into the cytoplasm. Once in the cytoplasm, *GagPol* mRNA is translated by the ribosome. The ribosome serves as an important regulator of *GagPol* gene expression. In the 1980's, Harold Varmus's lab discovered that *GagPol* translates into two major protein products, Gag and GagProPol, in the retroviruses RSV [48], Mouse Mammary Tumor Virus (MMTV) [49], and HIV-1 [50] regulated by ribosomal frameshifting. The *GagPol* mRNA forms a stem-loop structure that stops *GagPol* translation. When GagProPol is the translated product, the ribosome shifts open reading frames and translates through the RNA stem-loop. Retroviral ribosomal frameshifting regulates *GagPol* gene expression resulting in a Gag to GagProPol ratio of about 20:1 [50].

HIV-1 Assembly

Following translation, the 55 kD Gag and 160 kD GagProPol protein products (**Figure 2**) traffic towards the cellular plasma membrane (PM). The routes the Gag and GagProPol proteins take towards the membrane are still under investigation. There is evidence that the endosomal sorting complexes required for transport (ESCRT) proteins are involved with Gag trafficking [51, 52] and budding from the host cell [53-55]. ESCRT proteins primarily interact with the p6 late domain of Gag [56] and will be discussed later. Gag is the primary structural protein and is 20 times more abundant in the cell than GagProPol, which contributes the essential enzymes PR, RT, and IN.

It is generally accepted that the PM is the primary site of HIV-1 assembly [57]. Studies show that HIV-1 mutants can also assemble inside the cell. HIV-1 can replicate via the intracellular compartments multivesicular bodies when the HIV-1 has three matrix mutations and a truncated cytoplasmic tail of gp41 [58]. However, this chapter will focus on the PM as the primary site of HIV-1 assembly.

The Matrix (MA) domain, at the N-terminus of Gag or GagProPol, functions in virus assembly by targeting the protein to the PM. Gag is a substrate for post-translational modification by N-myristyl transferase (NMT) [59] resulting in the myristylated protein product myr+ Gag. The myr+ Gag is trafficked to the PM. The MA region of Gag is modified by covalent linkage of the 14 carbon fatty acid myristate to the 2^{nd} amino acid of the N-terminus of Gag [60]. Mutation of this glycine to alanine (MA-G2A) disrupts the Gag-PM association and inhibits formation of myr+ Gag causing and accumulation of myr- Gag in the cell [60]. Additionally, GagProPol can also be

myristatylated, but non-myristylated GagProPol can still be packaged into VLPs, due to the role of CA region in Gag and GagProPol assembly [61]. The role of the myristate Gag modification is so vital in VLP production that replacing the MA region with a myristate signal still causes Gag to form particles [62]. The smallest HIV *Gag* gene product capable of virus-like particle formation was a 28-kDa protein which consists of a few MA amino acids and the CA-SP1 domain [63]. Though a later study reported that minimal HIV-1 Gag constructs which have NC replaced by a leucine zipper and retaining only a myristyl anchor, the C-terminal third of CA-SP1, and a late assembly domain can produce HIV-1 like particle [64]. This indicates that CA-SP1 and post-translational myristate modification of Gag is important for virus assembly.

Following Gag myristoylation, the myristate moiety is buried inside of a molecular pocket in the protein. As a Gag monomer, the myristate is sequestered, though once Gag forms a trimer, the myristate moiety is exposed [65]. Thus, Gag:Gag multimerization can trigger trafficking towards the PM because myristate exposure is necessary for PM association. A study shows that genome binding can facilitate myristate exposure [66]. Current studies determined that myristate exposure is also caused by calmodulin binding at a 1:1 ratio with myristate(+) MA [67] and is also influenced by changes in pH [68]. Point mutations can also influence myristate exposure [69] . Once exposed, the myristate moiety targets the Gag protein towards lipid rafts in the PM. The change between myristate exposure and myristate concealment is termed the myristyl switch.

Myristoylation is an interesting therapeutic target. Myristate is a 14 carbon length fatty acid, and **Appendix B** of this thesis describes a 14 carbon fatty acid derivative, OK191, which has modest anti-HIV-1 activity. The anti-HIV-1 activity is even more pronounced when OK191 is in an ionic mixture with 2 glucamonium molecules (OK191G). Since a study demonstrated that glucosamine non-competitively inhibits NMT, and blocks HIV-1 release from the cell [59], and that OK191G is the same as OK191, except for the presence of two glucamonium ions; it is possible that OK191G targets NMT while, OK191 does not target NMT. Another study indicated that myristoylation can be an anti-HIV-1 target by showing a 14 carbon fatty acid that inhibited viral budding [70]. Furthermore, in **Appendix B**, transmission electron microscopy (TEM) results indicate that OK191G treatment of HIV-1 producing cells seems to trap HIV-1 particles on the cellular PM (**Appendix B, Figure 2b**). Also in **Chapters 2** and **3**, the anti-HIV-1 triterpene compounds OK117 and OK118 are betulinic aldehyde mixtures with glucamonium. OK117 and OK118 inhibit the late phase of HIV-1 replication [4]. Thus, myristoylation of HIV-1, and the cellular enzyme NMT, are logical targets for anti-HIV-1 drug development.

Once myristate is exposed, the MA part of Gag is able to interact with the PM. The myristate is thought to be embedded into the PM and maintains the interaction following virus budding and release. During viral entry, the MA protein is thought to play a role in formation of the pre-integration complex (PIC). MA must be phosphorylated by tyrosine kinase at the MA C-terminal region, and phosphorylation is important for the ability to infect a new cell and preintegration complex formation [71].

More specifically, MA phosphorylation of Ser-9, -67, -72, and -77 is important for an early post entry step during virus infection [72]. Furthermore, mutation of these specific serine residues prevents MA interaction with lipid rafts during HIV-1 assembly and can impair recruitment of envelope to the sites of viral budding [73]. Though MA phosphorylation mechanisms and consequences are mostly unknown, phosphorylation is an important post-translational modification of the MA region of Gag contributing to HIV-1 replication.

Multimerization of Gag and GagProPol is driven by interactions between the capsid (CA) regions of Gag and GagProPol. The CA region plays central role in GagProPol incorporation into HIV-1 during virus assembly. Non-myristoylated GagProPol interacts with Gag and is incorporated into HIV-1 particles [61] through CA:CA interactions. Thus, GagProPol myristoylation is not necessary for GagProPol packaging; rather the CA region is important for GagProPol packaging into particles [74]. The CA region, and more likely CA-SP1, is important for GagProPol interactions with Gag during HIV-1 assembly. It makes sense that myr- GagProPol is in HIV-1, because the absence of a myristate linkage to the PM would increase GagProPol's molecular flexibility. Increased GagProPol flexibility would make the initial PR intramolecular [75] cleavage more efficient during viral maturation. The CA domain is important for GagProPol incorporation into HIV-1 like particles.

Capsid (CA) is important for Gag:Gag recognition and assembly of Gag mulitmers during HIV-1 assembly [43, 76]. Residues in the C-terminus of CA promote CA to CA binding. A CA binding peptide, CAI, can inhibit Gag assembly by targeting

CA to CA recognition [77]. Recent data suggest that Gag self assembles to form a curved hexameric lattice while the immature particle assembles at the PM [76]. It is further thought that Gag:Gag interactions are coupled with interactions between the CA-SP1 domain of Gag [78]. CA and CA-SP1 regions of Gag and GagProPol are important for protein self-association during the assembly of HIV-1

There is debate on the role of SP1 in HIV-1 assembly. One reports says Gag:Gag interactions are mediated by the **I** (SP1-NC) region, and plays a central role in the assembly of HIV particles [79]. However, another study reports Gag self-association is not significantly influenced by the SP1 region; rather the SP1 functions in flexibility of the HIV-1 Gag polyprotein [80]. Another study concluded that SP1 and the first 13 amino acids of NC are required for RNA binding, indicating the importance of SP1 and NC in HIV-1 genomic encapsidation [81]. SP1 likely serves as a linker region between CA and NC during virus assembly. Thus, SP1 plays an important role in Gag:Gag interaction (in association with CA) while also contributing to the role of NC in RNA recognition during virus assembly.

During HIV-1 assembly, NC plays a critical role in gRNA packaging into the virus. The NC region of Gag and GagProPol has two zinc fingers that interact with the gRNA. The dimerization of gRNA during assembly is reliant upon NC and the dimerization initiation signal on the gRNA [82]. Also, MA binds the gRNA during virus assembly and can target RNA to PM [83, 84]. Furthermore, a recent report suggests NC and MA both interact with the gRNA and PM during virus assembly [85]. It is important

that the gRNA is packaged into the nascent viral particle and NC plays an essential role in Gag:gRNA interactions.

Lipid rafts in the PM have critical roles in HIV-1 assembly and release [86]. Recent data note that myristoylated MA (myr+MA) forms hexamers of MA trimers that preferentially targets MA to PM sites enriched in cholesterol [87] and phosphatidylinositol-(4,5)-bisphosphate (PI[4,5]P_2) [66, 84]. PI[4,5]P_2 regulates HIV-1 assembly [88] and MA binds PI[4,5]P_2 through head group and 2' acyl chain contacts [84]. It is currently accepted that lipid rafts are a major PM site for HIV-1 assembly [89].

Once Gag, GagProPol, the gRNA and various other components assemble at the PM, the virus then buds from the cell. The budding virus is released and undergoes maturation. The mature virus can then begin the replication cycle by infecting a new cell.

HIV-1 Budding and Release from Virus Producing Cell

HIV-1 budding from the virus producing cell is a late step in the virus replication cycle and has recently been reviewed [42, 51, 90-94]. The p6 late (**L**) domain in Gag binds with TSG101 and ALIX to recruit ESCRT proteins that function in fission of the virus from the cell [95]. The PTAP (Pro-Thr-Ala-Pro) amino acid sequence in p6 recruits the ESCRT proteins to the site of budding by binding the cellular protein TSG101 [96, 97]. The UEV domain in TSG101 binds to the PTAP domain on p6 [98]. However, if TSG101 is overexpressed, HIV-1 budding is inhibited via late domain functions [99], indicating there is fine balance between the TSG101 cellular concentration and virus budding.

Figure 3: HIV-1 Assembly, Budding, Release and Maturation

The *GagPol* gene's mRNA translates into a 20:1 ratio of Gag to GagProPol. During HIV-1 assembly: 2 genomic RNA (gRNA), about 5000 Gag, and about 250 GagProPol proteins traffic to the host cell's plasma membrane (PM). As the Gag, gRNA, and GagProPol form higher order multimers at the PM, the virus like particle protrudes from the cell surface, budding a nascent virus from the cell. Once the virus is released, the virus matures as a result of the viral Protease (PR) cleaving the Gag and GagProPol molecules. Distinct HIV-1 morphologies are shown: immature (**I**), mature eccentric (**E**), and mature regular (**R**). The **I** particle has a translucent core and the Gag protein is attached to the PM. The **E** particle likely has an elevated level of CA-SP1, in the particle, and is an intermediate morphology during maturation. In the **R** particle, the gRNA is coated with nucleocapsid (NC) and encapsidated into a conical viral core. The viral core is composed of CA multimers. Maturation is essential for the production of an infectious HIV-1 particle. The drawings of HIV-1 assembly, budding, release, and maturation coincide with the TEM images. The TEM images were taken at different stages of HIV-1 production from a *GagPol* expressing cell line (**Chapter 3**) with a JEOL1210 transmission electron microscope (Electron Microscopy BioServices; Frederick, Maryland).

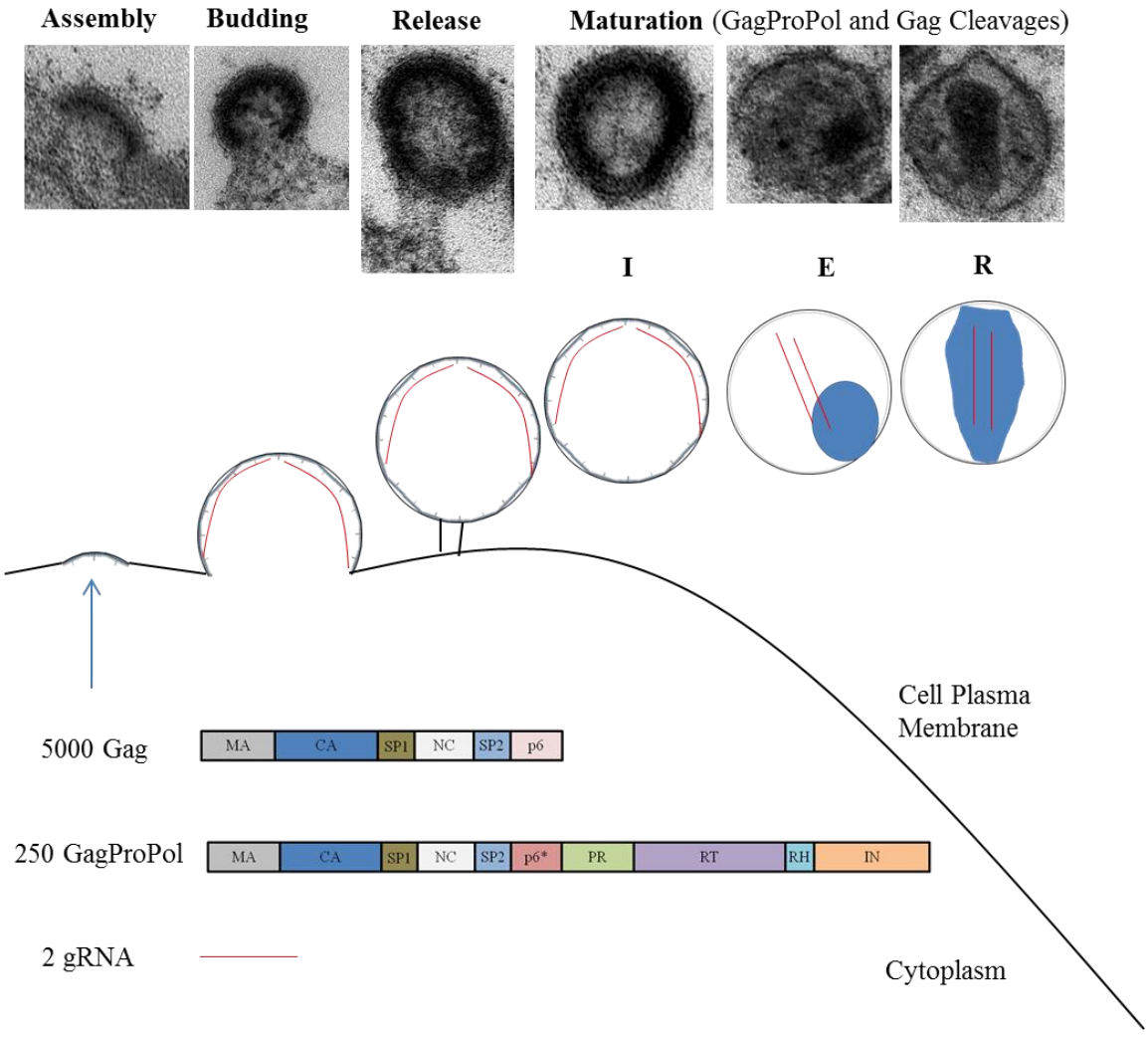

The Gag **L** domain p6 is important for production of HIV-1 [100] and phosporylation of p6 by ERK-2 from MAPK pathway influences virus release [101]. Also, variability in p6 influences budding [102] and p6 function [103]. The p6 interaction with ALIX is via the LYPX(n)L amino acid sequence [104, 105]. Recent data show that ALIX recruits the ubiquitin ligase Nedd4-1 to facilitate HIV-1 release through the LYPX(n)L **L** domain motif [53]. NC also engages ALIX through ALIX's BroI domain [106]. Furthermore, ESCRT machinery is dependent on NC-SP2 for HIV-1 release [107]. Thus, it is likely the entire Gag region including NC, SP2, and p6 interact with ALIX during fission of the particle from the cell. Finally, it should be noted that an ALIX fragment potently inhibits HIV-1 budding [108]. Therefore, ALIX plays in important role in the budding of HIV-1 from a host cell.

The HIV-1 accessory protein Vpu is a 16 kDa protein [109-111] that antagonizes the human protein Tetherin [112]. Tetherin is a cellular protein that links viral particles to the cell membrane. HIV-1's Vpu protein enhances the release of capsids produced by Gag constructs of widely divergent retroviruses [113]. Vpu's effect on particle release is different than p6's effect [114]. Though Vpu is an accessory protein for HIV-1 replication, further understanding of Vpu's antagonistic effect on Tetherin will further enhance our knowledge of HIV-1 release.

Viral budding and release offer targets for anti-HIV-1 therapy. The interactions of p6 with TSG101 and ALIX can be targets for anti-retroviral development. Furthermore, activation of the inositol (1,4,5)-triphosphate calcium gate receptor is required for HIV-1 Gag release [115] and could also be a target for suppressive HIV-1

Figure 4: GagProPol Processing Supplies Essential Viral Enzymes PR, RT, and IN
This figure shows a map of the GagPol protein product GagProPol. GagProPol is sequentially cleaved by the viral protease to form numerous protein products. The initial GagProPol cleavages are by an intramolecular mechanism. MA is at the N-Terminus of the protein and IN is at the C-terminus. The GagProPol proteins after cleavage are MA = Matrix, CA = Capsid, SP1 = Spacer Protein 1, NC = Nucleocapsid, SP2 = Spacer Protein 2, p6* = p6* is also called Transframe Protein (TFP), PR = Protease, RT = Reverse Transcriptase, RH = RNase H domain of Reverse Transcriptase, IN = Integrase. The proteins are sequentially cleaved, as illustrated from top to bottom, and there are numerous intermediate proteins during cleavage.

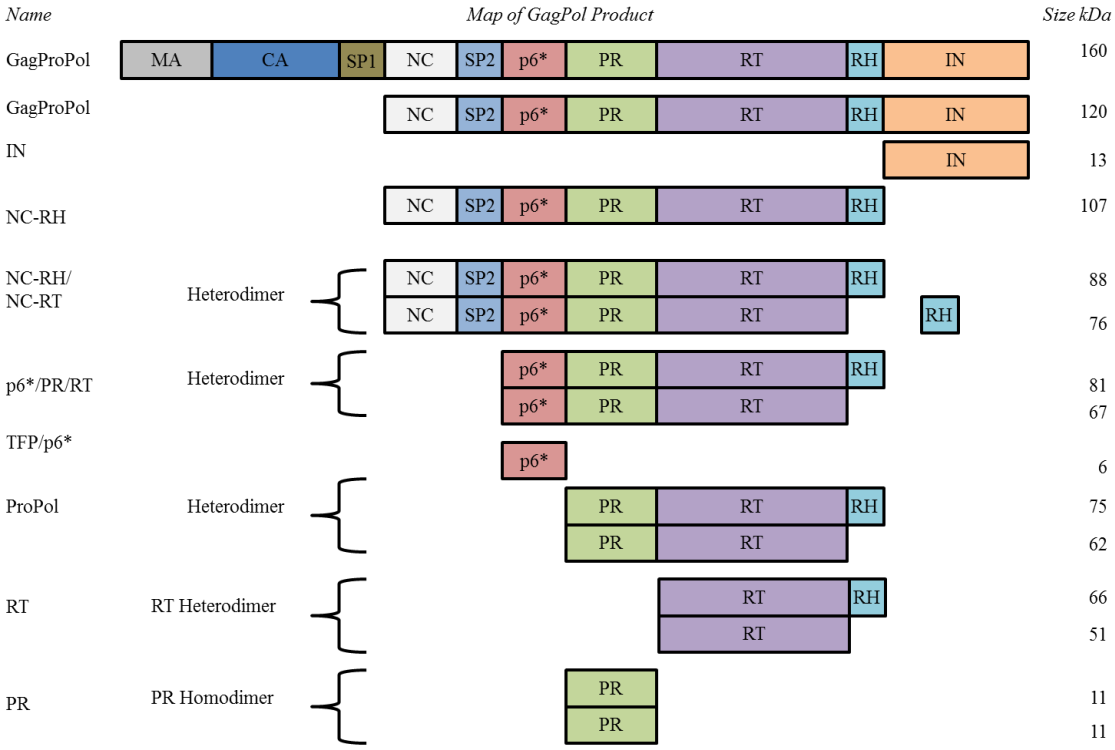

References: [45, 75, 116]

therapy. Lastly, Vpu is also an interesting viral target during the release of HIV-1 from a viral host cell. Following the release of a nascent HIV-1 particle, the virus undergoes a series of reactions that lead to a mature morphology. This thesis will focus on HIV-1 maturation as an anti-viral target using triterpene derivatives and antiretroviral agents.

HIV-1 Maturation and Cleavage of Gag and GagProPol

Maturation of the HIV-1 particle is a process that occurs as a result of proteolytic cleavages of the Gag and GagProPol proteins by the viral PR enzyme. Maturation occurs primarily after the virus has been released from the cell. Immature HIV-1 particles (**Figures 3, 5**) contain about 5,000 Gag proteins [117]. Since GagProPol is expressed at about $1/20^{th}$ the level of Gag, there are an estimated 250 molecules of GagProPol per HIV-1 particle. When GagProPol dimers occur the PR region of the molecule activates, and cleaves the GagProPol into protein products by an intramolecular mechanism [75] as portrayed in **Figure 4**. Once the excised PR dimer is free from the GagProPol precursors, PR's rate of enzymatic activity increases [118] and, *in trans*, cleaves Gag and GagProPol proteins in the virus particle at specific cleavage sites [75, 118].

GagProPol has 9 cleavage sites, while Gag has 5 cleavage sites. Cleavage of these proteins results in numerous protein products. **Figure 4** shows the ordered processing of the GagProPol protein into its subsequent products. GagProPol is most notable for supplying the essential viral enzymes, Reverse Transcriptase (RT), Protease (PR), and Integrase (IN). The PR domain of GagProPol dimers [75] proteolytically excises PR via an intramolecular mechanism. As stated in **Figure 1**, RT, PR, and IN are vital to the HIV-1 replication cycle. **Figure 5** shows the ordered processing of the Gag protein and its protein products. Gag supplies MA, CA, SP1, NC, SP2, and p6 to the particle. After maturation, the mature VLP core consists of 1,000 to 1,500 CA proteins; thus less than 1/3 of the total CA from Gag contributes to the mature HIV-1 core [117]. Mature HIV-1 contains $\leq$ 250 molecules of RT, IN, and PR per particle.

Figure 5: Gag Processing and HIV-1 Morphologies during HIV-1 Maturation
a) Map of HIV-1 Gag. Gag domains from N terminus to C-Terminus: MA = Matrix, CA = Capsid, SP1 = Spacer Protein 1, NC = Nucleocapsid, SP2 = Spacer Protein 2, p6 = p6 late domain. The 55 kDa Gag protein is sequentially cleaved by the viral protease at specific sites between the domains. The sequence of processing is illustrated from top to bottom of the figure. The cleavage of CA-SP1 is typically the last Gag cleavage. **b**) Transmission electron microscopy of HIV-1 morphologies. 293 cells that stably express HIV-1 *GagPol* and *Rev* were analyzed by electron microscopy. The Immature (**I**) morphology correlates with minimal Gag cleaveages in the virus particle. The Mature Eccentric (**E**) morphology is an intermediate step during viral maturation. The **E** morphology can be characterized by a condensed viral core that is often not centered in the virus. The **E** morphology correlates to intermediate levels of Gag processing. The Mature Regular (**R**) morphology for HIV-1 has a conical core and correlates to full Gag processing. Gag processing is essential for HIV-1 to infect a new cell.

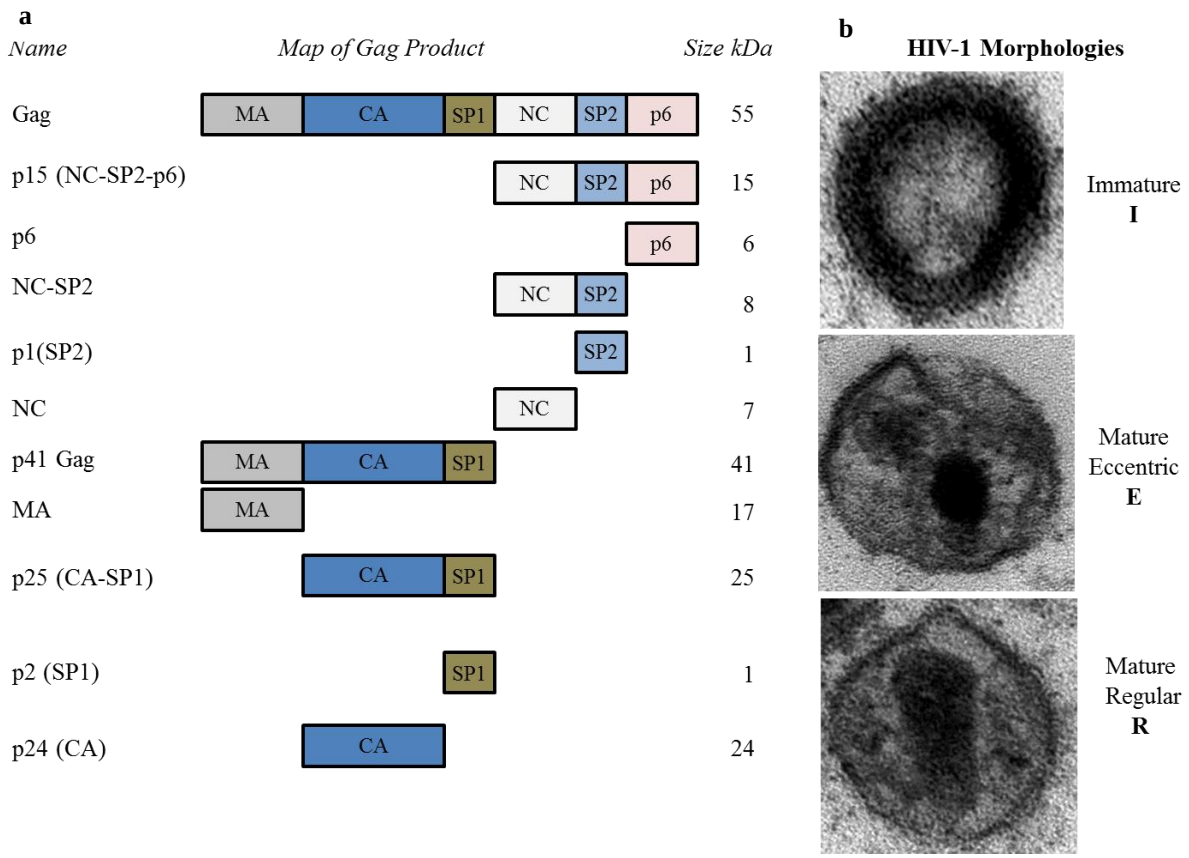

References: [45, 75, 116, 119]

During sequential processing virus morphology can be seen in various correlating stages (**Figures 3, 5**). Included in these stages are immature (**I**), mature eccentric (**E**), and mature regular (**R**). These maturation stages of the virus life cycle correspond with the ratios of *GagPol* products in the cells. For instance, if nearly 100% of the Gag in the

virus is the 55 kDa version of Gag the virus like particle (VLP) tends to be **I** morphology. As the concentration of the 25 kDa CA-SP1 is elevated, the **E** morphology is apparent. The **E** morphology predominates in the CA5 HIV-1 mutant that is defective at cleaving CA-SP1 into the products CA and SP1. When processing yields about 1,000 to 1,500 copies of the 24 kDa protein CA, the virus takes on the **R** morphology. The virus maturation is essential for the virus infect a nascent cell. In fact, even partial inhibition of Gag maturation results in noninfectious virus particles (**Chapter 3**).

Processed Gag and GagProPol are present in the cell (see **Chapter 3: Figures 5a, 6a, 7a**). This is evident by a number of Gag products in the whole cell lysates as witnessed by western blot. Additionally, Jean-Luc Darlix's lab published a remarkable gel that shows processed Gag and RNA are present in late endosomes, lysosome, and small vesicles [120]. Darlix also showed that zinc finger NC mutants cause the genomic HIV-1 RNA to dissociate from the intracellular compartments, while removal of NC caused processed Gag to accumulate in small vesicles and as soluble aggregates [120]. The role of processed Gag and GagProPol in cells is currently unclear.

Many of the Gag products are not well characterized, but have been reported by numerous studies. However, the predominant *Gagpol* gene product in the cell lysates is the 55 kD protein Gag. Gag itself has been shown capable of producing VLPs for many retroviruses. When Gag is expressed from a vector, it can produce high yields of immature VLPS, but since PR is absent, the VLPs never become mature. In **Chapter 3** of this thesis, there are data indicating a *GagPol* expressing cell line can also produce mature HIV-1 particles. Gag expressing cell lines produce lentiviral particles [121], and

HTLV-1 Gag can also form immature virus particles [122]. Gag products are also modified, and form interactions with host proteins. It is possible that Gag products get processed while the virus is budding and get endocytosed into the cell. If the virus is tethered to the cell via a Tetherin interaction, the delayed release may be enough time that the cell endocytosises the particle resulting in processed Gag inside the cell lysates. However, many of the intermediate Gag processing products are poorly defined in the literature.

Virus morphology has been investigated using electron microscopy and electron cryotomography. **Figure 3**, and data in **Chapter 3** and **Appendix B** use transmission electron microscopy (TEM) to study compound effects on virus morphology. The major difference between TEM and cryotomography is that with cryotomography the cell/virus samples are flash frozen in liquid nitrogen, while with TEM, the samples are embedded into a paraffin material and sectioned with a diamond knife into about 100 nM thickness. Both methods use an electron microscope for observation of the samples. In cryotomography, the sample remains frozen during microscopy, while typical TEM does not require freezing. Cryotomography gives much higher resolution images then TEM, due to better "intactness" of the sample.

Much of the generated data have been compiled into 3D reconstruction models from cryotomography data to determine the structures of the **I** [123] and **R** [124] virus morphologies. Very little is understood about intermediate virus morphologies like **E**. It should be noted that when the CA protein is free in the virus, the CA protein then oligermizes inside of the virus forming a viral core. Encapsidated inside the CA core are

the gRNA (coated with NC), RT, IN, and other proteins. Current technologies have limited the ability to investigate all the enzymatic reactions inside of the virus particle. However, the virus particle is very active during the maturation process inferring that the virus is more "alive" than assumed. Hopefully, with advances in technology, someday we will be able to visualize the viral maturation process.

The immature HIV-1 particle (**I**) is characterized by a membrane with an electron density caused by the 55 kDa Gag protein. The 55kDa Gag forms a hexameric lattice giving the curvature of the viral particle [76]. The core of the **I** particle is translucent until maturation begins. After maturation, the order of the viral proteins reorganizes [125] and forms an electron dense core. In general, the **I** particle looks like ring shape and can be visualized in **Figures 3** and **5**. The initiation of viral maturation is not fully characterized. However, recent data indicate that temperature, salt concentration, and pH changes can influence core formation [126]. For the **I** virus morphology to become **R**, the Gag and GagProPol proteins need to be cleaved by PR during viral maturation.

The cleavage rates of the Gag are important during maturation. There are five major cleavage sites in Gag with variable cleavage rates. Substitutions in the P1 position (N-terminus side of cleavage site) of MA/CA, CA/SP1, NC/SP2 can enhance the rate of cleavage greater than 60-fold, while the wild-type amino acid sequences at SP1/NC and SP2/p6 cleavage sites had optimal cleavage rate. Additionally, the size of the P1' amino acid (C-terminus of cleavage site) can influence the rate of cleavage and P1'-P1 regulate in *trans* the rate of cleavage [116]. Disruption of optimal Gag cleavage rates can cause errors in cleavage products.

As determined by a series of papers, published by Steve Pettit, Andrew Kaplan, and Ronald Swanstrom, the sequential cleavages of GagProPol and Gag are summarized in **Figure 4** and **5**. There are factors that influence the Gag cleavage rates, but they are not fully defined. Alteration of the proline at position 7 of SP1 suppresses viral infectivity in a strain dependent manner [127], while wild-type SP1 regulates the rate of cleavage at the CA-SP1 processing site. Deletion of SP1 resulted in less infectious virions. Lower pH selectively accelerates cleavage at CA-SP1 [128]. The appearance of free SP1 in viral particles regulates the cleavage of CA-SP1 in a feedback regulation process. A recent finding, by Eric Freed's lab, concludes CA-SP1 is a dominant inhibitor of HIV-1 replication [129]. Furthermore, the data in **Chapter 3**, indicates that CA-SP1 is an effective target for inhibiting HIV-1 replication with triterpene compounds.

The Gag precursor contains a specific HIV-1 protease cleavage site between the 7 kDa the SP2 proteins [130]. The SP2 region of HIV-1 Gag contains the frameshift stem-loop, GagProPol transframe and a protease cleavage site that are crucial for viral assembly, replication and infectivity [131]. Polymorphisms in SP2-p6/p6* of HIV type 1 can delay protease autoprocessing and increase drug susceptibility [132]. Also, polymorphisms in the NC-SP2 and SP2-p6 cleavage sites have can cause resistance to protease inhibitors [133]. Additionally, the 15, 9, and 7 kDa NC and NC-SP2 intermediates regulate the RNA during maturation [82]. Furthermore, the processing of the NC-SP2 site is dispensable for infectivity, while cleavage of SP2-p6 site is required for efficient integration by the infecting virus [134]. Also, Gag cleavage sites can coevolve with PR mutations. The AP2V mutation at the NC-SP2 cleavage site coevolved

with the V82A PR mutation which causes resistance to indinavir or ritonavir [135]. Also compensatory mutations were found at the HIV cleavage sites NC-SP2 and SP2-p6 in therapy-naive and therapy-experienced patients [136]. Lastly, it is noted that Gag processing intermediates interfere with replication [137] making them interesting therapeutic targets. After Gag and GagProPol cleavages, the virus becomes mature.

There are quite a few studies that have investigated the structures of mature (**R**) HIV-1. One cryoelectron microscopy study concludes that core growth inside of the virus develops from the narrow end towards the wider end of the core [138]. Also during maturation, the virus diameter remains unchanged at about 145 nm [139]. The core assembles due to CA:CA interactions and multimerization that can be disrupted with the CA binding peptide CAI [77]. Studies have also shown that CA mutants do not always form the typical conical core, rather they can form cylinders or spheres [140]. Other data says the CA is phosphorylated 3 times and electrostatic repulsions between HIV-1 capsid proteins modulates hexamer plasticity and in vitro assembly [141]. However, a recent model of the mature regular (**R**) viral core indicates the core is composed of 12 CA pentamers and ~250 CA hexamers; 5 pentamers at one end and 7 pentamers at other end of fullerene cone model, CAP-1 inhibits capsid assembly [142]. This model fits well with previous reports that roughly 1,500 CA are present in the mature HIV-1 core [117]. Also, the CA assembly inhibitor CAP-1 blocks proper core formation [142]. In all, the mature viral core forms a conical core after proteolytic processing of the Gag and GagProPol proteins. The maturation process is required for production of an infectious HIV-1 particle.

GagPol as a Retroviral Drug Target

Since *GagPol* is the most essential gene in a retrovirus, it is not surprising that 23 of the 25 United States Food and Drug Administration (FDA) approved anti-HIV-1 drugs target *GagPol* gene products [143]. The only two FDA approved compounds that do not target *GagPol* gene products are the fusion inhibitor enfuvirtide and the CCR5 co-receptor inhibitor maraviroc [143]. The remaining 23 FDA approved compounds inhibit the enzymatic *GagPol* gene products PR, RT, and IN.

There are numerous compounds, currently in development, targeting *GagPol* gene products and the late phase of HIV-1 replication. The novel compound BIT225 inhibits the release of HIV-1 from human macrophages [144]. 14 carbon fatty acids targeting Gag myristoylation inhibit viral budding [70]. The compound CAP-1 inhibits CA:CA interactions [78, 145]. Also, CA assembly can be inhibited by 1,5-dihydrobenzo[1,4]diazepine-2,4-dione compounds [146]. Metallacarboranes [147] and diamide can inhibit PR [148] as well. Peptides can inhibit HIV-1 assembly [149, 150]. Also, cyclic peptides targetting the Gag interaction with TSG101 can inhibit viral replication [151]. In all, there are many therapeutic strategies in development as anti-HIV-1 inhibitors.

Antiviral therapies can be expensive to develop and produce. To make the development of antiviral therapies cheaper, it would be ideal to have a less expensive source of the compound. Fortunately, the Birch tree, *Betula papryrifera*, an excellent source of triterpene compounds, is found all over the northern hemisphere. Triterpenes are compounds that polymerize in the bark of plants as serves as protective barriers

against pathogens for plants. The triterpene compound betulinic acid has approximately 30 carbons in an aromatic structure (**Chapter 2**). Triterpenes have shown to have many therapeutic uses. Compounds that inhibit HIV-1 replication that are derived from natural products could make antiviral therapy less expensive.

This thesis will focus on compounds derived from Birch trees. The bark of the Birch tree has suberin and triterpene compounds that function in plant defenses. This thesis investigates the use of derivatives of triterpene (**Chapters 2** and **3**) and fatty acid (**Appendix B**) derivatives (like suberin). Triterpenes can inhibit early [152] and late phase HIV-1 replication [4]. Thus, we screened over 1000 triterpene derivatives for anti-HIV-1 activity (**Chapter 2**), and discovered many that inhibited late phase replication.

As a control, the thesis uses Bevirimat as a reference compound. Bevirimat (BVM) inhibits core condensation and CA-SP1 processing [153]. Mutations that cause BVM resistance map to the CA-SP1 cleavage site [154] [155] as the sequence of CA-SP1 plays role in differential sensitivity to BVM in HIV-1 and SIV [156]. There are a variety of mutations at CA-SP1 cause BVM resistance, but the SP1-A1V mutation is most common [157] . Also, BVM associates with Gag in a 1:1 ratio [158] indicating that BVM associates with Gag. A recent paper indicates BVM stabilizes the immature (**I** morphology) lattice in HIV-1 [159]. Bevirimat and other triterpene derivatives are promising anti-HIV-1 agents. BVM will be further discussed in **Chapters 2** and **3**.

In conclusion, the late phase of HIV-1 replication has numerous drug targets including: gene expression, Gag and GagProPol trafficking in cells, virus budding, release, and maturation.

This thesis will investigate the development of natural products as anti-HIV-1 agents. Particularly, the goal of this research was to discover novel anti-HIV-1 compounds and to identify the molecular target of viral inhibition. To do accomplish this goal, compounds were derived from birch trees by Dr. Pavel Krasutsky's lab at University of Minnesota Duluth Natural Resource Research Institute and screened for anti-HIV-1 activity by Casey Dorr at University of Minnesota Institute for Molecular Virology in Dr. Louis Mansky's lab. Following identification of novel anti-viral compounds (**Chapter 2, Appendix B**), biological assays were performed (**Chapter 3, Appendix A**) to identify molecular target of viral inhibition.

Chapter 2

Triterpene Derivatives that Inhibit Human Immunodeficiency Virus Type 1 Replication

Casey Dorr[a], Sergiy Yemets[b], Oksana Kolomitsyna[b], Pavel Krasutsky[b] and Louis M. Mansky[a]

[a]*University of Minnesota, Institute for Molecular Virology; 18-242 Moos Tower, 525 Delaware St. SE, Minneapolis, MN 55455;*

[b]*University of Minnesota, Natural Resource Research Institute, 5013 Miller Trunk Highway, Duluth, MN 55811*

Figure 1: Graphical Abstract

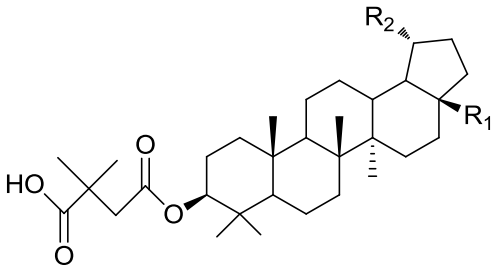

R_1 = CN, R_2 = $CH_3C{=}CH_2$ (**7**);
R_1 = HCO, R_2 = $HC(CH_3)_2$ (**18**);
R_1 = HCO, R_2 = $CH_3C{=}CH_2$ (**19**)

Newly synthesized triterpene derivatives were tested for anti-HIV-1 activity and cellular toxicity. Compounds **7**, **18** and **19** manifested highest activity and therapeutic index, which are comparable with bevirimat. These derivatives inhibit a late step in virus replication, likely virus maturation.

Human immunodeficiency virus type 1 (HIV-1), the etiologic agent of AIDS, remains a serious global public health problem. Highly active antiretroviral therapy (HAART) prevents viral replication and the development of AIDS. Though HIV-1 infection can be inhibited, antiretroviral drug resistance and off-target effects require the continual development of novel antiretroviral agents to combat HIV-1 infection for inclusion into HAART regimens.

Figure 2: Structure of Bevirimat

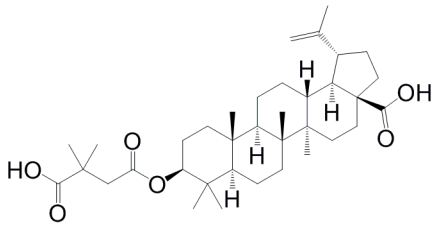

Fifteen of the 25 anti-HIV-1 drugs approved by the United States Food and Drug Administration (FDA) inhibit early steps in the HIV-1 life cycle. Specifically, these drugs target either viral entry, co-receptor recognition, fusion, reverse transcription, or integration [160]. The 10 approved anti-HIV-1 drugs that inhibit late steps in the HIV-1 life cycle all target the viral protease [160]. There are numerous late steps in the HIV-1 life cycle that could be potential drug targets. Examples of such targets include viral RNA transcription, protein translation, virus particle assembly, release, or maturation. Maturation of HIV-1 particles occurs primarily after virus release from infected cells. Maturation is a process that is targeted by the triterpene Bevirimat (3-*O*-(3'3'-dimethylsuccinyl) betulinic acid, PA-457, DSB) [153, 154, 156, 158, 161-166]. Bevirimat (**Figure 2**) inhibits HIV-1 maturation by preventing the cleavage of CA-SP1 (p25) Gag into Capsid (p24) and SP1 (p2) [153, 154, 156, 158, 161-166]. Bevirimat, in the absence of the viral protease, has also been shown to inhibit virus assembly.[167, 168] Drug resistance studies have revealed many resistance-bearing mutations at the carboxy-terminus of capsid and in the SP1 spacer peptide [156, 163, 166, 169, 170]. Bevirimat has been shown to inhibit HIV-1 replication in cell culture [153, 156, 161-166, 171] and has shown promise in clinical trials [172, 173], but has not been approved as a drug for the treatment of HIV-1 infection. The goal of this study was to identify other

triterpenes that could inhibit HIV-1 replication and would be useful for better understanding the mechanism of action and the structure-activity relationship. Such information would clearly be useful in the design of new derivatives that have potential for clinical translation.

Triterpenes have great potential for drug development [174]. Triterpenes can be extracted from natural sources and are abundant in *Betula paperifera* (North American Birch tree) [174]. Betulin was extracted and purified from Birch bark of *Betula paperifera* in accordance with a previously developed procedure [175]. Other precursors – betulinic aldehyde and betulinic acid - were synthesized from betulin by the method of electrochemical oxidation [176]. Further triterpene modifications were provided in accordance with newly developed **Schemes 1, 2 and 3.** All synthesized derivatives were characterized by ^{1}H and ^{13}C NMR and HRMS.

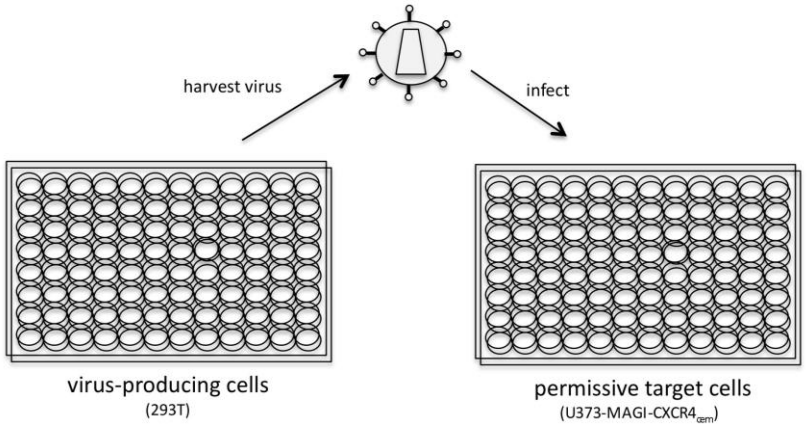

Figure 3: Assay for Antiretroviral Activity of Triterpene Derivatives

HIV-1 vector was cotransfected with a HIV-1 envelope expression plasmid into 293T cells in a 96-well tissue culture plate. Forty-eight hours post-trasfection, cell culture supernatants were harvested from the virus-producing cells and used to infect permissive target cells (i.e., U373-MAGI-CXCR4$_{cem}$ cells). Infected cells were harvested 48 hours postinfection and analyzed by flow cytometry. To test triterpene derivatives for antiretroviral activity, virus-producing cells (prior to harvesting virus) or permissive target cells after virus infection were exposed individually with each derivative at a range of concentrations (i.e., 5 nM to 50 μM).

The triterpene derivatives were screened for anti-HIV-1 activity using a single-cycle HIV-1 replication assay. This assay is particularly useful because it can differentiate whether a derivative targets the late or early steps in the viral life cycle (**Figure 3**). In the assay, 293T cells were transfected [97, 177] with the HIV-1 vector pHIG [177], which encodes for the green fluorescence protein (GFP), and a HIV-1 envelope vector, pIIINL4 Env [178]. The cell culture supernatant from the virus-producing cells was harvested, cellular debris removed, and used to infect HIV-1 permissive U373-MAGI- $CXCR4_{cem}$ target cells [179]. Permissive cells were all treated with the equivalent volume of compound treated virus containing supernatant as the no drug treatment control. The no drug treatment control virus had a multiplicity of infection (MOI) of 0.05. The low MOI reduces the possibility of multiple infections in individual target cells. Infected cells were monitored for GFP expression 48 h post infection by flow cytometry. GFP expression allowed for the monitoring of HIV-1 infection, and a reduction in the percentage of GFP-expressing target cells was indicative of a reduction in virus infectivity due to the antiretroviral activity of a triterpene derivative. To determine whether the triterpene derivatives could inhibit HIV-1 replication, virus-producing or permissive target cells were exposed to triterpene derivatives in a concentration range from 5 nM to 50 μM. The EC_{50} values were determined using Graph Pad Prism 5 statistical software.

Scheme 1: Synthesis of Anti-HIV-1 Triterpenes 4 and 7

(i) CF_3COOH, $CHCl_3$; (ii) KOH, EtOH; (iii) DMSA, DMAP, Py; (iv) $(CF_3CO)_2O$, $CHCl_3$; (v) KOH, MeOH

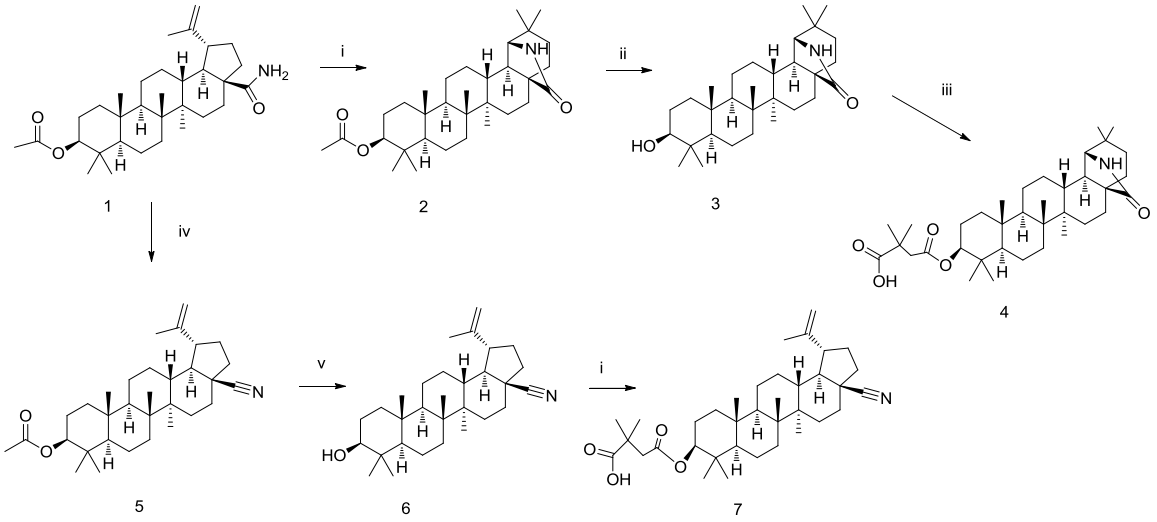

Scheme 2: Synthesis of Anti-HIV-1 Triterpenes 9 and 15

(i) DMSA, DMAP, Py; (ii) KOH, *t*-BuOH; (iii) $(CH_3O)_2SO_2$, K_2CO_3, DMF; (iv) $(CH_3CO)_2O$, Py; (v) $POCl_3$, Py; (vi) 1) KOH, *t*-BuOH; 2) HCl, H_2O

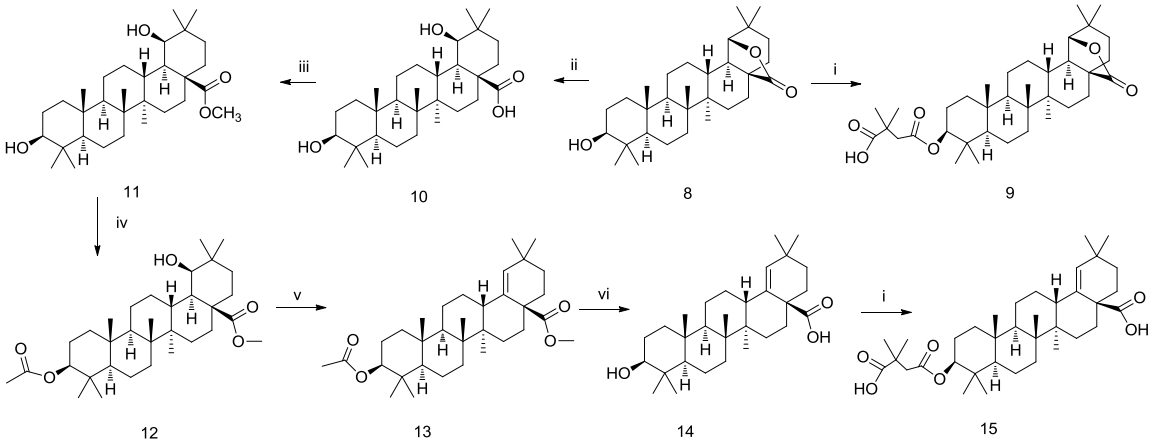

When permissive target cells were treated with the triterpene derivatives, none of the derivatives inhibited HIV-1 replication – testing up to concentrations of 50 μM. When treating virus-producing cells, bevirimat, 3-*O*-(3'3'-dimethylsuccinyl) betulinic acid inhibited HIV-1 replication with an EC_{50} value of 0.29 μM. The betulinic aldehyde derivatives (**18-21**) had EC_{50} values of 1.8 μM, 1.2 μM, 1.5 μM, and 1.4 μM, respectively. The betulinic nitrile derivative (**7**) had a similar EC_{50} value of 1.5 μM.

Scheme 3: Synthesis of Anti-HIV-1 Triterpenes 18, 19, 20, and 21
(i) H_2, Pd/C, THF/MeOH (ii) DMSA, DMAP, Py; (iii) *N*-methyl-D-glucamine, MeOH

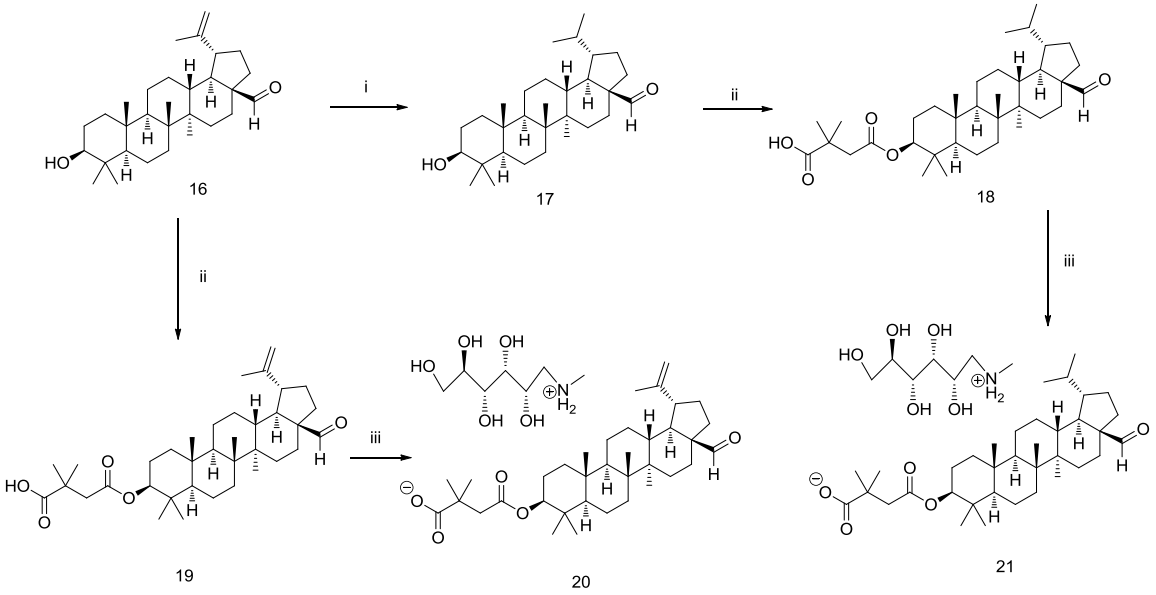

Derivatives (**4**) and (**9**) had EC_{50} values of 15 and 14 μM, respectively, which was ~10-fold less potent than the betulinic aldehyde or betulinic nitrile derivatives. Interestingly, derivative **15** was about 130 times less active than bevirimat, with an EC_{50} of 39 μM. Potential cell toxicity was assayed using a commercially available kit (CellTiter Non-Radioactive Cell Proliferation Assay, Promega) following the manufacturer's instructions (**Table 1**). Briefly, cells were treated with serial dilutions of each individual triterpene derivative and IC_{50} values were determined. If cell proliferation was not inhibited by at least 50% at the highest concentration tested, the estimated IC_{50} was reported as > the highest concentration tested in the assay. Bevirimat, the betulinic nitrile derivative (**7**), the betulinc aldehyde derivatives (**18**, **19**, and **21**), and the morolic acid derivative **15** had the lowest cellular toxicity values: IC_{50} >300 μM. The betulinic aldehyde derivative had an IC_{50} value of 29 μM. Derivatives **4** and **9** were less soluble than the other derivatives

analyzed in the study, and had minimal toxicity. The triterpene derivatives **4** and **9** were found to have IC_{50} values of >130 μM and >150 μM, respectively.

A therapeutic index (TI) value (i.e., TI = IC_{50}/EC_{50}) was determined for each of the triterpene derivatives. Bevirimat had a TI of >1000. The betulinic aldehydes (**18**, **19**, and **21)** and the betulinic nitrile derivative (**7)** had TI values of >160, >250, >210 and >200 respectively. The betulinic aldehyde derivative **20** had a TI of 19. Derivatives **4** and **9**, which were less soluble, had TI values of >10 and > 9.2, respectively. Finally, the dimethyl succinate derivative of morolic acid, **15,** had a TI value of >7.6.

Table 1: Antiretroviral Activity, Cell Toxicity, and Therapeutic Indices for Triterpene Derivatives

Triterpene derivative	Antiretroviral activity (treatment of virus-producing cells) EC_{50}, μM[a]	Antiretroviral activity (treatment of permissive-target cells) EC_{50}, μM[b]	Cell toxicity IC_{50}, μM[b]	Therapeutic index[c]
Bevirimat	0.28 (±0.09)	>50	>300	>1000
4	15 (±2.5)	>50	>150	>10
7	1.5 (±0.4)	>50	>300	>200
9	14 (±2.7)	>50	>130	>9.2
15	39 (±10)	>50	>300	>7.6
18	1.8 (±0.5)	>50	>300	>160
19	1.2 (±0.3)	>50	>300	>250
20	1.5 (±0.5)	>50	29	19
21	1.4 (±0.4)	>50	>300	>210

[a] Mean of four experiments, standard deviation is given in parentheses.
[b] Mean of three experiments.
[c] Therapeutic index = IC_{50} cytotoxicity/EC_{50} antiretroviral activity.

The 3,3-dimethylsuccinate functional group was common to all nine triterpene derivatives listed in **Table 1**. The difference in anti-HIV-1 activity between **15** and bevirimat suggests that the morolic acid scaffold is less active at inhibiting HIV-1

replication than the betulinic acid scaffold. In addition, the dimethylsuccinate group in the C-3 position of the derivatives may be important for antiretroviral activity. Furthermore, the C-28 position or the triterpene can be variable, having either a carboxylic acid (bevirimat), aldehyde (**18, 19, 20,** and **21**) or nitrile (**7**) group and still maintaining antiretroviral activity. Finally, dimethylsuccinates of 3β-hydroxyoleananes (**4**, **9**) or morolic acid (**15**) have antiretroviral activity. These observations provide useful information for further investigation of the structure-activity relationship.

In this study, several triterpene derivatives have been characterized to have anti-HIV-1 activity, using a novel single-cycle replication assay. These derivatives should be useful for better understanding the mechanism of action of bevirimat and the general structure-activity relationship. Though it is possible the compounds could inhibit virus release or the viral protease, it is most likely, due to structural similarity with bevirimat, that the compounds in **Table 1** inhibit HIV-1 replication by blocking CA-SP1 processing. It should be noted that the derivatives of 3-*O*-(3'3'-dimethylsuccinyl) betulinic aldehyde (**18**, **19**, **20**, and **21**) or 3-*O*-(3'3'-dimethylsuccinyl) betulinic nitrile (**7**) may be metabolized by aldolases or nitrolases and therefore represent prodrugs for bevirimat. In general, the derivatives analyzed in this study have the desirable and practical feature that they can be produced in high quantities and at low cost from Birch bark. In summary, the information from this study should be useful in the design of new derivatives that have potential for clinical translation.

Chapter 3

Anti-retroviral Triterpenes Target CA-SP1 and Inhibit Production of Infectious HIV-1

SY33 (compound 7 in **Chapter 2**) is a triterpene derived from the outer bark of Birch trees that potently inhibits the late phase of HIV-1 replication [4]. Triterpenes are compounds native to many plants and suspected to function as an innate defense against invading pathogens [174]. This study investigates the mechanism of anti-HIV-1 activity of a collection of triterpenes [4] while using a triterpene in clinical trials, bevirimat (BVM), as a control.

Bevirimat, 3-*O*-(3',3'-dimethylsuccinyl)betulinic acid is a triterpene with anti-HIV-1 activity [171] in clinical trials as an HIV-1 therapy. Bevirimat is also known as BVM, DSB [168], PA-457 [161], and YK-FH312 [180]. BVM inhibits HIV-1 maturation by preventing the cleavage of the CA-SP1 Gag product by HIV-1's Protease (PR) to CA and SP1 during HIV-1 maturation [153, 156, 158, 161, 163]. Inhibiting the CA-SP1 cleavage by BVM causes the virus to form a mature eccentric (**E**) core, much like the HIV-1 core seen in the CA-SP1 cleavage defective mutant CA-5 [129, 161]. The mature eccentric core, compared to immature (**I**) and mature regular (**R**), can be seen in **Figure 1** and correlates to the presence of accumulated CA-SP1 in HIV-1 particles. Thus, BVM, is known as the first compound known as an HIV-1 maturation inhibitor.

Maturation is a viable target during the production of retroviruses. Currently, anti-HIV-1 therapies like the protease inhibitor have been successful at blocking viral

replication, until resistance mutations arise in the protease (PR) gene [181]. Nelfinavir, a PR inhibitor, acts by blocking PR's enzymatic activity in HIV-1 [181, 182]. PR predominantly functions by cleaving the Gag and GagProPol proteins into smaller protein products after the virus has budding from the host cell. The 55 kDa Gag and 160 kDa GagProPol proteins are expressed from the *GagPol* mRNA in a 20:1 ratio regulated by ribosomal frameshifting during translation [50]. Gag is cleaved into the protein products, matrix (MA), capsid (CA), spacer protein 1 (SP1), nucleocapsid (NC), spacer protein 2 (SP2), and the p6 (**Figure 1**). GagProPol is primarily cleaved to the same products as Gag, with the addition of the transframe protein (p6*), and the essential viral enzymes PR, Reverse Transcriptase (RT), and Integrase (IN). Gag multimerizes and assembles into virus like particles (VLPs) that are released from the cell. Upon proteolytic cleavage of Gag, the virus undergoes maturation that correlates with the Gag cleavage process (**Figure 1**). For instance, if 55 kDa Gag is predominant in virus, the virus is likely immature (**I**); if CA-SP1 is in abundance, the virus is mature eccentric (**E**); and if CA is in high concentration, the virus forms mature regular (**R**) morphology. BVM is different than a PR inhibitor, because BVM seems to directly interact with the Gag substrate [158] rather than the PR enzyme. Numerous data have indicated that BVM specifically interacts with the CA-SP1 cleavage site inhibiting viral maturation [153, 156, 158, 161].

HIV-1 mutations can cause resistance to all known anti-viral strategies. Mutations that confer resistance to BVM localize to the CA-SP1 cleavage site in HIV-1 Gag [154-156, 163, 183]. Additionally, BVM is less effective against HIV-2 and many natural HIV-1 isolates are BVM resistant [148, 157, 184]. The most common occurring

Figure 1: HIV-1 Gag Processing and Bevirimat Resistance

a) Map of HIV-1 Gag. Gag domains from N terminus to C-Terminus: MA = Matrix, CA = Capsid, SP1 = Spacer Protein 1, NC = Nucleocapsid, SP2 = Spacer Protein 2, p6 = p6 late domain. The 55 kDa Gag protein is sequentially cleaved by the viral protease at specific sites between the domains. The last cleavage is cutting the 25 kDa CA-SP1 product into the 24 kDa CA and the 1 kDa SP1. The maturation inhibitor Bevirimat specifically inhibits the cleavage of CA-SP1. Alternatively, protease inhibitors, like Nelfinavir, target the viral protease and inhibit Gag processing very early, resulting in accumulation of large Gag products. An alanine to valine mutation in the first amino acid, at the N-terminus, of SP1 (SP1-A1V) decreases susceptibility to Bevirimat. **b**) Transmission electron microscopy of HIV-1 morphologies. 293 cells that stably express HIV-1 *GagPol* and *Rev* were analyzed by electron microscopy. The Immature (**I**) morphology correlates with minimal Gag cleaveages in the virus particle. The Mature Eccentric (**E**) morphology is an intermediate step during viral maturation. The **E** morphology can be characterized by a condensed viral core that is often not centered in the virus. The **E** morphology correlates to intermediate levels of Gag processing. The Mature Regular (**R**) morphology for HIV-1 has a conical core and correlates to full Gag processing. Gag processing is essential for HIV-1 to infect a new cell. If Gag processing is suppressed, like with a maturation or protease inhibitor, viral replication is inhibited.

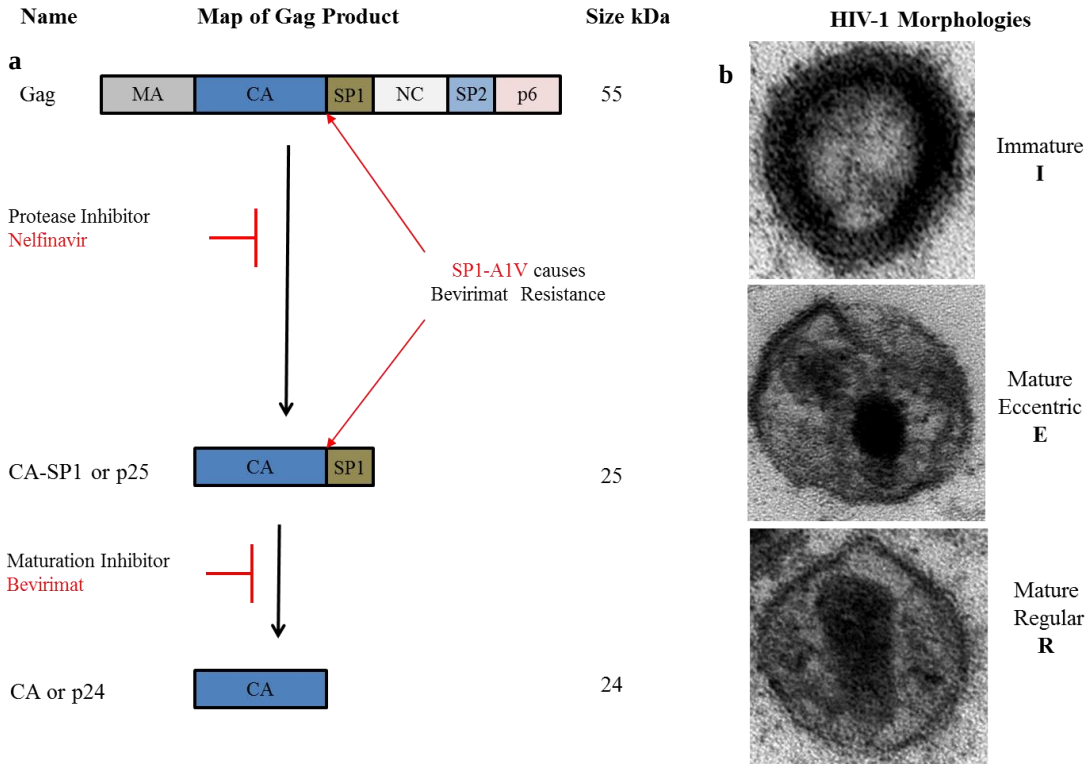

BVM resistance mutation is an alanine to valine mutation in the SP1 gene causing the genotype SP1-A1V [153-155, 161, 163]. CA-SP1 is still a good anti-HIV-1 target since BVM and other compounds that target CA-SP1 are quite potent at inhibiting HIV-1 replication. Antiviral potency can be described using the value EC_{50}. The EC_{50} is the

concentration of compound that inhibits viral replication by 50%. The EC_{50} for BVM has varied in the literature ranging from the nanomolar (nM) to micromolar (μM) concentrations depending on the assay. In single-cycle replication assay, treating only the virus producing cells BVM's EC_{50} is 280 nM [4], 0.35 nM in a spreading infection assay in H9 cells and IIIB HIV-1 [185], 7.8 nM in a spreading infection assay [161], and 10 μM at inhibiting CA-SP1 cleavage [164] and 8-10 μM at inhibiting Gag assembly in insect cells [168]. Though EC_{50} values vary in cell culture assays, BVM is proven to control HIV-1 replication in patients [172] until resistance occurs. Since BVM targets CA-SP1, and is effective at controlling HIV-1 replication prior to resistance, much more information is necessary to further understand the structure-function relationship between HIV-1 maturation inhibitors and the CA-SP1 molecular target.

Since BVM's discovery, a few compounds have been shown to have anti-HIV-1 maturation activity [186, 187] but there has not been a detailed comparative study published that investigates effectiveness of multiple maturation inhibitors. This study will investigate the mechanism of action of 8 novel anti-HIV-1 compounds that were recently described [4] while using BVM as the reference compound. This study tests if the triterpene compounds in **Figure 2** target CA-SP1 processing in HIV-1. Further analysis will investigate the mechanism of action of the compound SY33 (2,2-Dimethyl-4-[(28-nitrilolup-20-en-3β-yl)oxy]-4-oxobutanoic acid). SY33's effect on CA-SP1 processing is investigated using 3 separate virus release assays. The BVM resistant mutant SP1-A1V will be investigated for sensitivity to SY33 by single round HIV-1 assay, in spreading HIV-1 infection cultures over time, and molecularly for CA-SP1

Figure 2: Antiretroviral Triterpenes that Inhibit CA-SP1 Processing in HIV-1

a) Triterpene compound that were identified to inhibit the late phase of HIV-1 replication. **b.**) Virus release assay data show the compounds inhibit CA-SP1 processing to CA and SP1. 293T cells were transfected with an HIV-1 vector and then treated with the vehicle (V) of 1% DMSO, 10 or 50 µM of each compound. The supernatants were ultracentrifuged to harvest virus like particles (VLPs). VLP lysates were then assayed by immunoblot using an anti-HIV-1 capsid antibody. Nelfinavir, an HIV-1 protease inhibitor, and Bevirimat, an HIV-1 maturation inhibitor, were used as controls. The EC_{50} (compound concentration to inhibit 50% viral replication) for each compound is listed below the immunoblot data.

a. Triterpene Structures

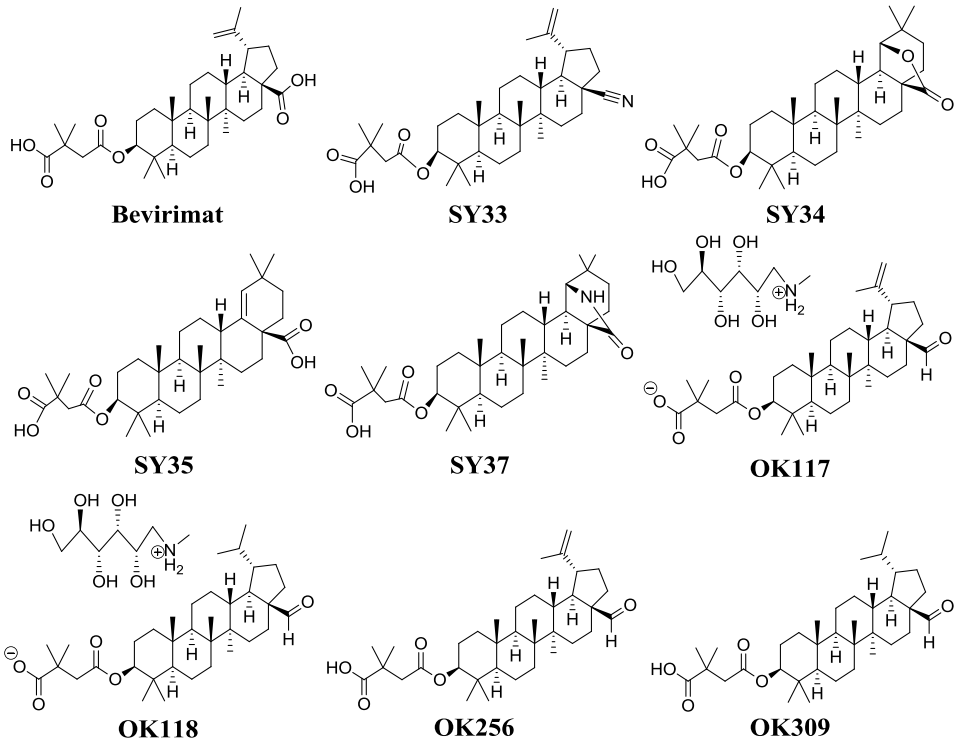

b. Antiretroviral Triterpenes Inhibit CA-SP1 to CA Processing in HIV-1

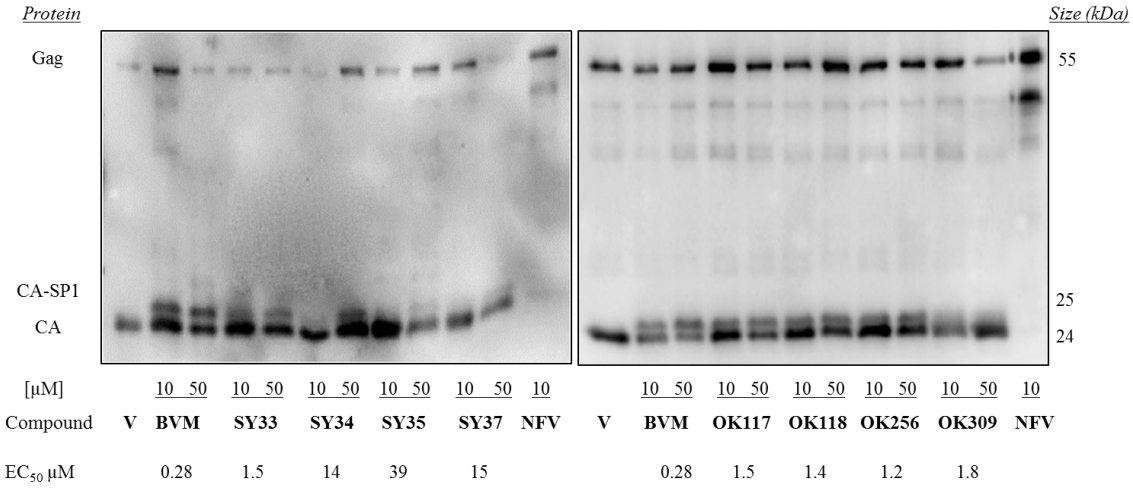

cleavage. There is currently no EC_{50} values published for BVM (or any other maturation inhibitor) against SP1-A1V. The only published information regarding BVM and SP1-A1V shows SP1-A1V resistance [154, 155, 161, 163], but does not determine EC_{50} value. This is the first study to look over broad compound concentration ranges of BVM (and SY33) against SP1-A1V which is then used to calculate EC_{50} values and therapeutic indices for BVM and SY33 against SP1-A1V. Lastly, SY33 will be investigated for its effect on HIV-1 morphology by TEM. Due to structural similarities between SY33 and BVM, it is hypothesized that SY33 will target CA-SP1 and function at inhibiting HIV-1 replication by a similar mechanism.

Results

Single-Round HIV-1 Replication Assay

BVM and SY33 inhibited wild-type HIV replication within the previously reported EC_{50} values of 0.28 µM or 1.5 µM, respectively [4] when treating only the production phase of the HIV-1 life cycle with compound. The noted difference is that the SP1-A1V mutant showed marked resistance to both BVM and SY33 (**Figure 3a, 3b, Table 1**). Particularly interesting is that at 5 µM BVM or SY33, the SP1-A1V virus replication appeared to increase (**Figure 3b**). This was also true for 25 µM, however, at 50 µM, SY33 inhibited SP1-A1V replication while at 50 µM BVM there was still greater than 100% replication. This indicates that at higher concentrations SY33 has slightly better potency than BVM at inhibiting the SP1-A1V mutant's replication. It is possible that SP1-A1V mutant has better fitness than wild-type HIV-1 in the presence of

moderately high BVM or SY33 concentrations. However, as the compound concentration is raised to 150 µM, both compounds inhibit the replication of the HIV-1 mutant SP1-A1V.

Figure 3: SY33 and Bevirimat Inhibit Wild-type HIV-1 and SP1-A1V Mutation Reduces Susceptibility to Both Compounds

Wild-type (**a**) or SP1-A1V (**b**) HIV-1 was produced by transfecting the respective HIV-1 molecular clone into 293T cells. 48 hours post-transfection, virus containing supernatants were harvested. The virus was titered by infecting CEM-GFP cells at increasing volumes of virus. Virus not used for titering was stored at -80^{o}c until further use. The CEM-GFP cells were analyzed by flow cytometry to determine % GFP^{+} CEM-GFP cells. Following viral titer, CEM-GFP cells were infected with either wild-type (**a**) or SP1-A1V (**b**) HIV-1 virus stocks at a multiplicity of infection (MOI) of 0.15. The CEM-GFP/HIV-1 cultures were then treated with 500 pM, 5 nM, 50 nM, 500 nM, 5 µM or 25 µM SY33 or Bevirimat. Each compound concentration was tested in triplicate. Compound treated cells were harvested and analyzed by flow cytometry. Note: this data is representative of a single experiment. It was repeated 4 times as stated in Table 1. **c**) Compound induced cell toxicity was assayed using the Promega non-radioactive cell proliferation assay with CEM-GFP cells. Toxicity data are normalized to the vehicle (1% DMSO) control. The toxicity data was repeated 3 times as stated in Table 1.

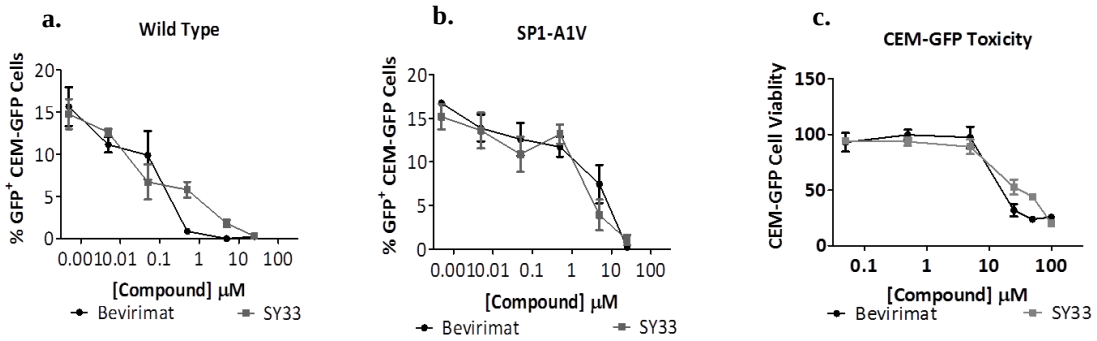

Spreading HIV-1 Infection Assay

Anti-HIV-1 activity caused by the compounds BVM or SY33 was evident in the spreading virus assay (**Figures 3a, 4, Table 1**). The wild-type virus was inhibited from replicating when treated with 25 µM of either compound for the entire 22 day experiment. The 25 µM concentration of SY33 or BVM was potent at completely inhibiting wild-type replication every time this experiment was performed. Likewise, 25

μM BVM or SY33 consistently inhibited replication of SP1-A1V replication in the spreading infection. Complete inhibition at 25 μM BVM or SY33 in the spreading infection assay is in-part due to modest toxicity in the CEM-GFP cell line. Antiviral differences were prominent at 5 μM compound concentrations, where wild-type replication potently was inhibited by BVM and SY33, while the SP1-A1V mutant replicated at 5 μM concentration of either compound. Resistance to BVM was most notable at 500 nM with the SP1-A1V mutant. At 500 nM, SP1-A1V replicated closely to that of the no drug (vehicle) treatment control. However, at 500 nM SY33 induced inhibition of SP1-A1V replication, but less potent than inhibiting wild-type HIV-1 with SY33. BVM at 50 nM was slightly more potent at inhibiting WT HIV-1 than SY33, while neither 50 nM BVM nor SY33 inhibited SP1-A1V replication. SY33 or BVM had minimal effect at inhibiting WT or SP1-A1V HIV-1 at concentrations of 5 nM and 500 pM. The infectivity data from Day 12, the day of detected peak replication, were used to calculate EC_{50} values for SY33 and BVM. SY33 inhibited 50% WT replication at 150 nM and at BVM 100 nM. Likewise, EC_{50} values were calculated for the SP1-A1V

Figure 4: SY33 and Bevirimat Inhibit Spreading HIV-1 Infection and SP1-A1V Causes Decreased Susceptibility to Both Compounds
a.) Vehicle (1% DMSO) treated. **b.**) SY33 treated Wild-type and SP1-A1V **c.**) BVM treated Wild-type and SP1-A1V

a. Vehicle

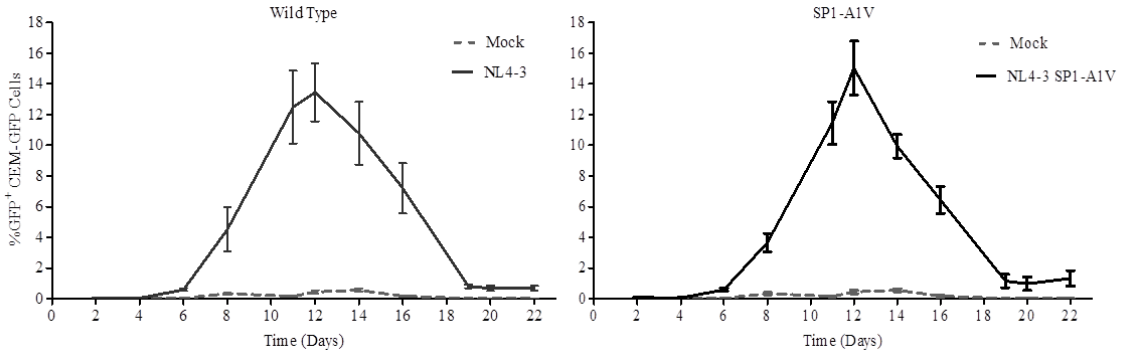

b . SY33

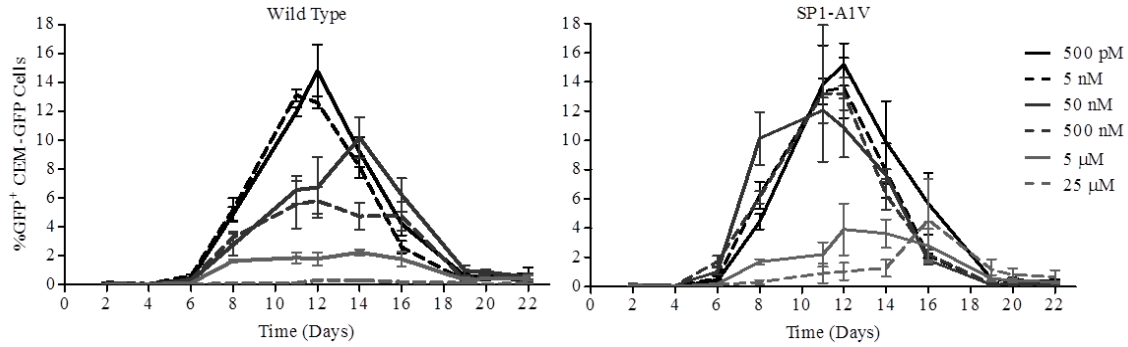

c. Bevirimat

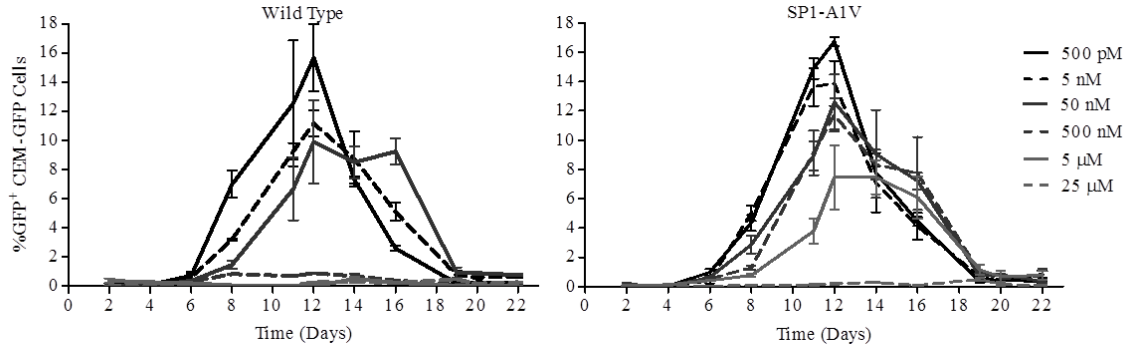

mutant of 2000 nM for SY33 and 2800 for BVM. Preliminary experiments with OK309, show that OK309 has similar potencies as SY33 in spreading infections at inhibiting wild-type and SP1-A1V (data not shown). As another control, Nelfinavir was tested for

anti-HIV-1 activity against the SP1-A1V mutant. As expected, Nelfinavir is potent at inhibiting the SP1-A1V mutant's replication with EC_{50} between 5 and 50 nM (data not shown). These data indicate that SY33 might be slightly better at inhibiting SP1-A1V, and BVM is better at inhibiting WT. However, SP1-A1V has resistance to both BVM and SY33.

Table 1: Therapeutic Indices using Replication Competent HIV-1 Assay

Compound	Genotype	EC_{50} (nM)[a]	IC_{50} (nM)[b]	Therapeutic Index[c]
SY33	WT	740 ± 300	46,000 ± 3,600	62
	SP1-A1V	13,000		3.5
Bevirimat	WT	230 ± 100	44,000 ± 10,000	190
	SP1-A1V	23,000		1.9

[a]EC_{50} = compound concentration for 50% antivirial activity; Mean and standard deviation from 4 independent experiments.
[b]IC_{50} = compound concentration for 50% cellular toxicity in CEM-GFP cells; Mean and standard deviation from 3 independent experiments.
[c]Therapeutic Index = IC_{50}/EC_{50}

Toxicity and Therapeutic Index

Toxicity data consistently show BVM to be slightly more toxic to the CEM-GFP cells than SY33 (**Table 1**). IC_{50} is the compound concentration to inhibit 50% cell viability. IC_{50} values in CEM-GFP human T-cells are 44,000 ± 10,000 µM for BVM and 46,000 ± 3,600 µM for SY33. However, for 293T human embryonic kidney cells, the IC_{50} values were both over 300 µM as previously reported [4]. The human H9 T-cell line had comparable sensitivity to BVM and SY33 as the CEM-GFP cells. Thus, the tested T-cell lines are more sensitive to compound toxicity than 293T cells.

Taken together, the toxicity data and the antiviral data indicate that SY33 is slightly less potent than BVM at inhibiting spreading HIV-1 infection for wild-type and possibly better than BVM at inhibiting SP1-A1V. SY33 has similar toxicity in T-cell lines as BVM. SY33 is slightly more potent at inhibiting SP1-A1V replication than BVM. However, using the single-cycle HIV-1 replication assay, SY33 and BVM are roughly the same potency at inhibiting SP1-A1V, and the SP1-A1V mutation might actually contribute to higher levels of viral replication (**Figure 5**). The effect on wild-type replication in the single-cycle assay shows BVM about 10 fold more potent than SY33 as reported [4].

Therapeutic indices were determined using the calculation T.I. = IC_{50} / EC_{50}. The therapeutic indices vary depending on the assay being used. For instance, in the single cycle assay, the IC_{50} for SY33 and BVM are both >300 μM. This high IC_{50} value leads to a high therapeutic index due to low toxicity in the 293T cell line. However, TI values are different in the spreading infection assay due to lower IC_{50} values. The CEM-GFP cells are more sensitive to compound-induced cellular toxicity than 293T cell. IC_{50} values in CEM-GFP cells are 44,000 μM for BVM or 46,000 μM for SY33. Additionally, the compounds are more potent in the spreading infection assay compared to the single cycle assay which also leads to differences in the therapeutic index of the compounds. As summarized in **Table 1**, the spreading infection assay indicates that BVM and SY33 have greater therapeutic value against wild-type HIV-1 than against the SP1-A1V mutant.

Virus Release Assays and Gag Processing

Virus release assays, and subsequent immunoblots indicate the compounds shown in **Figure 2a** cause the accumulation of CA-SP1 in HIV-1 particles **Figure 2b**. Two types of virus release assays were performed; M**ethod 1.** 293T cells were calcium phosphate transfected with the HIV-1 vector pHIG [4, 177, 188, 189] and treated with 10 or 50 µM BVM, OK117, OK118, OK256, OK309, SY33, SY34, SY35, or SY37, 10 µM NFV or DMSO (vehicle) in 10 ml cell culture volumes and VLPs were harvested by ultracentrifuge from a total volume of 20 ml per treatment group (**Figure 2b**); **Method 2.** 293T cells were polyethyleneimine (PEI) transfected with pHIG or pHIG SP1-A1V, then aliquoted into 1 mL cell cultures. These cultures were treated with 5 nM, 50 nM, 250 nM 500 nM, 5 µM, 25 µM, 50 µM, 75 µM, 110 µM, or 150 µM BVM or SY33 or with DMSO only control. The VLPs were harvested from the 1 mL cultures using a table top microcentrifuge (**Figure 5**). The VLPs from **Method 1** were used for immunoblotting. Experiments from **Method 2**, cell lysates and VLPs were collected and analyzed by immunoblotting. Furthermore, in **Method 2**, in parallel, single-cycle HIV-1 infectivity assays were performed to determine the correlation between infectivity and Gag processing caused by the compounds.

Using virus release assay **Method 1**, compounds OK117, OK118, OK256, OK309, SY33, SY34, SY35 and SY37 all demonstrated the ability to cause accumulation of CA-SP1 in VLPs in a concentration dependent manner (**Figure 2**). The betulinic aldehyde compounds OK117, OK118, OK256 and OK309 cause CA-SP1 to appear in the immunoblots at 10 µM and there is a visual increase in CA-SP1 product at 50 µM. It

should be noted that the CA-SP1 molecular phenotype does not directly correlate with the antiviral potencies of these compounds. As indicated in **Figure 2b**, at 10 μM of all the betulinic aldehyde compounds, the CA band is denser than CA-SP1 band in the immunoblot. However, the antiviral EC_{50} for these compounds using single-cycle assay with pHIG vector ranges between 1 and 2 μM [4] and as the compound concentration of the betulinic aldehydes reaches 50 μM, HIV-1 replication is virtually non-existent (data not shown), while at 50 μM, the CA (p24) gene product still seems more abundant that the CA-SP1 (p25) gene product. Thus, it seems that moderate accumulation of CA-SP1 in the VLPs is adequate to poison the HIV-1 particles from being infectious. Since CA-SP1 is also called p25 [190], this anti-HIV-1 effect can be coined "p25 particle poisoning". In general, the new term "particle poisoning" refers to interference with viral replication such that the viral particle is defective of infecting a normally permissive cell.

The non-betulinic aldehyde compounds described in this paper also indicate that CA-SP1 in minimal abundance is associated with defective HIV-1 replication. The compound SY33 is a betulinic nitrile compound that has similar potency to the betulinic aldehyde compounds with EC_{50} of 1.5 μM in single-round replication assay. SY33 treatment causes accumulation of CA-SP1 at 10 or 50 μM in virus release assay **1**, which leads to the observation that SY33 indeed targets CA-SP1 processing as a molecular mechanism of action. This also indicates that the C-28 position of the triterpene molecules can be variable with carboxylic acid [–COOH (BVM)], nitrile [-CN (SY33)], or aldehyde [-COH (OK117, OK118, OK256, OK309)] functional groups and still maintain the molecular target of CA-SP1. However, the carboxylic acid group in BVM

seems most potent at causing CA-SP1 accumulation in VLPs (**Figure 2**). It should be noted that carboxylic acid group is not enough to cause the CA-SP1 potency because SY35 has a carboxylic acid group in the C-28 position, but being a derivative of oleanic acid instead of betulinic acid (BVM) SY35 has a reduced anti-HIV-1 effectiveness (EC_{50} = 39 μM) [4] and ability to cause CA-SP1 accumulation in VLPs compared to BVM (**Figure 2**). Thus, these data indicate that the triterpene scaffold is significant and that the betulin structure is important since oleane structure decreases potency. Additionally, SY34 and SY37 show that the variability in the scaffold and polar anchor regions of the molecule influences the effectiveness of the compounds at inhibiting CA-SP1 processing. SY34 and SY37 are both derived from oleanic acid, but are more effective than SY35, however less effective than SY33. It should be noted that the dimethyl succinyl structure is found in all these compounds, and in virus release assay **Method 1**, CA-SP1 is evident in all treatment groups. Thus, dimethyl succinyl compound moiety might be important in targeting CA-SP1 region of Gag. These data support a conclusion that, though the C-28 functional group is variable, the dimethyl succinyl group and the betulin/oleane structures are important for causing CA-SP1 accumulation in HIV-1 particles.

SY33 was chosen for further analysis because it is structurally different than BVM by having C-28 nitrile instead of the carboxylic acid functional group of BVM. Also, SY33 has a good therapeutic index of >200 [4]. SY33 was tested side by side with BVM for effect on Gag processing against the BVM resistant mutant SP1-A1V and wild-type HIV-1. These experiments were tested over a broad range of concentrations and in smaller culture volumes compared to the release assay **Method 1**. The smaller

experiment format enabled more concentrations of compound to be tested per experiment due to differences in centrifuge rotors. The microcentrifuge can handle 24 cultures per spin, while the ultracentrifuge rotor can bear 12 cultures per spin. However, there is much less VLP harvested from the microcentrifuge **Method 2** than the ultracentrifuge **Method 1** due to smaller supernatant volume (20 ml in **Method 1** vs. 1 ml in **Method 2**). Also femto signal detection sensitivity was necessary for **Method 2** while pico sensitivity was adequate for the protein detection in **Method 1**. In all, SY33 was analyzed for influence on HIV-1 Gag processing by 2 different methods and against two genotypes.

In **Figure 5**, SY33 was tested in parallel with BVM using virus release assay **2**. **Figure 5** compares the compounds' molecular targets in the wild-type HIV-1 and the SP1-A1V mutant. When BVM treatment of wild-type HIV-1 reached the concentration of 0.5 µM, CA-SP1 was observed in the immunoblots. As BVM reached higher concentrations up to 150 µM, CA-SP1 accumulated in the VLPs (**Figure 5**). However, SY33 treatment by this method failed to show a large accumulation of CA-SP1 in the VLPs. The CA-SP1 band appears faintly in the immunoblots at 75 µM SY33 (**Figure 5**). However, wild-type VLPs treated with 110 or 150 µM SY33 show another molecular phenotype; the 55 kDa Gag is in high abundance. Interestingly, as SY33 seems to cause accumulation of the 55 kDa Gag product in wild-type VLPs, BVM seems to cause a slight decrease of 55 kDa Gag in WT VLPs at concentrations over 50 µM (**Figure 5**). Interestingly, at these high concentrations of BVM or SY33, there is virtually no HIV-1 replication, but the molecular phenotypes seem to be different. It seems that at high

concentrations, SY33 might influence the 55 kDa version of Gag to be present in VLPS, while BVM influences a 25 kDa version of Gag (CA-SP1) to accumulate in VLPs.

When analyzing SY33 and BVM for effect on Gag in VLPs from the SP1-A1V mutant (**Figure 5**), it was noticed that the CA-SP1 band was not evident in either treatment group, unless CA-SP1 is below the level of detection. Additionally, it was observed that SP1-A1V mutant less susceptibility to both SY33 and BVM in virus infectivity assays, indicating that CA-SP1 or SP1 is a molecular site of interaction with Gag for both SY33 and BVM. Interestingly, the accumulation of the 55 kD Gag product was less evident in the SY33 treated SP1-A1V particles than the wild-type particles. There is a possibility that the SP1-A1V mutation decreases interactions between Gag and SY33 or BVM. These molecular data indicate that SP1-A1V has less susceptibility to both BVM and SY33.

Further analysis of the Gag products in the cell lysates, reveals a particular phenomenon that was not expected. SY33 and BVM both appear to have a secondary mechanism of action by virus release assay **2 (Figures 5)**. Cell lysates, immunoblotted with anti-HIV-1 CA antibody indicate 55 kDa Gag accumulation in cell lysates at concentrations of $\geq$ 25 μM BVM or $\geq$ 50 μM SY33 (**Figure 5**). These data suggest that BVM and SY33 are able to cause Gag accumulation in cells. If so, these data are in agreement with reports from Pierre Boulanger's lab indicating high concentrations of BVM inhibits HIV-1 assembly [167, 168]. Interestingly, the accumulation of the 55 kDa Gag in cell lysates was observed in cells producing either wild-type or SP1-A1V HIV-1. Defective virus assembly, observed by full-length Gag accumulation in cells, could

explain why both wild-type and SP1-A1V HIV-1 replication at 75 µM and higher of BVM or SY33 is severely impaired. Thus, data from virus release assay **2** suggest SY33 and BVM have a primary molecular target of inhibiting CA-SP1 processing in VLPs and possibly a secondary molecular target of causing full-length Gag accumulation in cells.

Figure 5: **SP1-A1V Mutant Causes Decreased Susceptibility to Bevirimat or SY33. SY33 and Bevirimat Target CA-SP1, Inhibit Production of Infectious HIV-1 and Cause Gag Accumulation in Cells Producing Wild Type or SP1-A1V HIV-1.**
293T cells were mass transfected with a wild type or SP1-A1V HIV-1 vector, aliquoted, and then treated with increasing concentrations of Bevirimat or SY33 over a range of 0.005 µM to 150 µM. Cell lysates were harvested for immunoblotting using anti-HIV-1 capsid antibody (**a-d**). Supernatants were centrifuged to harvest virus like particles (VLPs) for immunoblotting (**e-h**). In parallel, the experiment was repeated with co-transfection of an HIV-1 Envelope plasmid. The supernatants from the co-transfected cells were used to infect CEM-GFP cells to determine infectivity (**i-l**). **a,e,i**) WT HIV-1 treated with Bevirimat. **b,f,j**) Wild type HIV-1 treated with SY33. **c,g,k**) SP1-A1V HIV-1 treated with Bevirimat **d,h,l**) SP1-A1V HIV-1 treated with SY33. Please note, the concentrations in the infectivity graphs correspond to the lanes in the immunoblots above the graph. These immunoblots and graphs are representative of this experiment that was repeated 3 independent times following the same protocol.

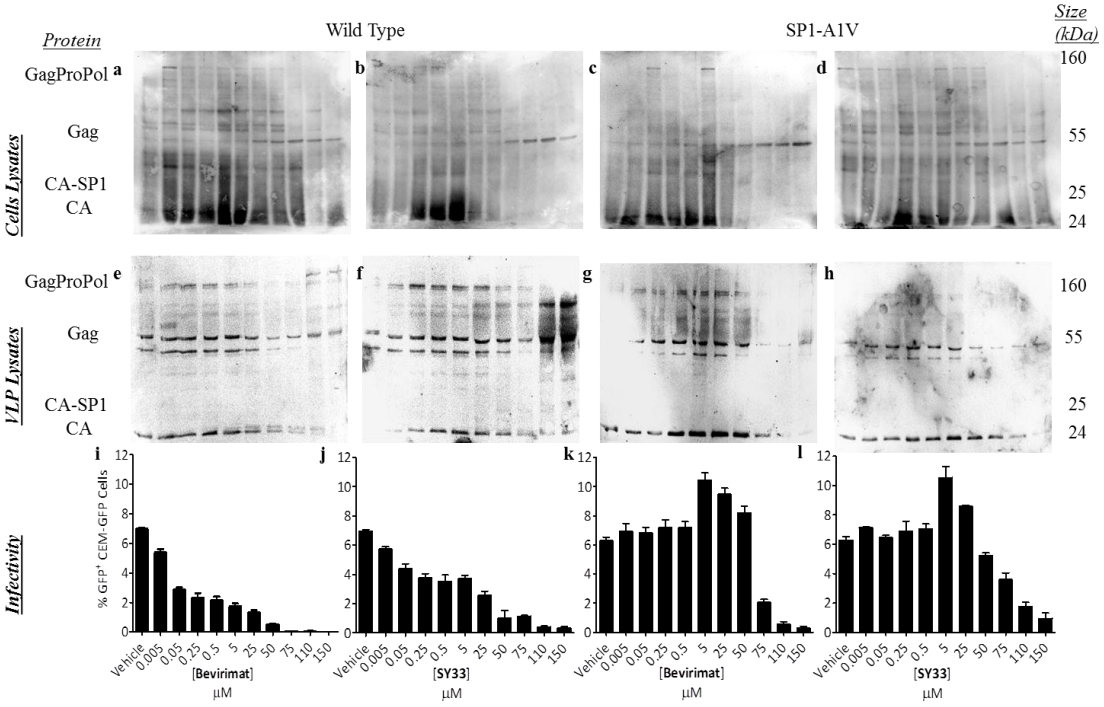

These virus release assays lead to the conclusion that the compounds described in **Figure 2a**, cause CA-SP1 to accumulate in VLPs. However, these novel compounds are not as potent at causing CA-SP1 to accumulate in VLPs as BVM. Since the anti-HIV-1 effect for OK117, OK118, OK256, OK309, and SY33 is approximately 10 fold less potent than BVM, it is reasonable that a 10 fold higher compound concentration is needed to cause same effect on CA-SP1 accumulation in VLPs as BVM. However, at higher concentrations of SY33, it seems a secondary mechanism of action might be occurring that causes an accumulation of 55 kDa Gag in wild-type VLPs. Additionally, results from **Method 2** suggest, at higher concentrations of BVM and SY33, there is a secondary mechanism of action that causes 55 kDa Gag to accumulate in cells regardless of WT or SP1-A1V genotype. Lastly, it seems that the femto detection sensitivity and microcentrifuge isolation method might contribute to limited CA-SP1 detection. These data support the recent observation from Eric Freed's Lab, that CA-SP1 is a dominant-negative regulator of HIV-1 replication [129]. CA-SP1 (p25) causes HIV-1 p25 particle poisoning when in relatively low abundance. Thus, the antiviral triterpenes in **Figure 2a** target CA-SP1 and inhibit the production of infectious HIV-1.

Transmission Electron Microscopy

Transmission Electron Microscopy (TEM) analysis of 50 µM SY33 or 50 µM BVM treated *GagPol* expressing cells reveals that SY33 and BVM cause HIV-1 VLPs to associate with cells. SY33 treated VLPs were typically immature, and in close association to cell membranes, and within vacuolar spaces. As seen in **Figure 6**, a few virus morphologies were witnessed with SY33 treatment including: mature regular (**R**),

mature eccentric (**E**), immature (**I**), and double budded particles. The doubled budded HIV-1 particles are rare in the literature. In 1995, the BC9101 strain of HIV-1 was isolated from a patient in China that caused double budded particles and virus trafficking to vacuolar spaces [191]. The authors attributed these defects to a defective start codon for the Vpu gene [191], however, no further studies, to my knowledge, have confirmed defective Vpu as causing double budded particles. Also, Vpu is not present in this experiment. However, Vpu's antagonist Tetherin [112] is likely in the cell line. PTAP mutants, in p6 of Gag, have been shown to produce double budded immature particles [192]. Additionally, electron dense regions that look like HIV-1 budding sites were witnessed. It is possible that SY33 interferes with HIV-1 budding and/or assembly.

The vehicle treated cells (1% DMSO) analyzed by TEM (**Figure 6**) resulted in very few VLPs in close association with the cells. However, western analysis of supernatants from the cell cultures proves that VLPs are produced in relatively high abundance of p24 from the *GagPol* expressing cells (data not shown). The vehicle treated cells revealed virus morphologies of **I**, **E**, and **R**, and some viruses in the process of budding. However, TEM analysis of vehicle treated *GagPol* expressing cells did not reveal any double budded particles. Most likely the majority of mature virions were not in close association with the cells because the virions were released into the supernatant.

TEM analysis of BVM treated *GagPol* cells resulted in numerous **I** particles localized to vacuolar spaces in the cell. The primary virus type witnessed after BVM treatement was **I**, though there were a few **E** morphologies. TEM analysis did not reveal any **R** HIV-1 particles after 50 µM BVM treatment. Since BVM is more potent than

SY33 at inhibiting CA-SP1 processing (**Figures 2b and 5**), it is logical that less **R** HIV-1 particles were witnessed in the BVM treatment group. It should also be noted that only one **R** particle was witnessed in the SY33 treatment group. In all, these data suggest BVM caused **I** or **E** HIV-1 morphology, and that BVM treated virions are in closer association to cells than vehicle treated, and that BVM and SY33 can increase likelihood of virions being directed to vacuolar spaces.

Figure 6: Electron Microscopy Suggests BVM and SY33 Cause VLP Accumulation Near Cells

293 cells that were stably transformed to express the HIV-1 *GagPol* and *Rev* genes were treated with a **a**) vehicle control (1% DMSO), **b**) 50 µM SY33 or **c**) 50 µM Bevirimat. After 40 hours treatment, the cells were fixed in glutaraldehyde, stained, embedded into paraffin, thin sectioned and virus particles in the cell periphery were observed by transmission electron microscopy.

a. Vehicle

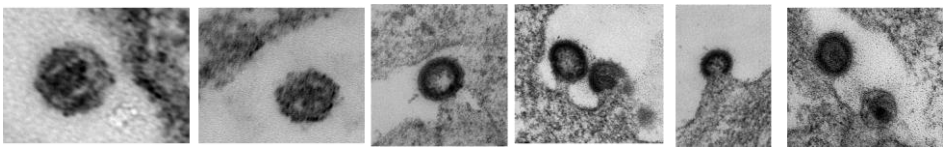

b. SY33

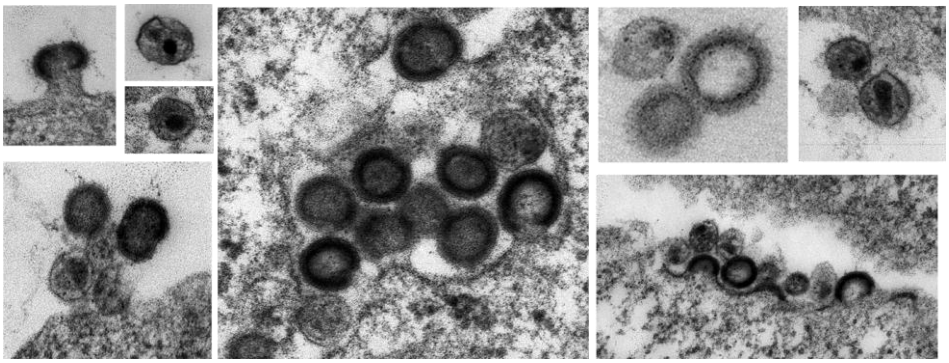

c. Bevirimat

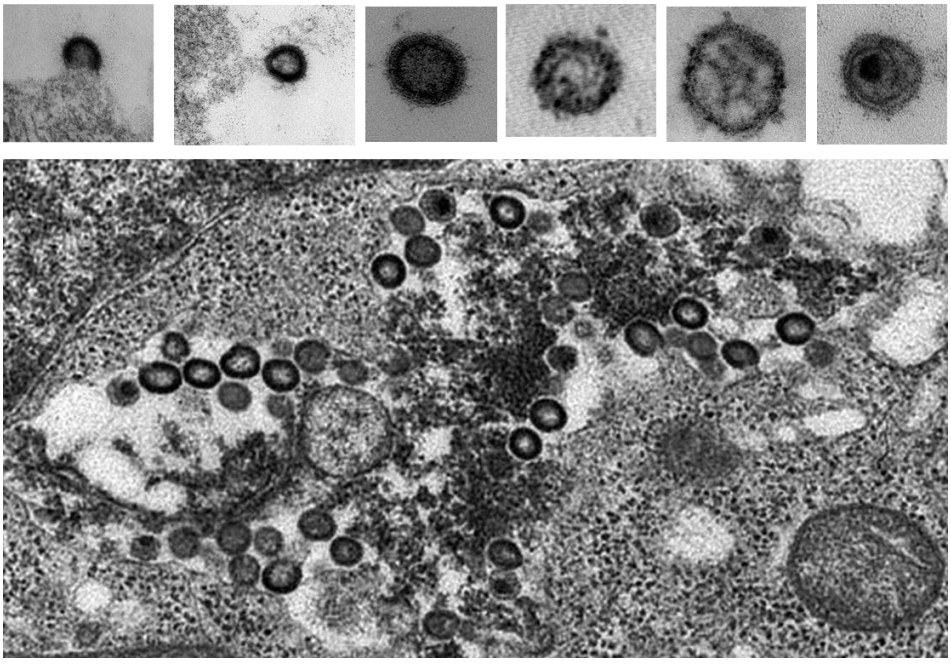

Discussion

The data in this chapter indicate that SY33 and the reported antiretroviral triterpenes target HIV-1 CA-SP1 region of the Gag protein. The compounds in **Figure 2** cause the Gag cleavage product CA-SP1 to accumulate in VLPs. SY33 causes CA-SP1 accumulation in VLPs by three different virus release assay methods (**Figures 2b, 5b, 7b**). SY33 also seems to cause accumulation of the 55 kDa Gag product in wild-type VLPs while BVM did not (**Figure 5b**). It is possible that the nitrile functional group of SY33 inhibits PR's enzymatic activity. This SY33 interference with PR is possible since a recent report showed that diamide can inhibit PR processing of HIV-1 Gag [148]. If SY33 interacts with PR, then it is likely full length Gag will accumulate in particles. In general this study determines antiretroviral triterpenes target CA-SP1.

This is the first study to look closely at the structure and activity relationships between multiple anti-HIV-1 maturation inhibitors. BVM is more effective at inhibiting wild-type CA-SP1 processing than the triterpene compound in **Figure 2**. Also, SP1-A1V has resistance to SY33 and BVM, indicating SP1-A1V resistance is not specific for the C-28 position of the triterpene molecule. SY33 has a nitrile in the C-28 position while BVM has a carboxylic functional group. The dimethyl succinyl moiety and the betulin scaffold seem important at targeting CA-SP1. Of course, other researchers have found other compound structures that can target CA-SP1 [186]. This study is the most detailed comparative study of multiple compounds that target CA-SP1.

Preliminary experiments testing SY33 against bevirimat resistant isolates CA-H226Y, CA-L231M, CA-L231F, SP1-A3V, SP1-V7A, and SP1-V7M [154, 155, 163] show variable levels of resistance to BVM and SY33 (data not shown). Furthermore, preliminary experiments selecting for SY33 resistant isolates through serial passage of NL4-3 or NL4-3 SP1-A1V in CEM-GFP cells gave rise to multiple mutations in CA, PR, SP1, NC and RT (**Appendix A**). However, the most consistent mutations to arise when replicating pNL4-3 in the presence of SY33 were SP1-A1V and SP1-A3V. Indeed, this study verifies that SP1-A1V causes resistance to SY33. The identified SP1-A3V mutations were accompanied by numerous other mutations in RT, CA, NC, and p6. Compensatory mutations occurring with SP1-A3V is somewhat expected as SP1-A3V replicates poorly. When SP1-A1V HIV-1 was passaged in the presence of 5 μM SY33 it was observed that the SP1-A1V mutation was conserved and continued to replicate in the presence of the higher SY33 concentrations of 5 μM. These preliminary resistance data support the data in this paper that SY33 has a similar mechanism of action as BVM by inhibiting HIV-1 replication by targeting CA-SP1 gag cleavage site.

It is possible BVM and SY33 have secondary mechanisms of action influenced by compound structure. The triterpenes SY33 and BVM have structures that are aromatic and non-polar linked to a polar dimethyl-succinate structure via epoxide linkage. This leads to the possibility that the dimethyl succinate structure interacts with the CA-SP1 cleavage site. Additionally, it is possible that at concentrations >5 μM, the aromatic region of compounds are interacting with the plasma membrane (PM). It is possible that at higher concentrations BVM and SY33 bridge the virus to the PM, influencing Gag and

GagPol trafficking, virus budding, or virus release. Preliminary TEM data suggest that BVM and SY33 increase the presence of VLPs in/and near PM. VLPs were witnessed in endosomal compartments, vacuole-like spaces, trapped in budding phase, and even double-budded pre-immature viral particles (**Figure 6**). It is possible that BVM and SY33 have a secondary mechanism of action by causing Gag accumulation inside cells.

The C-28 position of the triterpene influences the ability of the compound to inhibit CA-SP1 processing. It is unknown if the C-28 position interacts with the PR or the CA-SP1 Gag product. Resistance studies with SY33 and BVM indicate that the C-28 position can be –COOH, -CN, or possibly –COH, and SP1-A1V mutant maintains a level of resistance. It is possible that the dimethyl succinate group is interacting with the Gag and the nitryl group of SY33 interacts with the HIV-1 PR. This could be consistent with a recent report suggesting that diamide can inhibit HIV-1's PR [193]. Preliminary SY33 selection experiments also gave rise to SP1-A1V mutant. Since SY33 and BVM differ at C-28, but are equal at dimethyl-succinate, and that SP1-A1V has resistance to both compounds, it seems logical that the dimethyl-succinate is interacting with CA-SP1.

This study also confirms that modest levels of p25 (CA-SP1) in HIV-1 particles cause defective replication. The p25 particle poisoning effect likely inhibits the formation of the conical core as recently described [142] that is necessary for nascent infections. Taken together, our data, with supporting evidence from Eric Freed's lab, indicate that the accumulation of p25 in viral particle inflicts a poisoning effect on HIV-1 [129] termed "p25 particle poisoning." Thus, maturation inhibitors that cause p25 (CA-SP1) to build up in viral particles provide viable options for further development as

antiretroviral therapy. Taken together, this study concludes that certain antiretroviral triterpenes target CA-SP1 and inhibit the production of infectious HIV-1.

Materials and Methods

Compounds, DNA Constructs, Primers, and Cells

SY33, 2,2-Dimethyl-4-[(28-nitrilolup-20-en-3β-yl)oxy]-4-oxobutanoic acid; **SY34**, 2,2-Dimethyl-4-[(19β,28-epoxy-28-oxo-18α-oleanan-3β-yl)oxy]-4-oxobutanoic acid; **SY35**, 3β-[(3-Carboxy-3-methylbutanoyl)oxy]olean-18-en-28-oic acid; **SY37**, 2,2-Dimethyl-4-[(19β,28-epimino-28-oxo-18α-oleanan-3β-yl)oxy]-4-oxobutanoic acid; **OK117**, *N*-Methyl-D-glucamine 2,2-dimethyl-4-[(28-oxolup-20-en-3β-yl)oxy]-4-oxobutanoate; **OK118**, *N*-Methyl-D-glucamine 2,2-dimethyl-4-[(28-oxolupan-3β-yl)oxy]-4-oxobutanoate; **OK256**, 2,2-Dimethyl-4-[(28-oxolup-20-en-3β-yl)oxy]-4-oxobutanoic acid; **OK309**, 2,2-Dimethyl-4-[(28-oxolupan-3β-yl)oxy]-4-oxobutanoic acid; and **bevirimat**, 3-*O*-(3',3'-dimethylsuccinyl)betulinic acid, were synthesized from Birch bark extracts following our recently described methods [4]. The compounds were serially diluted in dimethyl-sulfoxide (DMSO) for biological assays.

For spreading HIV-1 replication assay, pNL4-3 [194] was the wild-type control, and pNL4-3 SP1-A1V [154, 155, 163] was the SP1-A1V mutant. The HIV-1 molecular clones were kind gifts from Eric Freed at NCI-Frederick.

For the single-round HIV-1 replication assay, pHIG SP1-A1V was constructed by excising the SbfI-SpeI fragment from pNL4-3 SP1-A1V [154, 155, 163] and inserting it

into pNL4-3 HIG [177, 188, 189]. pNL4-3 HIG SP1-A1V and pNL4-3 HIG were confirmed by sequence analysis of the *GagPol* gene using primers **NL516F,** 5'-TGC CCG TCT GTT GTG TGA CTC-3' [154, 163]; **NL645F,** 5'-AAC AGG GAC TTG AAA GCG-3' [163]; **NL1155F**, 5'-AGG AAA CAA CAG CCA GGT-3' [163]; **NL1410F**, 5'-GGA AGC TGC AGA ATG GGA TA-3' [154, 163]; **NL1754F**, 5'-TGG TCC AAA ATG CGA ACC-3' [154, 163]; **NL2135F**, 5'-TTC AGA GCA GAC CAG AGC CAA-3' [154, 163]; **NL2897R**, 5'-AAA ATA TGC ATC GCC CAC AT-3'[154, 163].

293T human embryonic kidney cells [195, 196] was used primarily for production of HIV-1 particles and were cultured in Dulbecco's Modification of Eagle's Media (DMEM) supplemented with 10% Fetal Calf Serum 3 (FC3). CEM-GFP cells were used as indicator cells permissive to HIV-1 infection and cultured in RPMI supplemented with 10% FC3. The CEM-GFP cells [197] fluoresce green when infected by HIV-1. The HIV-1 Tat protein activates a Green Fluorescent Protein (GFP) gene driven by an HIV-1 long terminal repeat (LTR) transcriptional promoter [197].

A 293 [198] cell line was used that stably expresses the codon-optimized HIV-1 *GagPol* and *Rev* genes. This cell line was developed in Nikunj Somia's lab. The cells produce HIV-1-like particles as confirmed by p24 ELISA of cellular and viral lysates (data not shown). The *GagPol* expressing 293 cell-line was also characterized by immunoblot analysis (data not shown) and transmission electron microscopy (**Figure 6**).

Single-Round HIV-1 Replication Assay

The pNL4-3 HIG vector pHIG [177, 188, 189] or pNL4-3 HIG SP1-A1V vector pHIG SP1-A1V were co-transfected into 293T cells using PEI method. Cells were harvested 20 hours post transfection, aliquoted into 24 well plates and treated with SY33 or Bevirimat, in triplicate of each concentration, at 5 nM, 50 nM, 250 nM, 500 nM, 5 µM, 25 µM, 50 µM, 75 µM, 110 µM, or 150 µM. Forty-eight hours later, virus containing supernatant was harvested, cell debris was removed by centrifugation, and frozen at -80 degrees Celsius. Supernatant that was treated with 1% DMSO was titrated into CEM-GFP cells. 72 hours post infection, the CEM-GFP cells were analyzed by Flow Cytometry to determine multiplicity of infection. Following viral titer of pHIG and pHIG SP1-A1V viruses, the compound-treated viruses were thawed and infected into CEM-GFP cells at a volume equivalent to a multiplicity of infection (MOI) of 0.07 compared to the DMSO control. 72 hours post infection, CEM-GFP cells were collected and analyzed by flow cytometry using a BD LSR II with HTS adapter. Flow cytometry data were analyzed with FlowJo software to determine percent GFP positive cells. Data were then analyzed with Graphpad statistical software to determine EC_{50} values. The EC_{50} values in **Table 1** do not directly correlate with the $\%GFP^{+}$ CEM-GFP cells in the graphs in **Figure 3** because the EC_{50} was derived from a curve best fit to the data. This experiment was performed 3 times, the data were normalized to no drug control, and combined to determine values in **Table 1** for WT and SP1-A1V HIV-1.

Toxicity Assay

Compounds were tested for potential cellular toxicity using the Promega non-radioactive cell proliferation assay following the manufacturer's directions with CEM-GFP cells. Toxicity was tested with serial dilutions of compounds up to 300 µM for 293T cells or 100 µM for CEM-GFP cells using 1% DMSO (v/v) as the vehicle control. Optical densities at 570 nM (OD570) data were obtained using a plate reader and data analyzed with Graphpad statistical software.

Virus Release Assays

Three virus release assays were performed to analyze the triterpene effect on HIV-1 Gag processing. As shown in **Figure 2b**, cells were transfected in 10 cm tissue culture plates with pHIG vector using calcium phosphate method [97, 177] and treated with 10 or 50 µM compound. Supernatants from two dishes were filtered, combined and a total volume of 20 mL of VLPs containing supernatant was pelleted at 25,000 x g for 2.5 hours using an ultracentrifuge. VLP pellets were lysed in RIPA buffer and stored at -20°C until immunoblot.

In **Figure 5**, 293T cells were transfected in 10 cm tissue culture plates with pHIG or pHIG SP1-A1V using polyethylenimine (PEI) transfection [199]. The cells were harvested 24 hours later and aliquoted into 24 well culture clusters. The cultures were then treated with 5 nM, 50 nM, 250 nM, 500 nM, 5 µM, 25 µM, 50 µM, 75 µM, 110 µM, or 150 µM BVM or SY33. 40 hours post compound treatment, supernatants were collected and centrifuged for 7 minutes at 4.0 x g to remove cell debris. The supernatant

was then transferred to a fresh 1.5 ml tube and centrifuged in a microcentrifuge for 2.5 hours at 13.2 x g. VLP containing pellets were lysed with RIPA buffer and stored at -20°C until immunoblot. Additionally, the transfected and treated 293T cells were lysed in RIPA buffer for immunoblot.

Immunoblotting

Cell lysates or VLP lysates from virus release assays were electrophoresed through 15% SDS-PAGE and transferred to nylon membranes (BIORAD) using the electric BIORAD trans-blot transfer method. Membranes were Ponceau stained to ensure protein transfer, then blocked in 5% milk TBS-T and treated with HIV-1 IIIB Strain rabbit anti-p24 polyclonal antibody (Advanced Biotechnologies, Inc) at a dilution of 1:7000. Immunoblots were exposed to secondary antibody and developed using pico or femto sensitivity detection substrate. Immunoblots were imaged using a BIO-RAD chemiluminscent apparatus.

Spreading HIV-1 Infection Assay

pNL4-3 [194] and pNL4-3 SP1-A1V [154, 155, 163] molecular clones were transfected into 293T cells using calcium phosphate method[97, 177]. Cells transfected with pNL4-3 or pNL4-3 SP1-A1V were pooled and aliquoted into wells of a 6 well dish and treated with SY33 or Bevirimat at 500 pM, 5 nM, 50 nM, 500 nM, 5 µM, 25 µM compound concentration or with DMSO such that all cultures were treated with 1% DMSO. Forty-eight hours later, supernatant was harvested, filtered and used to infect

CEM-GFP cells. Each virus supernatant was used to infect three cultures of CEM-GFP cells in 24 well culture dishes at an approximate MOI of 0.12. Compound was added to each CEM-GFP culture at same concentration as transfection. Every one to three days, CEM-GFP cultures were split 1:2 by removing cells and adding fresh RPMI 10% FC3 and compound such that the initial compound concentration was maintained throughout the entire experiment. Viral replication was monitored by detecting GFP expressing by flow cytometry using a LSR II with HTS adaptor. Flow cytometry data were analyzed with FlowJo software. This experiment was repeated at least 3 times.

Transmission Electron Microscopy

GagPol expressing cells were treated with 50 µM SY33, BVM, or 1% DMSO for 48 hours. The cells were fixed in glutaraldehyde and mailed to Electron Microscopy BioServices (Frederick, Maryland) to be sectioned and analyzed by transmission electron microscopy. Alternatively, this experiment was repeated, cells treated the same, and sent to the University of Minnesota Characterization Facility for sectioning. The samples were analyzed, by Casey Dorr, using a Jeol 1200 transmission electron microscope.

Epilogue

Taken together, the research in this thesis investigated the synthesis, discovery, and analysis of novel anti-HIV-1 compounds derived from Birch trees. In **Chapter 3**, the anti-HIV-1 mechanism of action was investigated using virus release assays, immunoblots, transmission electron microscopy, spreading and single round replication assays with the mutant SP1-A1V. The data indicate that the triterpene compounds inhibit the CA-SP1 processing to CA and SP1. However, the data also indicate that at higher concentrations, SY33 can inhibit release of HIV-1 from the host cell and possibly cause the 55 kDa Gag product to accumulate. Though this thesis describes the discovery of these anti-HIV-1 compounds, while doing follow up work investigating anti-HIV-1 mechanism, there are more experiments I recommend if someone continues this project.

To determine if SY33 (and OK191G) inhibits HIV-1 released from the virus producing cell, I recommend enzyme linked immunoabsorbant assay (ELISA), coupled with a cell toxicity assay. This experiment can be used to determine the mass of HIV-1 produced from a viable cell in the unit ng HIV-1 p24 per viable cell. Furthermore, if the ELISA does not work, I recommend using a Reverse Transcriptase activity assay (RT-assay) to determine the amount of HIV-1 RNA release per viable cell. As controls, I recommend a vehicle only (1% DMSO), and increasing concentrations of compound from ranges 5 nM to 150 µM. These experiments will further investigate if SY33 inhibits HIV-1 release from a virus producing cell.

The next set of experiments I recommend is to test Coffin's Razor and SY33. Coffin's Razor is a term coined by Guylaine Hache and Reuben Harris referring to the invariant correlation that HIV-1 (and most retroviruses) becomes resistant to all known anti-viral strategies [200]. Basically, the virus needs to replicate using a spreading infection assay in the presence of a compound until the virus mutates and becomes resistant to the compound. Following resistance, the mutation needs to be mapped using nucleotide sequencing. This resistance selection experiment is kind of tricky, but with patience and time, this assay can work. I tested this assay (**Appendix A**) and noticed that the SP1-A1V and SP1-A3V mutations arise with SY33 treatment. However, as discussed in **Chapter 3**, numerous other mutations arise with SY33 treatment. One problem with selecting for drug resistant HIV-1 is that the virus kills the cells in culture. I spoke with John Coffin about selecting for drug resistant HIV-1 while I was in Prague. Coffin told me that the virus has to be passaged into uninfected cells every three days because HIV-1 will kill off the cells. After my experiments, I recommend passing a third of the cell/virus culture into a fresh culture of T-cells and media every 2-5 days while increasing SY33 concentration with every other passage until virus is replicating in the presence of 5 to 25 μM. Additionally, with each passage, collect the cells (CEM-GFP cells in **Chapter 3**) and analyze by flow cytometry for virus replication (GFP expression). Also, extract the DNA from the cells at each passage, and then sequence using the primers in **Chapter 3**. I hypothesize that the mutations will arise after a few passages, and as SY33 concentration is increased, the predominant SY33 resistant mutation will overtake the virus population. I recommend doing this experiment in 1-5 ml cell culture volumes,

likely in 6 well culture clusters. Following, the discovery of the predominant SY33 selected mutants, the resistance must be verified. Selecting and verifying SY33 resistance mutations will further elucidate SY33's molecular target.

Another experiment I recommend is to test a panel of CA-SP1 mutants for resistance to SY33 and the other triterpene derivatives. I obtained from Eric Freed at the National Cancer Institute a panel of CA-SP1 mutants that are bevirimat resistant: CA-H226Y, CA-L231M, CA-L231F, SP1-A1V, SP1-A3V, SP1-V7A, and SP1-V7M. I did preliminary tests to determine if SY33 could inhibit these mutants in spreading infections assays. However, there was limited time for these tests. The preliminary data indicate there are some differences in these mutants' sensitivity to BVM and SY33. I think that further analysis could help determine the structure-activity relationship between CA-SP1 mutants and the structure of the triterpene. Such structure-activity relationship data could help us determine which part (dimethyl succinate, tritperpene) part of the compound is interacting with the CA or SP1 side of the CA-SP1 cleavage site.

Since spreading infection assays are somewhat difficult, I recommend cloning the CA-SP1 region of the CA-SP1 mutants into the pHIG vector for analysis by the single-round HIV-1 replication assay. This can be repeated the exact same way as I did to engineer pHIG SP1-A1V vector in **Chapter 3**. Simply, swap the SbfI-SpeI fragment from the mutants, and insert them into a SbfI, SpeI double digested HIG vector. The nice thing is the point mutations are already made, so the cloning should be easy. I used this strategy and made the pHIG-SP1-A1V vector, and sequence verified, in about 1 week. I

recommend testing the triterpenes in **Chapter 2** for anti-HIV-1 activity against CA-SP1 mutants using the single-round HIV-1 replication assay.

Further experiments I recommend are to do more extensive transmission electron microscopy analysis for effect of SY33 on HIV-1 morphology. To this end, I recommend treating the *GagPol* expressing cell line (**Chapter 3**) with 50 µM SY33, 50 µM BVM (control), or vehicle only negative control. This should be done in a large volume, possibly 2-10 10 cm culture dishes per experimental sample. Following 2 days of treatment, harvest, filter and ultracentrifuge the supernatant to pellet the HIV-1 like particles (a sucrose cushion may increase virus intactness). Then re-suspend the virus pellet, mount onto a grid for electron microscopy analysis. Alternatively, the virus might need to be embedded into paraffin and sectioned. Then analyze the virus by electron microscopy. The point of this method is to increase the number of virus counts to better assess statistics. The virus should be categorized into virus morphologies (like **E**, **R**, or **I**) and statistics done to determine the predominant virus morphology present after SY33 treatment. I hypothesize there will be few **R** particles, and mostly **E** or **I** with SY33 treatment. Electron microscopy is a classical retrovirology technique that can further elucidate the mechanism of SY33's anti-HIV-1 activity.

The next set of experiments I suggest for SY33 is to test toxicity in an animal model using bevirimat (BVM) as a standard. If SY33 is less toxic in an animal model than BVM then, SY33 might be better for use in humans than BVM. I also suggest testing if SY33 is converted to BVM in the animal model be by animal enzymes. As we stated in **Chapter 2**, SY33 might be a prodrug for BVM. Thus, SY33 might have dual

activity as SY33 and also when it is converted to BVM. Animal models might lead to SY33 being a better therapeutic against HIV-1 than BVM.

The fatty acid derivatives in **Appendix B** are just the beginning of a new class of compounds that can have therapeutic effects against HIV-1 replication. Compound OK191G has modest anti-HIV-1 activity, but I think there are other fatty acid derivatives that will be much more potent and likely lead to a new molecular target for suppressive HIV-1 therapy. Interestingly, the most potent fatty acid derivative we tested, was a derivative from a suberinic acid fraction from a Birch bark extract. The sample was potent with EC_{50} less than 10 μM. This sample, OK149, also appeared to inhibit CA-SP1 processing in virus release assays. However, we were never able to repeat the synthesis of OK149. Fatty acid derivatives might serve as effective anti-HIV-1 compounds with further scientific development.

Taken together, this thesis work developed an entirely new scientific project that did not exist prior to my graduate school career in Professor Mansky's lab. With the help of our chemist collaborators in Duluth, we discovered 8 novel triterpenes that inhibit late phase HIV-1 replication and 2 fatty acid derivatives with modest anti-HIV-1 activity. The data in this thesis suggest the triterpenes function similar to Bevirimat, but structural differences in the compounds have functional differences in the molecular mechanism of action. Further development of SY33 (and other compounds in **Chapters 2** and **3**) as an anti-HIV-1 therapy is warranted. Since these compounds are derived from Birch trees, and potently inhibit HIV-1 replication, this research furthers my notion that plants may be useful in the future at solving human health problems.

References

1. Tian, L., et al., *Green fluorescent protein as a tool for monitoring transgene expression in forest tree species.* Tree physiology, 1999. **19**(8): p. 541-546.
2. Lico, C., et al., *Peptide display on Potato virus X: molecular features of the coat protein-fused peptide affecting cell-to-cell and phloem movement of chimeric virus particles.* J Gen Virol, 2006. **87**(Pt 10): p. 3103-12.
3. Marusic, C., et al., *Chimeric plant virus particles as immunogens for inducing murine and human immune responses against human immunodeficiency virus type 1*. J Virol, 2001. **75**(18): p. 8434-9.
4. Dorr, C.R., et al., *Triterpene derivatives that inhibit human immunodeficiency virus type 1 replication.* Bioorg Med Chem Lett, 2011. 21:p. 542-545.
5. Dorr C.R., Y.S., Kolomitsyna O., Krasutsky P. and Mansky L.M. *Discovery of Modified Triterpene Compounds Derived from B. papyrifera that Inhibit HIV-1 Replication by Inhibition of Virus Maturation* in *Retroviruses*. 2009. Cold Spring Harbor, New York: Cold Spring Harbor Laboratory.
6. Dorr C, K.O., Yemets S, Somia N, Krasutsky P and Mansky LM. *Discovery of Novel Compounds From Betula papyrifera That Inhibit HIV-1 Maturation*. in *Centennial Retrovirus Meeting*. 2010. Prague, Czech Republic: Medimond s.r.l.
7. Rous, P., *A Sarcoma of the Fowl Transmissible by an Agent Separable from the Tumor Cells.* J Exp Med, 1911. **13**(4): p. 397-411.
8. Rous, P., *A Transmissible Avian Neoplasm. (Sarcoma of the Common Fowl.).* J Exp Med, 1910. **12**(5): p. 696-705.
9. Svoboda, J. *Background and Perspectives*. in *Centennial Retrovirus Meeting*. 2010. Prague, Czech Republic: Medimond s.r.l.
10. UNAIDS, *AIDS Epidemic Update*, 2009, Joint United Nations Programme on HIV/AIDS (UNAIDS) and World Health Organization (WHO): Geneva.
11. Barre-Sinoussi, F. and J.C. Chermann, *Lymphadenopathy associated virus (L.A.V.): its association with AIDS or prodromes.* Adv Exp Med Biol, 1985. **187**: p. 35-43.

12. Barre-Sinoussi, F. and J.C. Chermann, *The etiologic agent of AIDS.* Mt Sinai J Med, 1986. **53**(8): p. 598-608.
13. Barre-Sinoussi, F., et al., *Isolation of a T-lymphotropic retrovirus from a patient at risk for acquired immune deficiency syndrome (AIDS).* Science, 1983. **220**(4599): p. 868-71.
14. Barre-Sinoussi, F., et al., *Isolation of lymphadenopathy-associated virus (LAV) and detection of LAV antibodies from US patients with AIDS.* JAMA, 1985. **253**(12): p. 1737-9.
15. Sarngadharan, M.G., et al., *HTLV-III: the etiologic agent of AIDS.* Princess Takamatsu Symp, 1984. **15**: p. 301-8.
16. *From the Centers for Disease Control and Prevention. 1993 revised classification system for HIV infection and expanded surveillance case definition for AIDS among adolescents and adults.* JAMA : the journal of the American Medical Association, 1993. **269**(6): p. 729-30.
17. Mansky, L.M., *HIV mutagenesis and the evolution of antiretroviral drug resistance.* Drug Resist Updat, 2002. **5**(6): p. 219-23.
18. Coffin, J.M., Hughes, S. H., Varmus, H. E. , *Retroviruses*1997, Woodbury, New York: Cold Spring Harbor Laboratory Press.
19. Haase, A.T., *Pathogenesis of lentivirus infections.* Nature, 1986. **322**(6075): p. 130-6.
20. Wertheim, J.O. and M. Worobey, *Dating the age of the SIV lineages that gave rise to HIV-1 and HIV-2.* PLoS Comput Biol, 2009. **5**(5): p. e1000377.
21. Temin, H.M. and S. Mizutani, *RNA-dependent DNA polymerase in virions of Rous sarcoma virus.* Nature, 1970. **226**(5252): p. 1211-3.
22. Yamashita, M. and M. Emerman, *Retroviral infection of non-dividing cells: old and new perspectives.* Virology, 2006. **344**(1): p. 88-93.
23. Lewis, P., M. Hensel, and M. Emerman, *Human immunodeficiency virus infection of cells arrested in the cell cycle.* The EMBO journal, 1992. **11**(8): p. 3053-8.
24. Dalgleish, A.G., et al., *The CD4 (T4) antigen is an essential component of the receptor for the AIDS retrovirus.* Nature, 1984. **312**(5996): p. 763-7.

25. Klatzmann, D., et al., *T-lymphocyte T4 molecule behaves as the receptor for human retrovirus LAV.* Nature, 1984. **312**(5996): p. 767-8.
26. Feng, Y., et al., *HIV-1 entry cofactor: functional cDNA cloning of a seven-transmembrane, G protein-coupled receptor.* Science, 1996. **272**(5263): p. 872-7.
27. Deng, H., et al., *Identification of a major co-receptor for primary isolates of HIV-1.* Nature, 1996. **381**(6584): p. 661-6.
28. Dragic, T., et al., *HIV-1 entry into CD4+ cells is mediated by the chemokine receptor CC-CKR-5.* Nature, 1996. **381**(6584): p. 667-73.
29. Alkhatib, G., et al., *CC CKR5: a RANTES, MIP-1alpha, MIP-1beta receptor as a fusion cofactor for macrophage-tropic HIV-1.* Science, 1996. **272**(5270): p. 1955-8.
30. Moyle, G., *Stopping HIV fusion with enfuvirtide: the first step to extracellular HAART.* J Antimicrob Chemother, 2003. **51**(2): p. 213-7.
31. Maertens, G.N., S. Hare, and P. Cherepanov, *The mechanism of retroviral integration from X-ray structures of its key intermediates.* Nature, 2010. **468**(7321): p. 326-9.
32. Baltimore, D., *RNA-dependent DNA polymerase in virions of RNA tumour viruses.* Nature, 1970. **226**(5252): p. 1209-11.
33. Moelling, K., *Further characterization of the Friend murine leukemia virus reverse transcriptase-RNase H complex.* J Virol, 1976. **18**(2): p. 418-25.
34. Moelling, K., *Comparison between an avian and a murine viral reverse transcriptase-RNase H complex.* Bibl Haematol, 1975(43): p. 121-4.
35. Moelling, K., *Reverse transcriptase and RNase H: present in a murine virus and in both subunits of an avian virus.* Cold Spring Harb Symp Quant Biol, 1975. **39 Pt 2**: p. 969-73.
36. Moelling, K., *Characterization of reverse transcriptase and RNase H from friend-murine leukemia virus.* Virology, 1974. **62**(1): p. 46-59.
37. Stahlhut, M., et al., *Purification and characterization of HIV-1 reverse transcriptase having a 1:1 ratio of p66 and p51 subunits.* Protein Expr Purif, 1994. **5**(6): p. 614-21.

38. Watson, J.D. and F.H. Crick, *Genetical implications of the structure of deoxyribonucleic acid.* Nature, 1953. **171**(4361): p. 964-7.
39. Watson, J.D. and F.H. Crick, *Molecular structure of nucleic acids; a structure for deoxyribose nucleic acid.* Nature, 1953. **171**(4356): p. 737-8.
40. Crick, F.H., *On protein synthesis.* Symp Soc Exp Biol, 1958. **12**: p. 138-63.
41. Crick, F., *Central dogma of molecular biology.* Nature, 1970. **227**(5258): p. 561-3.
42. Bieniasz, P.D., *The cell biology of HIV-1 virion genesis.* Cell Host Microbe, 2009. **5**(6): p. 550-8.
43. Ganser-Pornillos, B.K., M. Yeager, and W.I. Sundquist, *The structural biology of HIV assembly.* Curr Opin Struct Biol, 2008. **18**(2): p. 203-17.
44. Krausslich, H.G., A.M. Traenckner, and F. Rippmann, *Expression and characterization of genetically linked homo- and hetero-dimers of HIV proteinase.* Adv Exp Med Biol, 1991. **306**: p. 417-28.
45. Pettit, S.C., et al., *Ordered processing of the human immunodeficiency virus type 1 GagPol precursor is influenced by the context of the embedded viral protease.* J Virol, 2005. **79**(16): p. 10601-7.
46. Weber, I.T., et al., *Crystallographic analysis of human immunodeficiency virus 1 protease with an analog of the conserved CA-p2 substrate -- interactions with frequently occurring glutamic acid residue at P2' position of substrates.* Eur J Biochem, 1997. **249**(2): p. 523-30.
47. Aiken, C., *Pseudotyping human immunodeficiency virus type 1 (HIV-1) by the glycoprotein of vesicular stomatitis virus targets HIV-1 entry to an endocytic pathway and suppresses both the requirement for Nef and the sensitivity to cyclosporin A.* J Virol, 1997. **71**(8): p. 5871-7.
48. Jacks, T. and H.E. Varmus, *Expression of the Rous sarcoma virus pol gene by ribosomal frameshifting.* Science, 1985. **230**(4731): p. 1237-42.
49. Jacks, T., et al., *Two efficient ribosomal frameshifting events are required for synthesis of mouse mammary tumor virus gag-related polyproteins.* Proc Natl Acad Sci U S A, 1987. **84**(12): p. 4298-302.

50. Jacks, T., et al., *Characterization of ribosomal frameshifting in HIV-1 gag-pol expression.* Nature, 1988. **331**(6153): p. 280-3.
51. Fujii, K., J.H. Hurley, and E.O. Freed, *Beyond Tsg101: the role of Alix in 'ESCRTing' HIV-1.* Nat Rev Microbiol, 2007. **5**(12): p. 912-6.
52. Stuchell, M.D., et al., *The human endosomal sorting complex required for transport (ESCRT-I) and its role in HIV-1 budding.* J Biol Chem, 2004. **279**(34): p. 36059-71.
53. Sette, P., et al., *The ESCRT-associated protein Alix recruits the ubiquitin ligase Nedd4-1 to facilitate HIV-1 release through the LYPXnL L domain motif.* J Virol, 2010. **84**(16): p. 8181-92.
54. Morita, E., et al., *Human ESCRT and ALIX proteins interact with proteins of the midbody and function in cytokinesis.* EMBO J, 2007. **26**(19): p. 4215-27.
55. Morita, E., et al., *Identification of human MVB12 proteins as ESCRT-I subunits that function in HIV budding.* Cell Host Microbe, 2007. **2**(1): p. 41-53.
56. Im, Y.J., et al., *Crystallographic and Functional Analysis of the ESCRT-I /HIV-1 Gag PTAP Interaction.* Structure, 2010. **18**(11): p. 1536-47.
57. Jouvenet, N., et al., *Plasma membrane is the site of productive HIV-1 particle assembly.* PLoS Biol, 2006. **4**(12): p. e435.
58. Joshi, A., et al., *Evidence that productive human immunodeficiency virus type 1 assembly can occur in an intracellular compartment.* J Virol, 2009. **83**(11): p. 5375-87.
59. Zhdankin, V.V., et al., *1-(Organosulfonyloxy)-3(1H)-1,2-benziodoxoles: Preparation and Reactions with Alkynyltrimethylsilanes.* J Org Chem, 1996. **61**(19): p. 6547-6551.
60. Bryant, M. and L. Ratner, *Myristoylation-dependent replication and assembly of human immunodeficiency virus 1.* Proc Natl Acad Sci U S A, 1990. **87**(2): p. 523-7.
61. Park, J. and C.D. Morrow, *The nonmyristylated Pr160gag-pol polyprotein of human immunodeficiency virus type 1 interacts with Pr55gag and is incorporated into viruslike particles.* J Virol, 1992. **66**(11): p. 6304-13.

62. Lee, P.P. and M.L. Linial, *Efficient particle formation can occur if the matrix domain of human immunodeficiency virus type 1 Gag is substituted by a myristylation signal.* J Virol, 1994. **68**(10): p. 6644-54.
63. Wang, C.T., H.Y. Lai, and J.J. Li, *Analysis of minimal human immunodeficiency virus type 1 gag coding sequences capable of virus-like particle assembly and release.* J Virol, 1998. **72**(10): p. 7950-9.
64. Accola, M.A., B. Strack, and H.G. Gottlinger, *Efficient particle production by minimal Gag constructs which retain the carboxy-terminal domain of human immunodeficiency virus type 1 capsid-p2 and a late assembly domain.* J Virol, 2000. **74**(12): p. 5395-402.
65. Tang, C., et al., *Entropic switch regulates myristate exposure in the HIV-1 matrix protein.* Proc Natl Acad Sci U S A, 2004. **101**(2): p. 517-22.
66. Alfadhli, A., R.L. Barklis, and E. Barklis, *HIV-1 matrix organizes as a hexamer of trimers on membranes containing phosphatidylinositol-(4,5)-bisphosphate.* Virology, 2009. **387**(2): p. 466-72.
67. Ghanam, R.H., et al., *Binding of calmodulin to the HIV-1 matrix protein triggers myristate exposure.* J Biol Chem, 2010.
68. Fledderman, E.L., et al., *Myristate Exposure in the Human Immunodeficiency Virus Type 1 Matrix Protein Is Modulated by pH.* Biochemistry, 2010.
69. Saad, J.S., et al., *Point mutations in the HIV-1 matrix protein turn off the myristyl switch.* J Mol Biol, 2007. **366**(2): p. 574-85.
70. Lindwasser, O.W. and M.D. Resh, *Myristoylation as a target for inhibiting HIV assembly: unsaturated fatty acids block viral budding.* Proc Natl Acad Sci U S A, 2002. **99**(20): p. 13037-42.
71. Gallay, P., et al., *HIV-1 infection of nondividing cells: C-terminal tyrosine phosphorylation of the viral matrix protein is a key regulator.* Cell, 1995. **80**(3): p. 379-88.
72. Kaushik, R. and L. Ratner, *Role of human immunodeficiency virus type 1 matrix phosphorylation in an early postentry step of virus replication.* J Virol, 2004. **78**(5): p. 2319-26.

73. Bhatia, A.K., et al., *Mutation of critical serine residues in HIV-1 matrix result in an envelope incorporation defect which can be rescued by truncation of the gp41 cytoplasmic tail.* Virology, 2009. **384**(1): p. 233-41.
74. Huang, M. and M.A. Martin, *Incorporation of Pr160(gag-pol) into virus particles requires the presence of both the major homology region and adjacent C-terminal capsid sequences within the Gag-Pol polyprotein.* J Virol, 1997. **71**(6): p. 4472-8.
75. Pettit, S.C., et al., *Initial cleavage of the human immunodeficiency virus type 1 GagPol precursor by its activated protease occurs by an intramolecular mechanism.* J Virol, 2004. **78**(16): p. 8477-85.
76. Briggs, J.A., et al., *Structure and assembly of immature HIV.* Proc Natl Acad Sci U S A, 2009. **106**(27): p. 11090-5.
77. Bartonova, V., et al., *Residues in the HIV-1 capsid assembly inhibitor binding site are essential for maintaining the assembly-competent quaternary structure of the capsid protein.* J Biol Chem, 2008. **283**(46): p. 32024-33.
78. Tang, C., et al., *Antiviral inhibition of the HIV-1 capsid protein.* J Mol Biol, 2003. **327**(5): p. 1013-20.
79. Sandefur, S., et al., *Mapping and characterization of the N-terminal I domain of human immunodeficiency virus type 1 Pr55(Gag).* J Virol, 2000. **74**(16): p. 7238-49.
80. Newman, J.L., et al., *Flexibility in the P2 domain of the HIV-1 Gag polyprotein.* Protein Sci, 2004. **13**(8): p. 2101-7.
81. Morellet, N., et al., *Helical structure determined by NMR of the HIV-1 (345-392)Gag sequence, surrounding p2: implications for particle assembly and RNA packaging.* Protein Sci, 2005. **14**(2): p. 375-86.
82. Jalalirad, M. and M. Laughrea, *Formation of immature and mature genomic RNA dimers in wild-type and protease-inactive HIV-1: differential roles of the Gag polyprotein, nucleocapsid proteins NCp15, NCp9, NCp7, and the dimerization initiation site.* Virology, 2010. **407**(2): p. 225-36.

83. Chukkapalli, V., S.J. Oh, and A. Ono, *Opposing mechanisms involving RNA and lipids regulate HIV-1 Gag membrane binding through the highly basic region of the matrix domain.* Proc Natl Acad Sci U S A, 2010. **107**(4): p. 1600-5.
84. Alfadhli, A., A. Still, and E. Barklis, *Analysis of human immunodeficiency virus type 1 matrix binding to membranes and nucleic acids.* J Virol, 2009. **83**(23): p. 12196-203.
85. Datta, S.A., et al., *HIV-1 Gag Extension: Conformational Changes Require Simultaneous Interaction with Membrane and Nucleic Acid.* J Mol Biol, 2010.
86. Ono, A. and E.O. Freed, *Plasma membrane rafts play a critical role in HIV-1 assembly and release.* Proc Natl Acad Sci U S A, 2001. **98**(24): p. 13925-30.
87. Finzi, A., et al., *Productive human immunodeficiency virus type 1 assembly takes place at the plasma membrane.* J Virol, 2007. **81**(14): p. 7476-90.
88. Ono, A., et al., *Phosphatidylinositol (4,5) bisphosphate regulates HIV-1 Gag targeting to the plasma membrane.* Proc Natl Acad Sci U S A, 2004. **101**(41): p. 14889-94.
89. Waheed, A.A. and E.O. Freed, *Lipids and membrane microdomains in HIV-1 replication.* Virus Res, 2009. **143**(2): p. 162-76.
90. Hurley, J.H., et al., *Membrane budding.* Cell, 2010. **143**(6): p. 875-87.
91. Pincetic, A. and J. Leis, *The Mechanism of Budding of Retroviruses From Cell Membranes.* Adv Virol, 2009. **2009**: p. 6239691-6239699.
92. McDonald, B. and J. Martin-Serrano, *No strings attached: the ESCRT machinery in viral budding and cytokinesis.* J Cell Sci, 2009. **122**(Pt 13): p. 2167-77.
93. Marsh, M., K. Theusner, and A. Pelchen-Matthews, *HIV assembly and budding in macrophages.* Biochem Soc Trans, 2009. **37**(Pt 1): p. 185-9.
94. Fujii, K., et al., *Functional role of Alix in HIV-1 replication.* Virology, 2009. **391**(2): p. 284-92.
95. Dussupt, V., et al., *Basic residues in the Nucleocapsid domain of Gag are critical for late events of HIV-1 budding.* J Virol, 2010.
96. Usami, Y., et al., *The ESCRT pathway and HIV-1 budding.* Biochem Soc Trans, 2009. **37**(Pt 1): p. 181-4.

97. Dorweiler, I.J., et al., *Role of the human T-cell leukemia virus type 1 PTAP motif in Gag targeting and particle release.* J Virol, 2006. **80**(7): p. 3634-43.

98. Pornillos, O., et al., *Structure of the Tsg101 UEV domain in complex with the PTAP motif of the HIV-1 p6 protein.* Nat Struct Biol, 2002. **9**(11): p. 812-7.

99. Demirov, D.G., et al., *Overexpression of the N-terminal domain of TSG101 inhibits HIV-1 budding by blocking late domain function.* Proc Natl Acad Sci U S A, 2002. **99**(2): p. 955-60.

100. Huang, M., et al., *p6Gag is required for particle production from full-length human immunodeficiency virus type 1 molecular clones expressing protease.* J Virol, 1995. **69**(11): p. 6810-8.

101. Hemonnot, B., et al., *The host cell MAP kinase ERK-2 regulates viral assembly and release by phosphorylating the p6gag protein of HIV-1.* J Biol Chem, 2004. **279**(31): p. 32426-34.

102. Holguin, A., A. Alvarez, and V. Soriano, *Variability in the P6gag domains of HIV-1 involved in viral budding.* AIDS, 2006. **20**(4): p. 624-7.

103. Stys, D., I. Blaha, and P. Strop, *Structural and functional studies in vitro on the p6 protein from the HIV-1 gag open reading frame.* Biochim Biophys Acta, 1993. **1182**(2): p. 157-61.

104. Dussupt, V., et al., *The nucleocapsid region of HIV-1 Gag cooperates with the PTAP and LYPXnL late domains to recruit the cellular machinery necessary for viral budding.* PLoS Pathog, 2009. **5**(3): p. e1000339.

105. Strack, B., et al., *AIP1/ALIX is a binding partner for HIV-1 p6 and EIAV p9 functioning in virus budding.* Cell, 2003. **114**(6): p. 689-99.

106. Popov, S., et al., *Human immunodeficiency virus type 1 Gag engages the Bro1 domain of ALIX/AIP1 through the nucleocapsid.* J Virol, 2008. **82**(3): p. 1389-98.

107. Popova, E., S. Popov, and H.G. Gottlinger, *Human immunodeficiency virus type 1 nucleocapsid p1 confers ESCRT pathway dependence.* J Virol, 2010. **84**(13): p. 6590-7.

108. Munshi, U.M., et al., *An Alix fragment potently inhibits HIV-1 budding: characterization of binding to retroviral YPXL late domains.* J Biol Chem, 2007. **282**(6): p. 3847-55.

109. Strebel, K., T. Klimkait, and M.A. Martin, *A novel gene of HIV-1, vpu, and its 16-kilodalton product.* Science, 1988. **241**(4870): p. 1221-3.

110. Strebel, K., et al., *Molecular and biochemical analyses of human immunodeficiency virus type 1 vpu protein.* J Virol, 1989. **63**(9): p. 3784-91.

111. Strebel, K., *HIV accessory genes Vif and Vpu.* Adv Pharmacol, 2007. **55**: p. 199-232.

112. Neil, S.J., T. Zang, and P.D. Bieniasz, *Tetherin inhibits retrovirus release and is antagonized by HIV-1 Vpu.* Nature, 2008. **451**(7177): p. 425-30.

113. Gottlinger, H.G., et al., *Vpu protein of human immunodeficiency virus type 1 enhances the release of capsids produced by gag gene constructs of widely divergent retroviruses.* Proc Natl Acad Sci U S A, 1993. **90**(15): p. 7381-5.

114. Schwartz, M.D., R.J. Geraghty, and A.T. Panganiban, *HIV-1 particle release mediated by Vpu is distinct from that mediated by p6.* Virology, 1996. **224**(1): p. 302-9.

115. Ehrlich, L.S., et al., *Activation of the inositol (1,4,5)-triphosphate calcium gate receptor is required for HIV-1 Gag release.* J Virol, 2010. **84**(13): p. 6438-51.

116. Pettit, S.C., et al., *Replacement of the P1 amino acid of human immunodeficiency virus type 1 Gag processing sites can inhibit or enhance the rate of cleavage by the viral protease.* J Virol, 2002. **76**(20): p. 10226-33.

117. Briggs, J.A., et al., *The stoichiometry of Gag protein in HIV-1.* Nat Struct Mol Biol, 2004. **11**(7): p. 672-5.

118. Pettit, S.C., et al., *Processing sites in the human immunodeficiency virus type 1 (HIV-1) Gag-Pro-Pol precursor are cleaved by the viral protease at different rates.* Retrovirology, 2005. **2**: p. 66.

119. Moore, M.D., et al., *Suboptimal inhibition of protease activity in human immunodeficiency virus type 1: effects on virion morphogenesis and RNA maturation.* Virology, 2008. **379**(1): p. 152-60.

120. Grigorov, B., et al., *Intracellular HIV-1 Gag localization is impaired by mutations in the nucleocapsid zinc fingers.* Retrovirology, 2007. **4**: p. 54.
121. Krausslich, H.G., et al., *Analysis of protein expression and virus-like particle formation in mammalian cell lines stably expressing HIV-1 gag and env gene products with or without active HIV proteinase.* Virology, 1993. **192**(2): p. 605-17.
122. Grigsby, I.F., et al., *Biophysical analysis of HTLV-1 particles reveals novel insights into particle morphology and Gag stochiometry.* Retrovirology, 2010. **7**: p. 75.
123. Wright, E.R., et al., *Electron cryotomography of immature HIV-1 virions reveals the structure of the CA and SP1 Gag shells.* EMBO J, 2007. **26**(8): p. 2218-26.
124. Benjamin, J., et al., *Three-dimensional structure of HIV-1 virus-like particles by electron cryotomography.* J Mol Biol, 2005. **346**(2): p. 577-88.
125. Fuller, S.D., et al., *Cryo-electron microscopy reveals ordered domains in the immature HIV-1 particle.* Curr Biol, 1997. **7**(10): p. 729-38.
126. Barklis, E., et al., *Characterization of the in vitro HIV-1 capsid assembly pathway.* J Mol Biol, 2009. **387**(2): p. 376-89.
127. Hill, M.K., et al., *Alteration of the proline at position 7 of the HIV-1 spacer peptide p1 suppresses viral infectivity in a strain dependent manner.* Curr HIV Res, 2007. **5**(1): p. 69-78.
128. Pettit, S.C., et al., *The p2 domain of human immunodeficiency virus type 1 Gag regulates sequential proteolytic processing and is required to produce fully infectious virions.* J Virol, 1994. **68**(12): p. 8017-27.
129. Checkley, M.A., et al., *The capsid-spacer peptide 1 Gag processing intermediate is a dominant-negative inhibitor of HIV-1 maturation.* Virology, 2010. **400**(1): p. 137-44.
130. Wondrak, E.M., et al., *The gag precursor contains a specific HIV-1 protease cleavage site between the NC (P7) and P1 proteins.* FEBS Lett, 1993. **333**(1-2): p. 21-4.

131. Semeniuk, C.A., et al., *Multiple T-cell epitopes overlap positively-selected residues in the p1 spacer protein of HIV-1 gag.* AIDS, 2009. **23**(7): p. 771-7.
132. Whitehurst, N., et al., *Polymorphisms in p1-p6/p6* of HIV type 1 can delay protease autoprocessing and increase drug susceptibility.* AIDS Res Hum Retroviruses, 2003. **19**(9): p. 779-84.
133. Bally, F., et al., *Polymorphism of HIV type 1 gag p7/p1 and p1/p6 cleavage sites: clinical significance and implications for resistance to protease inhibitors.* AIDS Res Hum Retroviruses, 2000. **16**(13): p. 1209-13.
134. Coren, L.V., et al., *Mutational analysis of the C-terminal gag cleavage sites in human immunodeficiency virus type 1.* J Virol, 2007. **81**(18): p. 10047-54.
135. Prabu-Jeyabalan, M., et al., *Structural basis for coevolution of a human immunodeficiency virus type 1 nucleocapsid-p1 cleavage site with a V82A drug-resistant mutation in viral protease.* J Virol, 2004. **78**(22): p. 12446-54.
136. Verheyen, J., et al., *Compensatory mutations at the HIV cleavage sites p7/p1 and p1/p6-gag in therapy-naive and therapy-experienced patients.* Antivir Ther, 2006. **11**(7): p. 879-87.
137. Muller, B., et al., *HIV-1 Gag processing intermediates trans-dominantly interfere with HIV-1 infectivity.* J Biol Chem, 2009. **284**(43): p. 29692-703.
138. Briggs, J.A., et al., *The mechanism of HIV-1 core assembly: insights from three-dimensional reconstructions of authentic virions.* Structure, 2006. **14**(1): p. 15-20.
139. Briggs, J.A., et al., *Structural organization of authentic, mature HIV-1 virions and cores.* EMBO J, 2003. **22**(7): p. 1707-15.
140. Ganser-Pornillos, B.K., et al., *Assembly properties of the human immunodeficiency virus type 1 CA protein.* J Virol, 2004. **78**(5): p. 2545-52.
141. Brun, S., et al., *Electrostatic repulsion between HIV-1 capsid proteins modulates hexamer plasticity and in vitro assembly.* Proteins, 2010. **78**(9): p. 2144-56.
142. Pornillos, O., et al., *X-ray structures of the hexameric building block of the HIV capsid.* Cell, 2009. **137**(7): p. 1282-92.
143. Mehellou, Y. and E. De Clercq, *Twenty-six years of anti-HIV drug discovery: where do we stand and where do we go?* J Med Chem, 2010. **53**(2): p. 521-38.

144. Khoury, G., et al., *Antiviral efficacy of the novel compound BIT225 against HIV-1 release from human macrophages.* Antimicrob Agents Chemother, 2010. **54**(2): p. 835-45.

145. Kelly, B.N., et al., *Structure of the antiviral assembly inhibitor CAP-1 complex with the HIV-1 CA protein.* J Mol Biol, 2007. **373**(2): p. 355-66.

146. Fader, L.D., et al., *Discovery of a 1,5-dihydrobenzo[b][1,4]diazepine-2,4-dione series of inhibitors of HIV-1 capsid assembly.* Bioorg Med Chem Lett, 2010.

147. Cigler, P., et al., *From nonpeptide toward noncarbon protease inhibitors: metallacarboranes as specific and potent inhibitors of HIV protease*. Proc Natl Acad Sci U S A, 2005. **102**(43): p. 15394-9.

148. Monroe, E.B., et al., *Hydrogen/Deuterium Exchange Analysis of HIV-1 Capsid Assembly and Maturation.* Structure, 2010. **18**(11): p. 1483-91.

149. Sticht, J., et al., *A peptide inhibitor of HIV-1 assembly in vitro.* Nat Struct Mol Biol, 2005. **12**(8): p. 671-7.

150. Zhang, H., et al., *A cell-penetrating helical peptide as a potential HIV-1 inhibitor.* J Mol Biol, 2008. **378**(3): p. 565-80.

151. Tavassoli, A., et al., *Inhibition of HIV budding by a genetically selected cyclic peptide targeting the Gag-TSG101 interaction.* ACS Chem Biol, 2008. **3**(12): p. 757-64.

152. Dorr, P., et al., *Maraviroc (UK-427,857), a potent, orally bioavailable, and selective small-molecule inhibitor of chemokine receptor CCR5 with broad-spectrum anti-human immunodeficiency virus type 1 activity.* Antimicrob Agents Chemother, 2005. **49**(11): p. 4721-32.

153. Li, F., et al., *Determinants of activity of the HIV-1 maturation inhibitor PA-457.* Virology, 2006. **356**(1-2): p. 217-24.

154. Adamson, C.S., et al., *Impact of human immunodeficiency virus type 1 resistance to protease inhibitors on evolution of resistance to the maturation inhibitor bevirimat (PA-457).* J Virol, 2009. **83**(10): p. 4884-94.

155. Adamson, C.S., et al., *Polymorphisms in Gag spacer peptide 1 confer varying levels of resistance to the HIV- 1 maturation inhibitor bevirimat.* Retrovirology, 2010. **7**: p. 36.

156. Zhou, J., C.H. Chen, and C. Aiken, *The sequence of the CA-SP1 junction accounts for the differential sensitivity of HIV-1 and SIV to the small molecule maturation inhibitor 3-O-{3',3'-dimethylsuccinyl}-betulinic acid.* Retrovirology, 2004. **1**: p. 15.

157. Seclen, E., et al., *High prevalence of natural polymorphisms in Gag (CA-SP1) associated with reduced response to Bevirimat, an HIV-1 maturation inhibitor.* AIDS, 2010. **24**(3): p. 467-9.

158. Zhou, J., et al., *Inhibition of HIV-1 maturation via drug association with the viral Gag protein in immature HIV-1 particles.* J Biol Chem, 2005. **280**(51): p. 42149-55.

159. Keller, P.W., et al., *The HIV-1 Maturation Inhibitor Bevirimat Stabilizes the Immature Gag Lattice.* J Virol, 2010.

160. Mehellou, Y. and E. De Clercq, *Twenty-six years of anti-HIV drug discovery: where do we stand and where do we go?* J Med Chem, 2009. **53**(2): p. 521-38.

161. Li, F., et al., *PA-457: a potent HIV inhibitor that disrupts core condensation by targeting a late step in Gag processing.* Proc Natl Acad Sci U S A, 2003. **100**(23): p. 13555-60.

162. Zhou, J., et al., *Small-molecule inhibition of human immunodeficiency virus type 1 replication by specific targeting of the final step of virion maturation.* J Virol, 2004. **78**(2): p. 922-9.

163. Adamson, C.S., et al., *In vitro resistance to the human immunodeficiency virus type 1 maturation inhibitor PA-457 (Bevirimat).* J Virol, 2006. **80**(22): p. 10957-71.

164. Sakalian, M., et al., *3-O-(3',3'-dimethysuccinyl) betulinic acid inhibits maturation of the human immunodeficiency virus type 1 Gag precursor assembled in vitro.* J Virol, 2006. **80**(12): p. 5716-22.

165. Zhou, J., C.H. Chen, and C. Aiken, *Human immunodeficiency virus type 1 resistance to the small molecule maturation inhibitor 3-O-(3',3'-dimethylsuccinyl)-betulinic acid is conferred by a variety of single amino acid substitutions at the CA-SP1 cleavage site in Gag.* J Virol, 2006. **80**(24): p. 12095-101.

166. Adamson, C.S., et al., *Polymorphisms in Gag spacer peptide 1 confer varying levels of resistance to the HIV- 1 maturation inhibitor bevirimat.* Retrovirology. **7**: p. 36.

167. DaFonseca, S., et al., *The 3-O-(3',3'-dimethylsuccinyl) derivative of betulinic acid (DSB) inhibits the assembly of virus-like particles in HIV-1 Gag precursor-expressing cells.* Antivir Ther, 2007. **12**(8): p. 1185-203.

168. Dafonseca, S., et al., *The inhibition of assembly of HIV-1 virus-like particles by 3-O-(3',3'-dimethylsuccinyl) betulinic acid (DSB) is counteracted by Vif and requires its Zinc-binding domain.* Virol J, 2008. **5**: p. 162.

169. Heider, D., J. Verheyen, and D. Hoffmann, *Predicting Bevirimat resistance of HIV-1 from genotype.* BMC Bioinformatics. **11**: p. 37.

170. Verheyen, J., et al., *High prevalence of bevirimat resistance mutations in protease inhibitor-resistant HIV isolates.* AIDS. **24**(5): p. 669-73.

171. Hashimoto, F., et al., *Anti-AIDS agents--XXVII. Synthesis and anti-HIV activity of betulinic acid and dihydrobetulinic acid derivatives.* Bioorg Med Chem, 1997. **5**(12): p. 2133-43.

172. Yebra, G. and A. Holguin, *The maturation inhibitor bevirimat (PA-457) can be active in patients carrying HIV type-1 non-B subtypes and recombinants.* Antivir Ther, 2008. **13**(8): p. 1083-5.

173. Smith, P.F., et al., *Phase I and II study of the safety, virologic effect, and pharmacokinetics/pharmacodynamics of single-dose 3-o-(3',3'-dimethylsuccinyl)betulinic acid (bevirimat) against human immunodeficiency virus infection.* Antimicrob Agents Chemother, 2007. **51**(10): p. 3574-81.

174. Krasutsky, P.A., *Birch bark research and development.* Nat Prod Rep, 2006. **23**(6): p. 919-42.

175. Krasutsky, P.A.K., I. V.; Krastuskyy, D. A., *Depolymerization extraction of compounds from birch bark*, in *WIPO IP Services*, W.I.P. Organization, 2007.

176. Krasutsky, P.A.M., K., *Synthesis of betulonic and betulinic aldehydes* in *WIPO IP Services* W.I.P. Organization, 2006.

177. Dapp, M.J., et al., *5-Azacytidine can induce lethal mutagenesis in human immunodeficiency virus type 1.* J Virol, 2009. **83**(22): p. 11950-8.

178. Murakami, T. and E.O. Freed, *The long cytoplasmic tail of gp41 is required in a cell type-dependent manner for HIV-1 envelope glycoprotein incorporation into virions.* Proc Natl Acad Sci U S A, 2000. **97**(1): p. 343-8.

179. Vodicka, M.A., et al., *Indicator cell lines for detection of primary strains of human and simian immunodeficiency viruses.* Virology, 1997. **233**(1): p. 193-8.

180. Kanamoto, T., et al., *Anti-human immunodeficiency virus activity of YK-FH312 (a betulinic acid derivative), a novel compound blocking viral maturation.* Antimicrob Agents Chemother, 2001. **45**(4): p. 1225-30.

181. Resch, W., et al., *Nelfinavir-resistant, amprenavir-hypersusceptible strains of human immunodeficiency virus type 1 carrying an N88S mutation in protease have reduced infectivity, reduced replication capacity, and reduced fitness and process the Gag polyprotein precursor aberrantly.* J Virol, 2002. **76**(17): p. 8659-66.

182. Perry, C.M. and P. Benfield, *Nelfinavir.* Drugs, 1997. **54**(1): p. 81-7; discussion 88.

183. Heider, D., J. Verheyen, and D. Hoffmann, *Predicting Bevirimat resistance of HIV-1 from genotype.* BMC Bioinformatics, 2010. **11**: p. 37.

184. Wainberg, M.A. and J. Albert, *Can the further clinical development of bevirimat be justified?* AIDS, 2010. **24**(5): p. 773-4.

185. Kashiwada, Y., et al., *3-O-Glutaryl-dihydrobetulin and related monoacyl derivatives as potent anti-HIV agents.* Bioorg Med Chem Lett, 2004. **14**(23): p. 5851-3.

186. Blair, W.S., et al., *New small-molecule inhibitor class targeting human immunodeficiency virus type 1 virion maturation.* Antimicrob Agents Chemother, 2009. **53**(12): p. 5080-7.

187. Qian, K., et al., *Anti-AIDS agents 81. Design, synthesis, and structure-activity relationship study of betulinic acid and moronic acid derivatives as potent HIV maturation inhibitors.* J Med Chem, 2010. **53**(8): p. 3133-41.

188. Clouser, C.L., S.E. Patterson, and L.M. Mansky, *Exploiting drug repositioning for discovery of a novel HIV combination therapy.* J Virol, 2010. **84**(18): p. 9301-9.

189. Sadler, H.A., et al., *APOBEC3G contributes to HIV-1 variation through sublethal mutagenesis.* J Virol, 2010. **84**(14): p. 7396-404.

190. Margot, N.A., C.S. Gibbs, and M.D. Miller, *Phenotypic susceptibility to bevirimat in isolates from HIV-1-infected patients without prior exposure to bevirimat.* Antimicrob Agents Chemother, 2010. **54**(6): p. 2345-53.

191. Li, Q.G., et al., *The morphogenesis of a Chinese strain of HIV-1 forming inclusion bodies in Jurkat-tat III cells.* J Acquir Immune Defic Syndr Hum Retrovirol, 1995. **9**(2): p. 103-13.

192. Demirov, D.G., J.M. Orenstein, and E.O. Freed, *The late domain of human immunodeficiency virus type 1 p6 promotes virus release in a cell type-dependent manner.* J Virol, 2002. **76**(1): p. 105-17.

193. Daniels, S.I., et al., *The initial step in human immunodeficiency virus type 1 GagProPol processing can be regulated by reversible oxidation.* PLoS One, 2010. **5**(10): p. e13595.

194. Adachi, A., et al., *Production of acquired immunodeficiency syndrome-associated retrovirus in human and nonhuman cells transfected with an infectious molecular clone.* J Virol, 1986. **59**(2): p. 284-91.

195. Pear, W.S., et al., *Production of high-titer helper-free retroviruses by transient transfection.* Proc Natl Acad Sci U S A, 1993. **90**(18): p. 8392-6.

196. DuBridge, R.B., et al., *Analysis of mutation in human cells by using an Epstein-Barr virus shuttle system.* Mol Cell Biol, 1987. **7**(1): p. 379-87.

197. Gervaix, A., et al., *A new reporter cell line to monitor HIV infection and drug susceptibility in vitro.* Proc Natl Acad Sci U S A, 1997. **94**(9): p. 4653-8.
198. Graham, F.L., et al., *Characteristics of a human cell line transformed by DNA from human adenovirus type 5.* J Gen Virol, 1977. **36**(1): p. 59-74.
199. Boussif, O., et al., *A versatile vector for gene and oligonucleotide transfer into cells in culture and in vivo: polyethylenimine.* Proc Natl Acad Sci U S A, 1995. **92**(16): p. 7297-301.
200. Hultquist, J.F. and R.S. Harris, *Leveraging APOBEC3 proteins to alter the HIV mutation rate and combat AIDS.* Future Virol, 2009. **4**(6): p. 605.
201. Saermark, T., et al., *Characterization of N-myristoyl transferase inhibitors and their effect on HIV release.* AIDS, 1991. **5**(8): p. 951-8.

Appendix A

Passaging and Genotyping of HIV-1 in Human T-cells in Presence of SY33

> *"Though it is not a great hypothesis driven experiment, the best experiment in retrovirology is too passage the hell out of the virus and identify mutants. You will always generate interesting data."*
>
> John Coffin at Centennial Retrovirus Meeting in Prague, Czech Republic 2010

To further investigate SY33's antiviral target, HIV-1 was serially passaged in the presence of SY33 or Bevirimat; the virus genome was then sequenced to identify virus genotype. Since the virus is likely to develop resistance to the antiviral compound, mutants identified that replicate in high concentrations of SY33 or Bevirimat, might decrease the virus' susceptibility to the compound. Often, the identified mutants indicate the protein that the compound molecularly targets. Since SY33 is structurally similar to Bevirimat and targets CA-SP1, I hypothesize that the experiment would identify mutations near the CA-SP1 cleavage site that decrease SY33 drug susceptibility.

The passaging experiment can be divided into two separate experiments. The first part of the experiment was done identically as indicated in the materials and methods section of **Chapter 3**. These data are represented in **Appendix A, Figure 1** (Experiment 1). On day 33 of experiment 1, the CEM-GFP cells were centrifuged in a 96-well culture plate to pellet the cells. The supernatant was removed, and the cells were resuspended in 1% DMSO cell culture freezing solution. The 96-well plate was then covered, wrapped and stored at -80 ºC for nearly one year. The 96-well plate was then removed from the freezer, thawed, cells pelleted, and then resuspended in RPMI media with 10% FC3. The cells were immediately treated with the same compound concentration as to prior the freezing. Also, 10,000 fresh CEM-GFP cells were added to each cell culture well. Two

days later the aliquots of the cells were harvested for flow cytometry, and the remaining cell culture was passaged to a 5 ml cultures with 10,000 CEM-GFP cells added. On day 8, the cells were either passaged to new cell cultures or harvested. The harvested cells were analyzed by flow cytometry or the genomic DNA was extracted. Cells were then serially passaged in the 5 ml cultures, the compound concentration was raised to 25 uM on day 12, cells were analyzed by flow cytometry, and on day 35 genomic DNA was extracted again.

To identify HIV-1 genotypes, a 2.3 kb section of the HIV-1 *GagPol* gene was cloned and sequenced using the primers listed in material and methods in **Chapter 3**. The genomic DNA isolated on Day 8 or Day 35 of experiment 2 was used as the PCR template with PCR primers **NL645F** [163] and **NL2897R** [154, 163]. The resultant PCR products were then purified using a PCR cleanup kit, then ligated overnight into the pGEM-T-Easy vector. The ligation products were then transformed into chemically competent *E. coli* cells, and plated onto LB agar plates containing Ampicillin, X-Gal, and IPTG (for blue/white colony screening). White colonies were picked from the plates, and mini-prepped to isolate insert containing pGEM-T-Easy plasmids. The plasmids were restriction enzyme digested to ensure inserts were present. The plasmids were then sent to Functional Biosciences (Madison, Wisconsin) to be sequenced using the sequencing primers listed in **Chapter 3** (**NL1155F** [163]; **NL1410F** [154, 163]; **NL1754F** [154, 163]; **NL2135F** [154, 163]). The sequences were then analyzed using DNAStar Lasergene software and identified mutants are listed in **Figure 1**, **Table 1**, and **Table 2**. For each cell/virus culture, 1-4 sequences were identified.

Figure 1: Passaging and Genotyping of HIV-1 in Human T-cells in Presence of SY33
HIV-1 molecular clones were passaged in the presence of SY33 in CEM-GFP cells. The founder virus is the virus that initially infected the cells. Viral replication was monitored by assessing GFP expression with a flow cytometer. In experiment 1, the cell/virus culture was split every 1-3 days and then the cells were frozen at -80ºC. For experiment 2, the cells were thawed and virus was passaged for an additional 35 days. On days 8 and 35 of experiment 2, genomic DNA was isolated and the HIV-1 *GagPol* gene was sequenced. In red of each graph is the kinetics of a vehicle control. Identified genotypes in each culture are on graphs. **a)** Wild-type HIV-1 was passaged the presence of 5 µM SY33. On day 19 of experiment 2, [SY33] was raised to 25 µM. **b)** SP1-A1V HIV-1 mutant was passaged in the presence of 5 µM SY33. On day 19 of experiment 2, [SY33] was raised to 25 µM. **c)** SP1-A1V HIV-1 mutant was passaged in the presence of 25 µM SY33 for entirety of experiments 1 and 2.

a. Replication of WT HIV-1 Founder Virus with SY33 Treatment

Experiment 1

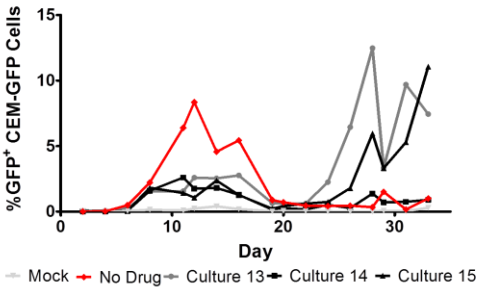

Experiment 2

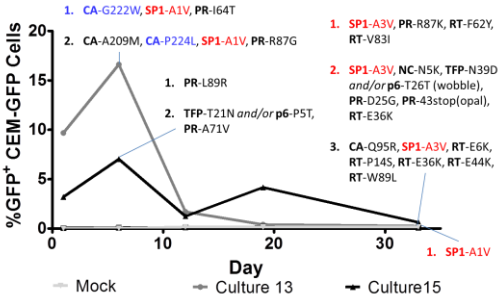

b. Replication of SP1-A1V HIV-1 Founder Virus with 5 µM SY33 Treatment

Experiment 1

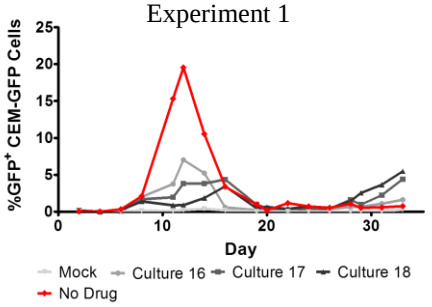

Experiment 2

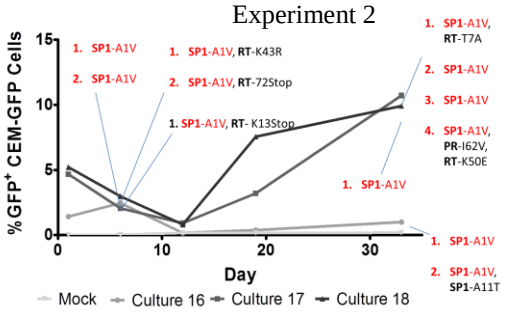

c. Replication of SP1-A1V HIV-1 Founder Virus with 25 µM SY33 Treatment

Experiment 1

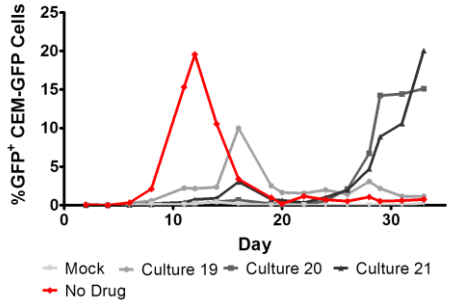

Experiment 2

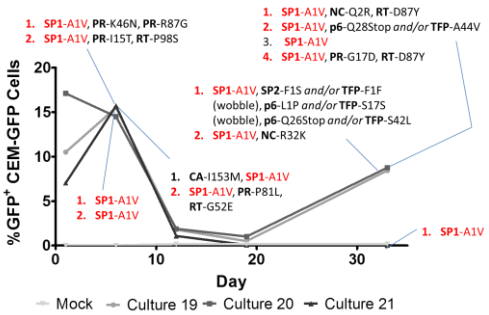

Table 1: HIV-1 Genotypes Identified in Passaging Experiment with Wild-Type Founder Virus

Treatment[a]	Culture[b]	Day[c]	% GFP$^+$ CEM-GFP Cells[d]	HIV-1 Genotypes Identified in Culture[e]
Vehicle	3	35	14	1. **SP1**-A1V, **NC**-F6L 2. **CA**-E113G, **SP1**-A1V
Vehicle	6	35	16	1. **SP1**-A1V
50 nM BVM	28	8	0.7	1. **CA**-L151R, **RT**-E28K, **RT**-K74R
5 nM BVM	29	8	0.2	1. **CA**-K203E
5 nM BVM	30	8	0.3	1. **CA**-T107A 2. **CA**-S178P, **SP1**-S5N, **PR**-H69R
5 µM SY33	13	8	`17	1. **CA**-G222W, **SP1**-A1V, **PR**-I64T 2. **CA**-A209M, **CA**-P224L, **SP1**-A1V, **PR**-R87G
25 µM SY33	13	35	0.1	1. **SP1**-A1V
5 µM SY33	15	8	7.0	1. **PR**-L89R 2. **TFP**-T21N *and/or* **p6**-P5T, **PR**-A71V
25 µM SY33	15	35	0.1	1. **SP1**-A3V, **PR**-R87K, **RT**-F62Y, **RT**-V83I 2. **SP1**-A3V, **NC**-N5K, **TFP**-N39D *and/or* **p6**-T26T (wobble), **PR**-D25G, **PR**-W43stop(opal), **RT**-E36K 3. **CA**-Q95R, **SP1**-A3V, **RT**-E6K, **RT**-P14S, **RT**-E36K, **RT**-E44K, **RT**-W89L
500 pM SY33	22	8	0.1	1. **RT**-E42G, **RT**-G45R 2. **NC**-T12S, **RT**-G45R
500 pM SY33	23	8	0.1	1. **PR**-V82I 2. **RT**-E80G

[a] Concentration of compound in culture. Vehicle = 1% DMSO
[b] Arbitraty number of individual cell and virus culture
[c] Day from experiment 2 (as in **Appendix A, Figure 1**) that genotypes were identified
[d] Percentage of CEM-GFP cells that are actively expressing HIV-1
[e] Identified genotypes in individual cultures after sequencing HIV-1 *GagPol* gene.

Table 2: HIV-1 Genotypes Identified in Passaging Experiment with SP1-A1V Founder Virus

Treatment[a]	Culture[b]	Day[c]	% GFP$^+$ CEM-GFP Cells[d]	HIV-1 Genotypes Identified in Culture[e]
Vehicle	9	35	11	1. **CA**-S102, **SP1**-A1V, **NC**-F16L, **p6**-K33R *and/or* **TFP**-Q49Q (wobble), **PR**-I62V 2. **CA**-V221A, **SP1**-A1V, **RT**-K67E
Vehicle	12	35	10	1. **CA**-F168, **SP1**-A1V 2. **SP1**-A1V, **SP2**-G14G (wobble) *and/or* **TFP**-E15K
50 nM BVM	25	8	0.1	1. **SP1**-A1V, **p6**-S3G *and/or* **TFP**-E19G
25 µM BVM	25	35	2.0	1. **SP1**-A1V
500 nM BVM	26	8	18	1. **CA**-T188A, **SP1**-A1V, **NC**-K46R 2. **SP1**-A1V, **PR**-P79L
25 µM BVM	26	35	3.0	1. **SP1**-A1V 2. **CA**-L151Q, **SP1**-A1V
5 µM BVM	27	8	17	1. **SP1**-A1V, **NC**-T49A
25 µM SY33	19	8	15	1. **SP1**-A1V 2. **SP1**-A1V
25 µM SY33	19	35	8.0	1. **SP1**-A1V, **NC**-Q2R, **RT**-D87Y 2. **SP1**-A1V, **p6**-Q28Stop (amber) *and/or* **TFP**-A44V 3. **SP1**-A1V 4. **SP1**-A1V, **PR**-G17D, **RT**-D87Y
25 µM SY33	20	8	15	1. **SP1**-A1V, **PR**-K46N, **PR**-R87G 2. **SP1**-A1V, **PR**-I15T, **RT**-P98S
25 µM SY33	20	35	8.0	1. **SP1**-A1V, **SP2**-F1S *and/or* **TFP**-F1F (wobble), **p6**-L1P *and/or* **TFP**-S17S (wobble), **p6**-Q26Stop (amber) *and/or* **TFP**-S42L 2. **SP1**-A1V, **NC**-R32K
25 µM SY33	21	8	16	1. **CA**-I153M, **SP1**-A1V 2. **SP1**-A1V, **PR**-P81L, **RT**-G52E
25 µM SY33	21	35	2.5	1. **SP1**-A1V
5 µM SY33	16	8	0.1	1. **SP1**-A1V, **RT**- K13Stop (amber)
25 µM SY33	16	35	0.3	1. **SP1**-A1V 2. **SP1**-A1V, **SP1**-A11T
5 µM SY33	17	8	2.0	1. **SP1**-A1V 2. **SP1**-A1V
25 µM SY33	17	35	10	1. **SP1**-A1V
5 µM SY33	18	8	3.0	1. **SP1**-A1V, **RT**-K43R 2. **SP1**-A1V, **RT**-W72Stop (amber)
25 µM SY33	18	35	11	1. **SP1**-A1V, **RT**-T7A 2. **SP1**-A1V 3. **SP1**-A1V 4. **SP1**-A1V, **PR**-I62V, **RT**-K50E

[a] Concentration of compound in culture. Vehicle = 1% DMSO
[b] Arbitraty number of individual cell and virus culture
[c] Day from experiment 2 (as in **Appendix A, Figure 1**) that genotypes were identified
[d] Percentage of CEM-GFP cells that are actively expressing HIV-1
[e] Identified genotypes in individual cultures after sequencing HIV-1 *GagPol* gene.

The results show that numerous mutants were identified. Most notably, is that the SP1-A1V mutation arose in the presence of SY33. However, the SP1-A1V mutation also arose with only vehicle treatment. Thus, it is possible the SP1-A1V mutation has some replicative advantage in cell culture over the wild-type HIV-1. However, there is not enough data here to conclude SP1-A1V replicates better than wild-type HIV-1. Additionally, when using SP1-A1V as the founder virus, the SP1-A1V mutation was consistently identified even with SY33 or Bevirimat treatment. Thus, it is likely that SP1-A1V is a common mutation that decreases susceptibility to either Bevirimat or SY33. Furthermore, this data support the claim that SY33 targets the CA-SP1 cleavage site, or more precisely SP1.

Though this data set is interesting, due to time constraints, I was not able to repeat this experiment and gather more genotypic data. If I repeated this experiment, I would avoid the freezing cycle. Actually, due to experiments 1 and 2, the sequences on day 35 were actually in culture for 68 days. However, it was good to know the cells can be frozen for a year in 96 well culture clusters. To repeat this experiment, I would do the entire experiment in 5 ml cultures in 6-well culture clusters. Also, the virus/cell mixture should be passaged every 2-4 days into cultures with fresh CEM-GFP cells (as done in Experiment 2). It is important to add fresh permissive cells to the cultures with each passage because HIV-1 kills the cells (John Coffin, personal communication). This is why the virus typically "peaks" in HIV-1 kinetics experiments. The virus "crashes" because the permissive cells die off. If fresh permissive cells are added with each passage, the virus can maintain high infection rates. In repeating this experiment, I

would suggest raising the compound concentration with each (or every other) passage. Also, with each passage, harvest cells for flow cytometry and extract DNA. The DNA can be used to identify mutants in culture. Lastly, I recommend getting more sequences from each culture. In this experiment only 1-4 sequences were identified per culture making it difficult to determine the predominant genotype in each culture. The flow cytometry can be used to identify the phenotype of the culture as infectivity of the virus.

Once the mutants are identified, they need to be verified. I recommend taking the mini-prep stock that was used for sequencing (since it was ligated and mini-prepped, it should be a monogenic plasmid stock) and use it for cloning. The sequence of interest can be PCR'ed or restriction digested from the pGEM-T-Easy vector and inserted into the pHIG HIV-1 vector or the pNL4-3 HIV-1 molecular clone. These new reagents can then be used to verify if the mutation alters susceptibility to SY33, Bevirimat, or any other antiviral strategy. Alternatively, the identified mutations can be introduced by site-directed mutagenesis, but since the mutations are already cloned into pGEM-T-Easy, time can be saved by using this method.

In all, **Appendix A** provides data and experimental information for passaging and identifying HIV-1 genotypes in culture. Particularly, this data set supports the claim that SY33 targets CA-SP1.

Appendix B

Fatty Acid Derivatives that Inhibit HIV-1 Replication

The observation that the triterpene compounds in **Chapters 2** and **3** have similar structures led to reasoning that the ring structure of the antiviral compounds could be substituted with a flexible carbon chain and maintain anti-HIV-1 activity. The flexible carbon chains will make the compounds lighter, more mobile, and have better permeability. We hypothesized that the dimethyl succinyl group had to be linked to a polar functional group some distance away and the compounds would inhibit HIV-1 replication.

To test this hypothesis, Dr. Pavel Krasutsky's research group in Duluth, Minnesota synthesized a collection of fatty acid derivatives that linked methylated succinates to other succinates, glutarates, carboxylic acids, aldehydes, or nitriles. The new library of compounds consisted of about 300 compounds with carbon lengths ranging from 4 carbons to 30 carbons lengths. The novel compounds were screened for anti HIV-1 activity using the assay in **Chapter 2**, **Figure 2**.

Antiviral screening identified a number of compounds with modest anti-HIV-1 activity. The compounds were tested three times for anti-HIV-1 activity. Using the screening assay, both virus producing and virus permissive cells were treated with compounds over a dilution range of 100 nM to 500 µM. However none of the compounds had great anti-HIV-1 potency. Reported in **Table 1** are compounds OK191G, OK191 and OK192BG. The EC_{50} was most potent for OK191G at 33 µM and OK191 was 51 µM. OK192BG had an extrapolated EC_{50} value of roughly 1000 µM.

Table 1: Therapeutic Index of Fatty Acid Derivatives

Compound	EC_{50} (µM)	IC_{50} (µM)	Therapeutic Index
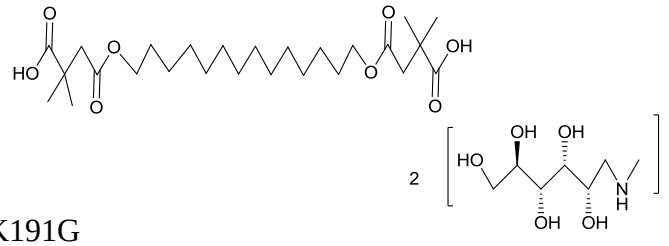 OK191G	33	>500	>15
 OK191	51	110	2
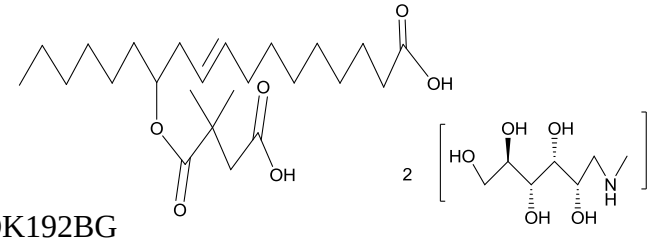 OK192BG	>500	>500	---
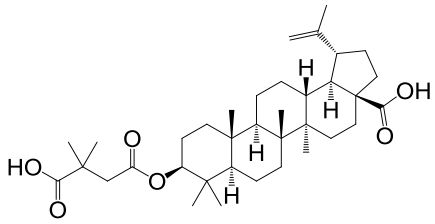 Bevirimat	0.18	>500	>2700

Antiviral compounds were tested for cellular toxicity, using the Promega non-radioactive cell proliferation assay following the manufacturer's directions with 293T cells as in **Chapters 2** and **3** using Bevirimat as a control. Compound concentrations were tested up to 500 µM. Therapeutic indices were derived using the toxicity and antiviral data. OK191 has therapeutic index of 2 and OK191G of 15. Thus, OK191G and OK191 have anti-HIV-1 activity.

Figure 1: Compound OK191G Treated HIV-1 is Trapped on Cellular Plasma Membrane

293T cells were transfected and treated with a vehicle control (1% DMSO) or 200 µM OK191G. Forty hours post treatment the cells were fixed, stained, embedded, sectioned and visualized under a transmission electron microscope. The HIV-1 like particles in the OK191G treatment group were consistently found attached to the cell membrane.

a. Vehicle Treated

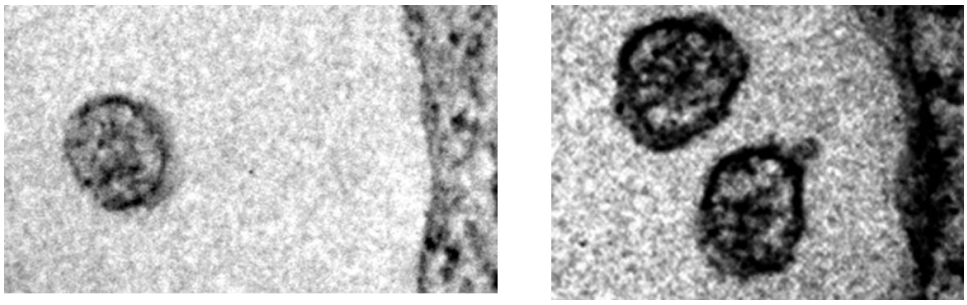

b. OK191G Treated

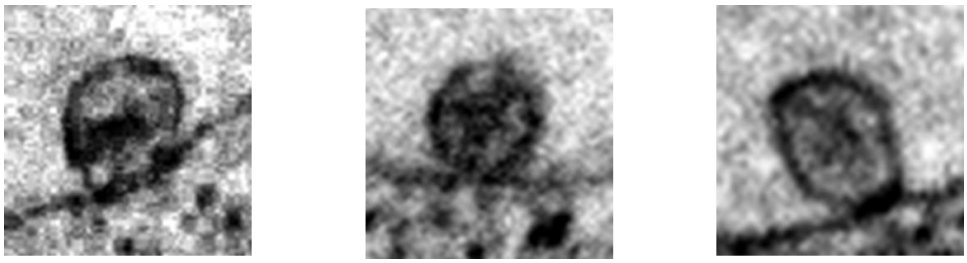

OK191G was analyzed by Transmission Electron Microscopy at University of Minnesota's Characterization Facility for morphological effects on HIV-1. Briefly, 293T cells were transfected with pHIG and treated with 200 µM OK191G. The cells were embedded and sectioned at the Characterization Facility and analyzed by transmission electron microscopy as in **Chapter 3**. Interestingly, mature regular morphology particles appeared to be trapped on the cell membrane with an electron dense ring between the nascent virus particle and the cell membrane (**Figure 2b**). The electron dense ring is similar to an observation that the human cellular protein CEP55 plays a role in the fission

of particles from the cell membrane [54]. It is possible that OK191G targets CEP55, or the ESCRT proteins, during viral budding. If OK191G inhibits cellular membrane fission, OK191G may be able to inhibit cytokinesis. If OK191 can inhibit cytokinesis, OK191 might have therapeutic use as an anti-cancer agent. Electron microscopy indicates that OK191G can cause HIV-1 to be trapped on a cell's plasma membrane.

OK191G was more active against HIV-1 than OK191. OK191 is 2 dimethyl succinates linked to each other with a 14 carbon fatty acid chain. Meanwhile, OK191G is the same compound, as a dianion, mixed with two glucamonium molecules. Glucosamine is shown to inhibit the N-mystryl transferase [200]. Since OK191G, OK191, and myristate are derivatives of 14 carbon fatty acids, myristoylation is essential for HIV-1 assembly, and myristate derivatives can inhibit HIV-1 replication [70], it is possible OK191G inhibits HIV-1 assembly by targeting Gag myristoylation.

This short data set indicates that fatty acid derivatives can inhibit HIV-1 replication. Electron microscopy data suggest it is possible that the compound OK191G can inhibit the release of nascent HIV-1 from the virus producing cell.